



SKB rapport R-98-01

August 1997

Cross-prediction of the groundwater
chemistry at the SKB sites in Sweden

Pilot study

Christina Skårman, Marcus Laaksoharju

Intera KB

Svensk Kärnbränslehantering AB

Swedish Nuclear Fuel and Waste Management Co

SKB, Box 5864, S-102 40 Stockholm, Sweden

Tel 08-665 28 00 Fax 08-661 57 19

Tel +46 8 665 28 00 Fax +46 8 661 57 19

**CROSS-PREDICTION OF THE
GROUNDWATER CHEMISTRY AT
THE SKB SITES IN SWEDEN**

PILOT STUDY

Christina Skårman, Marcus Laaksoharju

Intera KB

August 1997

This report concerns a study which was conducted for SKB. The conclusions and viewpoints presented in the report are those of the author(s) and do not necessarily coincide with those of the client.

**CROSS-PREDICTION OF THE
GROUNDWATER CHEMISTRY AT THE
SKB SITES IN SWEDEN**

Pilot study

August, 1997

**Christina Skårman, INTERA KB
Marcus Laaksoharju, INTERA KB**

Abstract

The possibility to perform a large scale prediction throughout Sweden was tested. The aim of the work was: to collect data and create a groundwater database for current and future use; to see if there is any correlation between data at different sites; to perform a modelling where the groundwater composition at different regions in Sweden is predicted.

The outcome of the predictions were compared with the measured data at different sites. The results show that it is possible but more work needs to be done to improve the prediction models. More measurements at depth are needed to enable the use of 3D models. It is also important to include hydrogeological parameters in the groundwater chemical prediction models that are used.

Abstract (Swedish)

Möjligheten att utföra storskaliga grundvattenpredikteringar för olika undersökningsplatser i Sverige har testats. Ett syfte med arbetet var att skapa en grundvattendatabas. Det andra syftet var en omfattande korrelations analys för att finna samband i data, samt att utföra ett test där grundvattensammansättningen i olika svenska undersökningsområden predikterades.

Utfallet av predikteringarna jämfördes med uppmätta värden från olika områden. Resultatet visar att det är möjligt att utföra denna typ av predikteringar men mera arbete krävs för att förbättra modellerna. Fler mätningar behövs från djupa borrhål för att 3D modeller skall bli tillförlitliga. Det är även nödvändigt att inkludera hydrogeologiska parametrar i modellerna.

TABLE OF CONTENTS

TABLE OF CONTENTS	2
1. BACKGROUND AND AIM	3
2. STRATEGY	4
3. PREDICTION METHODS	5
3.1. Kriging	5
3.2. Multiple Linear regression	5
4. RESULTS OF THE PREDICTIONS	6
5. DISCUSSION	19
ACKNOWLEDGEMENTS	20
REFERENCES	21
APPENDIX A: FINNSJÖN	22
APPENDIX B: FJÄLLVEDEN	27
APPENDIX C: FORSMARK	32
APPENDIX D: GIDEÅ	36
APPENDIX E: KAMLUNGE	41
APPENDIX F: KARLSHAMN	46
APPENDIX G: KLIPPERÅS	50
APPENDIX H: KRÅKEMÅLA	55
APPENDIX I: LANSJÄRV	59
APPENDIX J: STRIPA	64
APPENDIX K: SVARTBOBERGET	68
APPENDIX L: TAAVINUNNANEN	73
APPENDIX M: ZINKGRUVAN	78

1. BACKGROUND AND AIM

In Wikberg and Gustafsson (1993), Wikberg et al. (1994a) and Wikberg et al. (1994b) the groundwater chemistry in the Äspö hard rock laboratory was predicted. The major components Cl, Ca, Na, SO₄ and HCO₃ describe the groundwater composition well and were predicted by regression analyses, principal component analyses, neural network and kriging. Kriging is especially suitable when predicting the groundwater in a region.

Development and evaluation of prediction models and strategies are important for a number of reasons. When selecting new sites a well performed prediction of the new site will lower the cost, decrease the time spent and increase the effectiveness. A prediction model such as the one in this report also evaluates the current knowledge about the systems. The evaluation will help answer the question: What do we really know compared to what we think we know? A prediction like the one below will indicate how much information it is possible to draw from a new predicted site. It will also take into account what is needed to improve the prediction models to be able to perform reliable predictions at new sites.

The aim of our current work is as follows: to collect data and create a database for current and future use; to see if there is any correlation between data at different sites; to perform a pilot study and predict the groundwater composition in different regions in Sweden. The strategy is to perform cross-predictions (see Chapter 2) based on Sveriges Geologiska Undersökningars (SGU) brunnsarkiv (the Swedish Geological Survey, archive of well data (pers. comm. Sten Sandström, 1994) in combination with site characterisation data in GEOTAB (successor to SICADA), the Swedish Nuclear Fuel and Waste Management Company (SKB) database (pers. comm. Ann-Chatrin Nilsson, 1994). In the early part of the project a Neural Network and the 3D spatial location of the sampling points were used to predict Cl and the predicted Cl was to be used to predict the other groundwater constituents. The results showed that the deep samples were too few so that no meaningful predictions were obtained. Simplifications were needed. Using Kriging and the 2D spatial location of the sampled points the Cl versus sampling depth was predicted. To illustrate the results of the different site predictions the following elements were calculated using multiple linear regression: Cl, HCO₃, Ca, SO₄, K, S, Fe, TOC, and pH.

2. STRATEGY

The data from 14 SKB sites include 151 observations (between 2 and 55 observations per site). In order to accommodate the limitations of 2D kriging the mean (CI versus sampling depth) for each site was calculated and used for predictions. The well data contain 253 observations at different sample locations on the Swedish mainland and at sampling depth >120m.

The predictions were performed as cross-predictions. This means that the first site to be predicted was excluded from the dataset before the prediction took place. When the next site was to be predicted the first site was included and the second site was excluded from the dataset. This procedure was repeated for all sites. The Äspö, Finnsjön, Fjällveden, Forsmark, Gideå, Kamlunge, Karlshamn, Klipperås, Kråkemåla, Lansjärv, Stripa, Svartboberget, Taavinunnanen, and Zinkgruvan sites were predicted. The locations of the observations are shown in *Figure 2-1*.

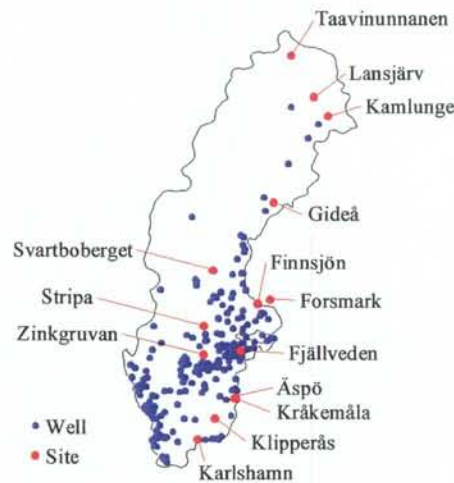


Figure 2-1. Map of Sweden showing the sample locations of the well and site observations.

The predictions were performed as a sequential combination of two statistical prediction methods: kriging followed by multiple linear regression. In the first prediction phase the mean (CI versus sampling depth) was predicted, using kriging, for each site. In the second phase the predicted CI versus sampling depth and the important location parameters were used in a multiple linear regression to predict the element concentration at different sites and depths.

3. PREDICTION METHODS

3.1. KRIGING

Kriging is based on the theory that unknown values physically close in location to a known value would also be numerically close to that known value. Unknown values far away from a known value would be more uncertain. All values have an uncertainty, a variance, associated with it. There are different ways of estimating the unknown values and their corresponding variances. Kriging seeks the minimum variance of the error of estimation. When estimating the missing or unknown values, the closest known values and their variance functions are used to estimate the unknown value and the variance of the estimate (Henley, 1981; Fortner, 1992). The computer program used was SURFER for Windows (1994).

3.2. MULTIPLE LINEAR REGRESSION

The multiple linear regression model is based on the least-square method that minimises the distance between the observed values and the equation of the model. The linear regression model states the following assumptions. The observations are independent, normally distributed, the variance is the same, and the relationship between dependent and independent variables is linear (Kleinbaum et al., 1988). The computer program used was STATISTICA for Windows (1995) and STATGRAPHICS PLUS for Windows (1994).

4. RESULTS OF THE PREDICTIONS

The results of the predictions are compared with measured data and shown in relation to depth (*Figures 4-1 - 4-22*). The prediction error for the multiple linear regression is also shown. The error shown is the smallest assumable error. The true overall prediction error is larger. A general prediction error includes measurement error, analysis error, misfit to the applied distribution, kriging error etc. The error interval is not a confidence interval. As seen in some of the *Figures 4-1 - 4-14* the predicted Cl content is negative. Negative predictions would by definition be set at zero. About half of the sites have too few locations (i.e. there were few existing boreholes), and it is therefore not possible to see any trends in the measurements.

The Cl predictions for the Äspö site are low but follow the measured trend (*Figure 4-1*).

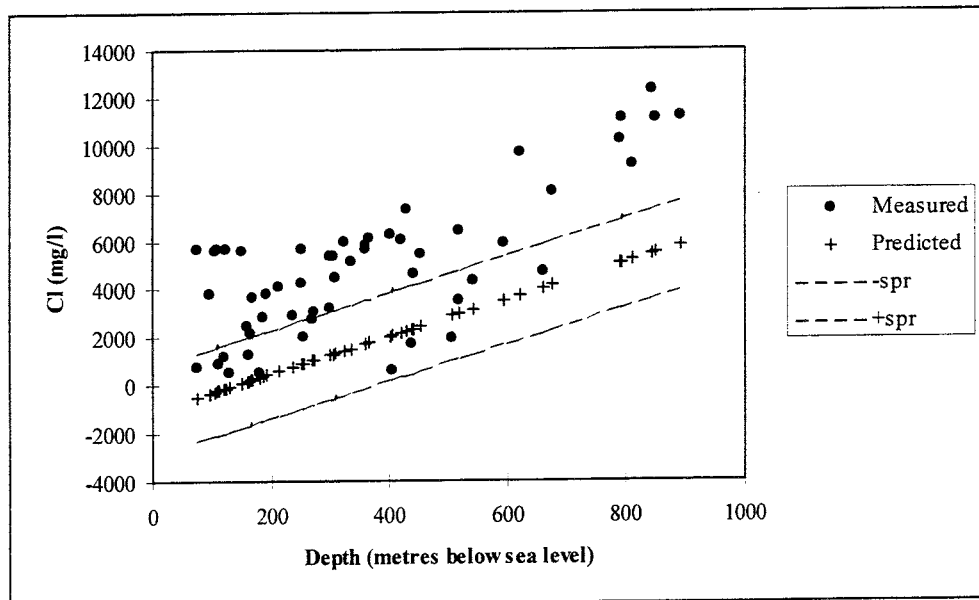


Figure 4-1. The measured (dots) and predicted (crosses) Cl content at the Äspö site in relation to the depth below sea level. The dotted lines show \pm the standard deviation of the prediction (s_{pr}).

The Cl predictions for the Finnsjön site are low but follow the measured main trend for most observations. In the southern part of the Finnsjön site there are some low Cl measurements that are predicted too high at greater depths (*Figure 4-2*).

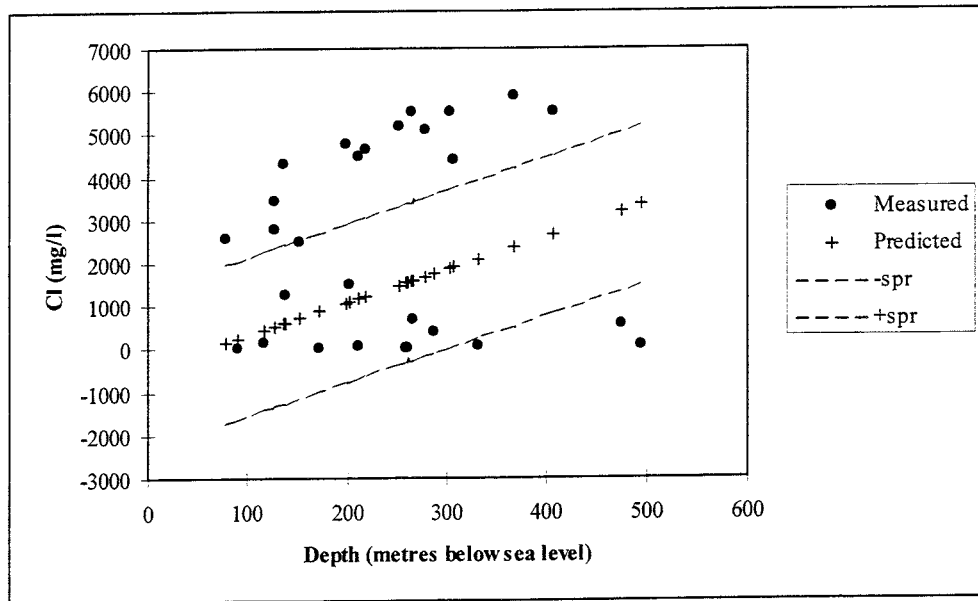


Figure 4-2. The measured (dots) and predicted (crosses) Cl content at the Finnsjön site in relation to the depth below sea level. The dotted lines show \pm the standard deviation of the prediction (s_{pr}).

At the Fjällveden site the measured Cl content is generally low. However, the predictions follow a different trend to the measured one - the deeper the depth, the higher the prediction (Figure 4-3).

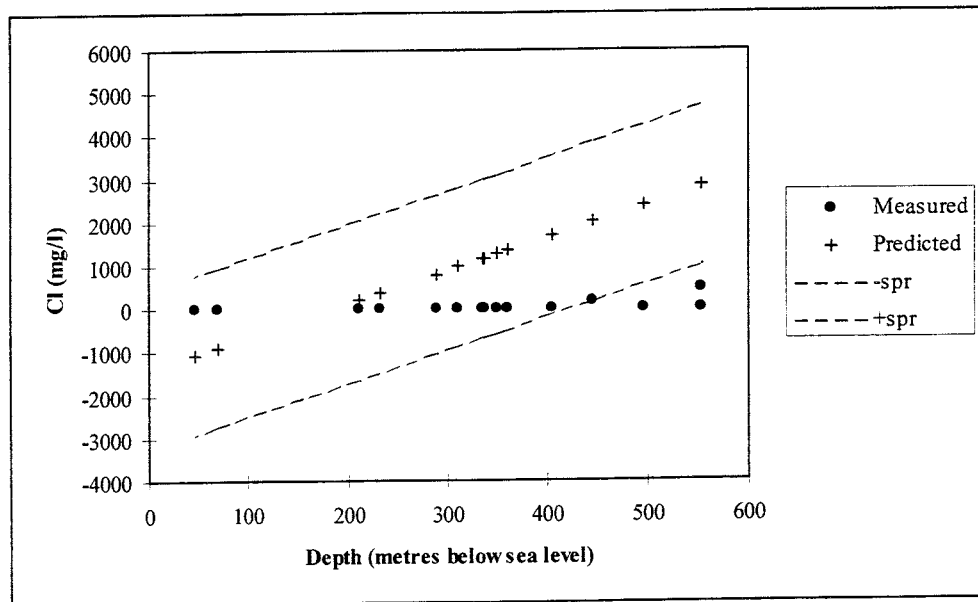


Figure 4-3. The measured (dots) and predicted (crosses) Cl content at the Fjällveden site in relation to the depth below sea level. The dotted lines show \pm the standard deviation of the prediction (s_{pr}).

The Forsmark site is located underneath the Baltic Sea. The prediction model does not recognise the Baltic Sea influence and the Cl predictions are low compared to the measured Cl content (*Figure 4-4*).

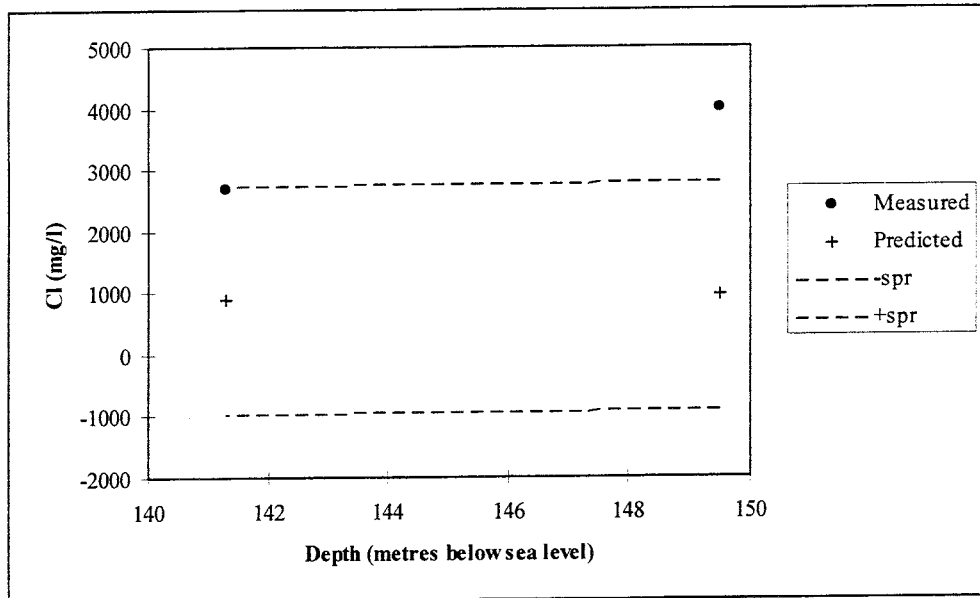


Figure 4-4. The measured (dots) and predicted (crosses) Cl content at the Forsmark site in relation to the depth below sea level. The dotted lines show \pm the standard deviation of the prediction (s_{pr}).

The Cl content at the Gideå site is low at depth. However, the predicted trend does not correspond to the measured one - thus the predictions at depth are high. No prediction is one standard deviation or more from the corresponding measurement (*Figure 4-5*).

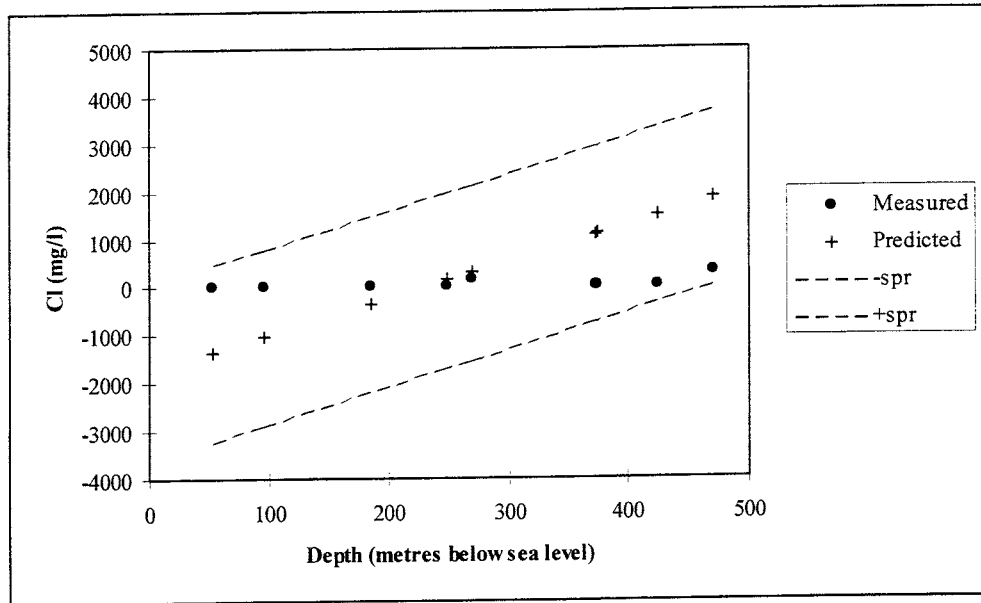


Figure 4-5. The measured (dots) and predicted (crosses) Cl content at the Gideå site in relation to the depth below sea level. The dotted lines show \pm the standard deviation of the prediction (s_{pr}).

The Cl content at the Kamlunge site is low at depth. However, the predicted trend does not correspond to the measured one - thus the deep predictions are high (Figure 4-6).

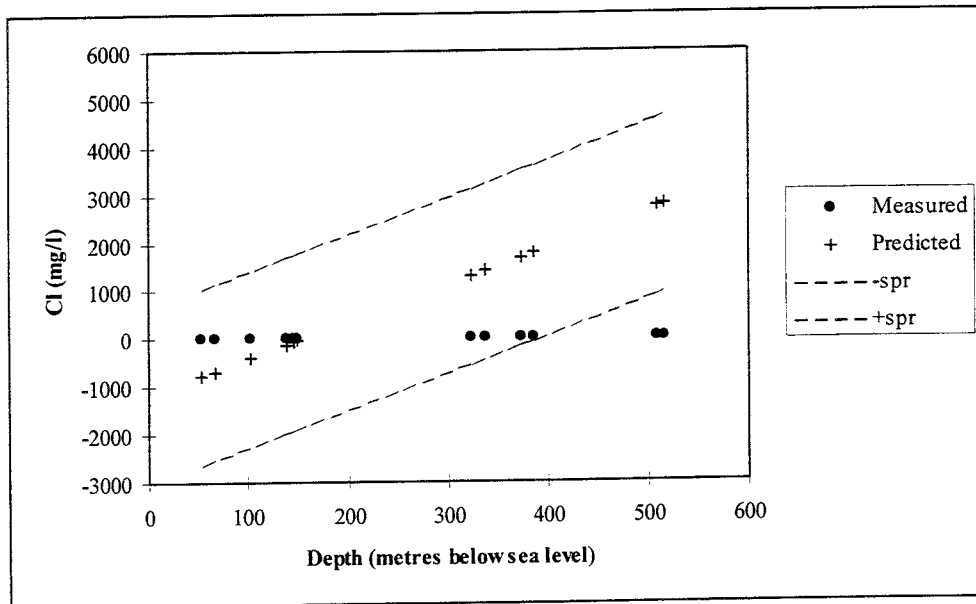


Figure 4-6. The measured (dots) and predicted (crosses) Cl content at the Kamlunge site in relation to the depth below sea level. The dotted lines show \pm the standard deviation of the prediction (s_{pr}).

The Cl content at the Karlshamn site is low at depth. However, the predicted trend does not correspond to the measured one - thus the predictions at depth are high. No prediction is one standard deviation or more from the corresponding measurement (*Figure 4-7*).

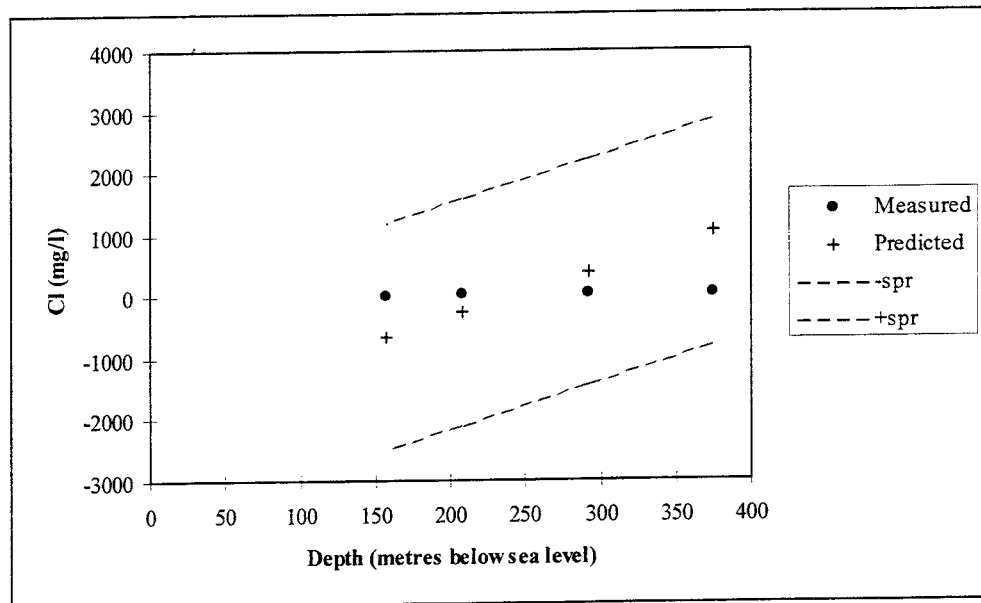


Figure 4-7. The measured (dots) and predicted (crosses) Cl content at the Karlshamn site in relation to the depth below sea level. The dotted lines show \pm the standard deviation of the prediction (s_{pr}).

The Cl content at the Klipperås site is low at depth. The predicted trend does not correspond to the measured one - thus the predictions at depth are high (*Figure 4-8*).

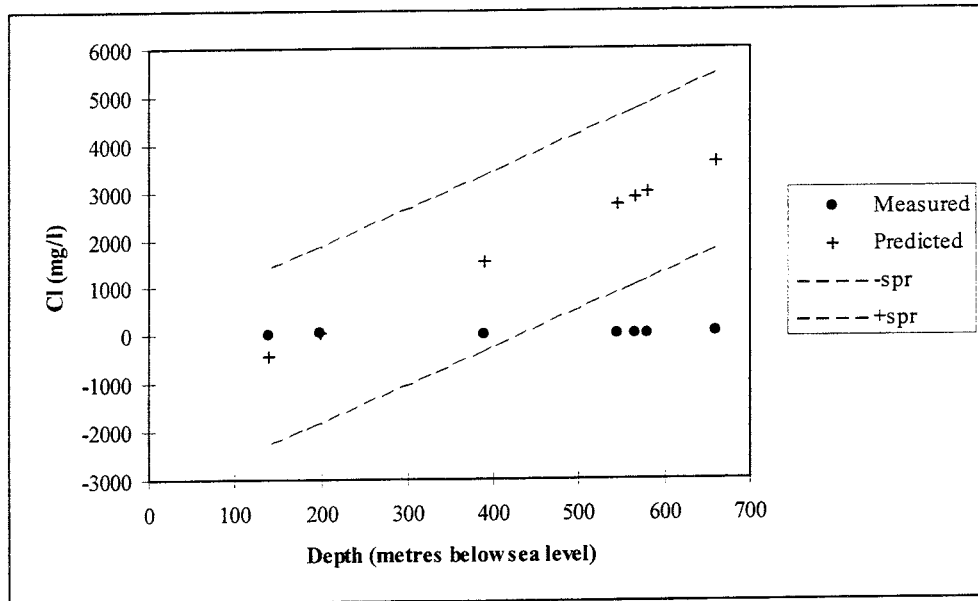


Figure 4-8. The measured (dots) and predicted (crosses) Cl content at the Klipperås site in relation to the depth below sea level. The dotted lines show \pm the standard deviation of the prediction (s_{pr}).

The Cl predictions for the Kråkemåla site are high (Figure 4-9).

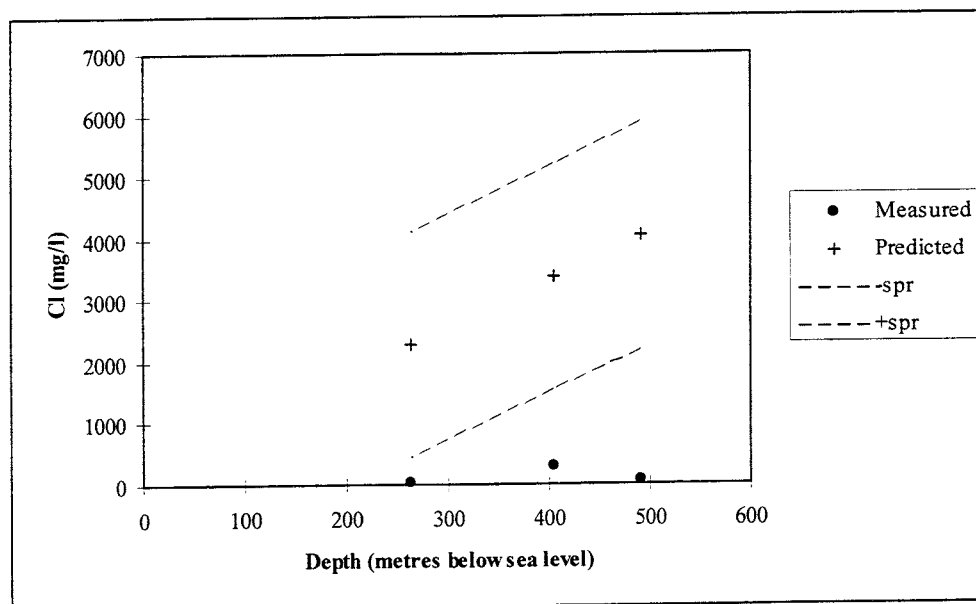


Figure 4-9. The measured (dots) and predicted (crosses) Cl content at the Kråkemåla site in relation to the depth below sea level. The dotted lines show \pm the standard deviation of the prediction (s_{pr}).

The Cl predictions for the Lansjärv site are negative and should by definition be set to zero and correspond to the Cl content measured at the site (Figure 4-10).

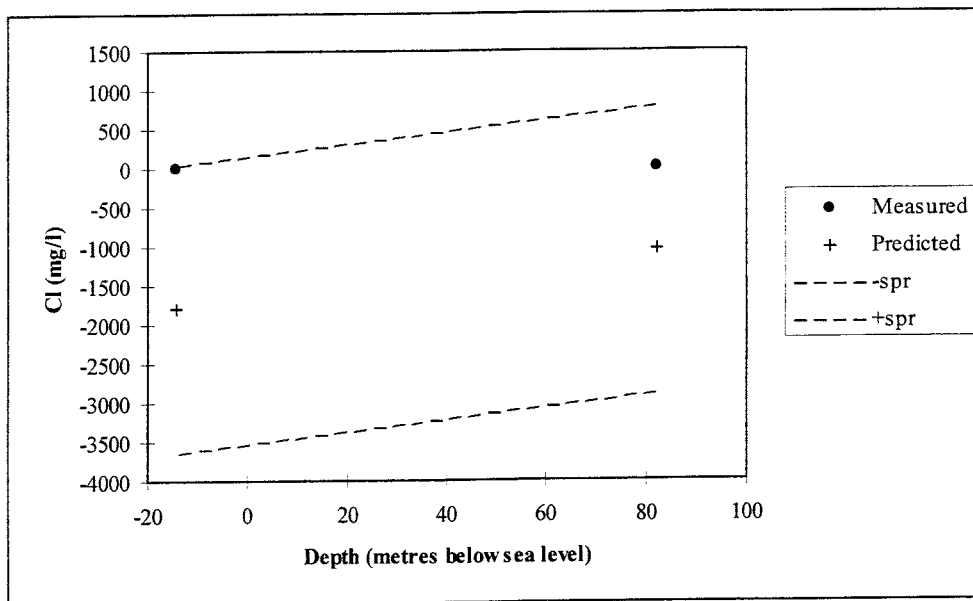


Figure 4-10. The measured (dots) and predicted (crosses) Cl content at the Lansjärv site in relation to the depth below sea level. The dotted lines show \pm the standard deviation of the prediction (s_{pr}).

The Cl content at the Stripa site is low at depth. The predicted trend does not correspond to the measured one - thus the predictions at depth are high (Figure 4-11).

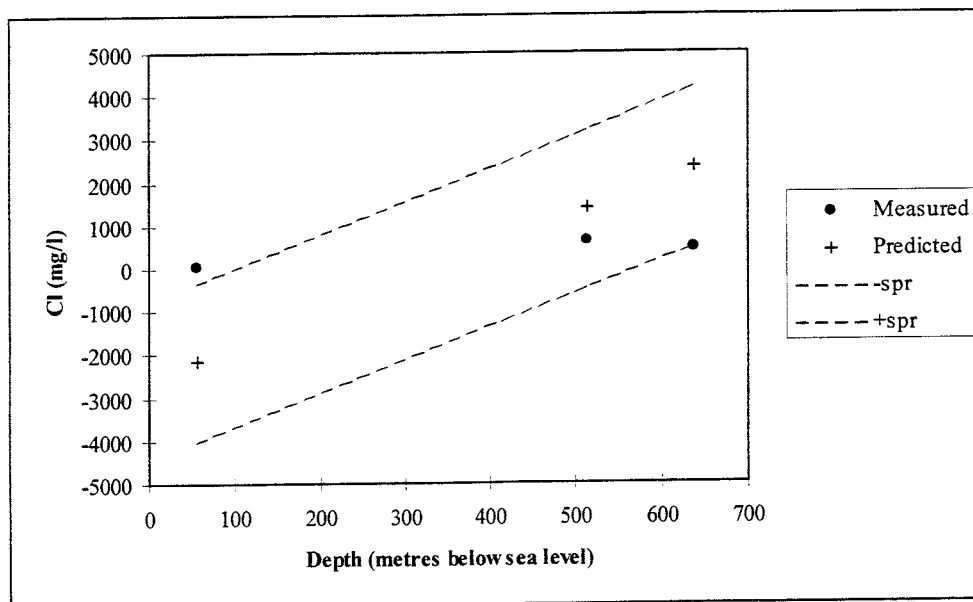


Figure 4-11. The measured (dots) and predicted (crosses) Cl content at the Stripa site in relation to the depth below sea level. The dotted lines show \pm the standard deviation of the prediction (s_{pr}).

The Cl content at the Svartboberget site is low at depth. The predicted trend does not correspond to the measured one - thus the predictions at depth are high (Figure 4-12).

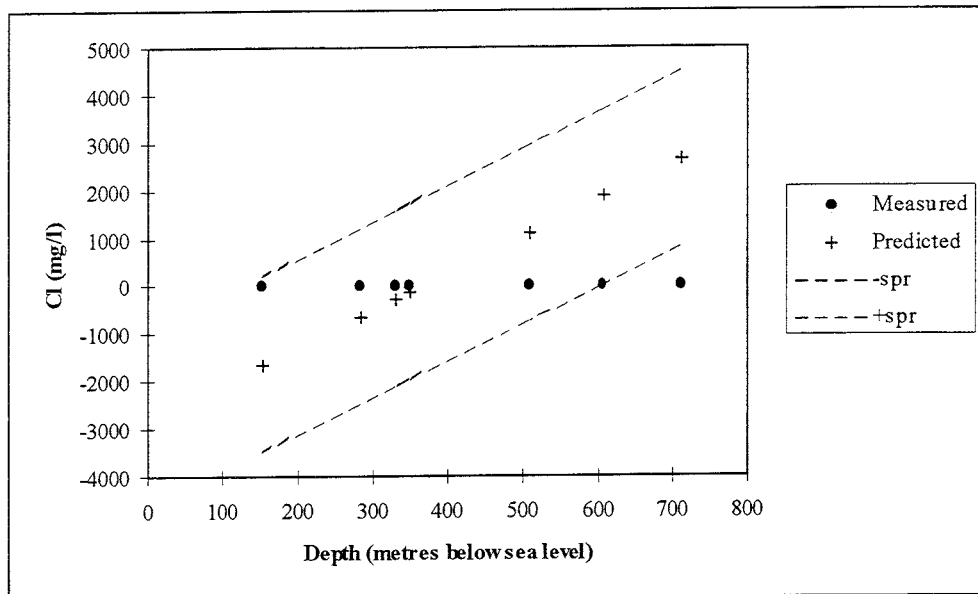


Figure 4-12. The measured (dots) and predicted (crosses) Cl content at the Svartboberget site in relation to the depth below sea level. The dotted lines show \pm the standard deviation of the prediction (s_{pr}).

The Cl predictions for the Taavinunnen site are negative and should by definition be set to zero and correspond to the Cl content measured at the site (Figure 4-13).

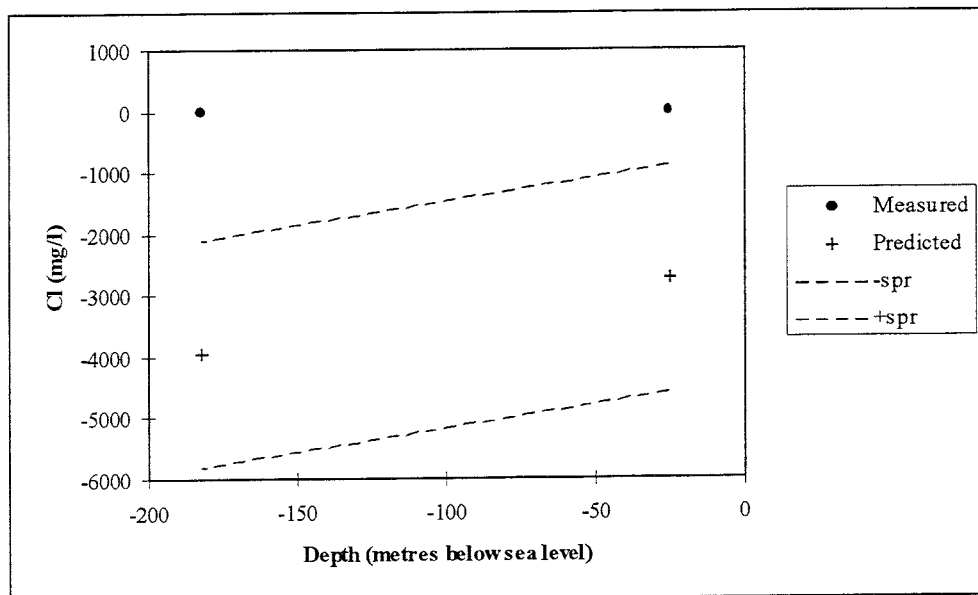


Figure 4-13. The measured (dots) and predicted (crosses) Cl content at the Taavinunnen site in relation to the depth below sea level. The dotted lines show \pm the standard deviation of the prediction (s_{pr}).

The Cl predictions at the Zinkgruvan site are low and the increase with depth is smaller than the two measured observations indicate (Figure 4-14).

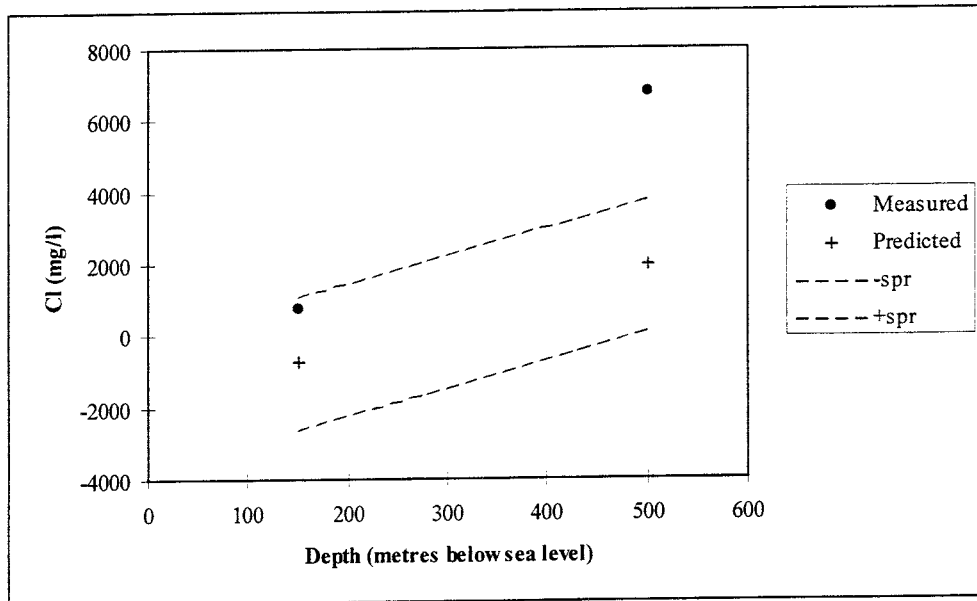


Figure 4-14. The measured (dots) and predicted (crosses) Cl content at the Zinkgruvan site in relation to the depth below sea level. The dotted lines show \pm the standard deviation of the prediction (s_{pr}).

The HCO_3 predictions at the Äspö site describe the measured HCO_3 content below 150m well. The predictions are low at a shallower depth (Figure 4-15).

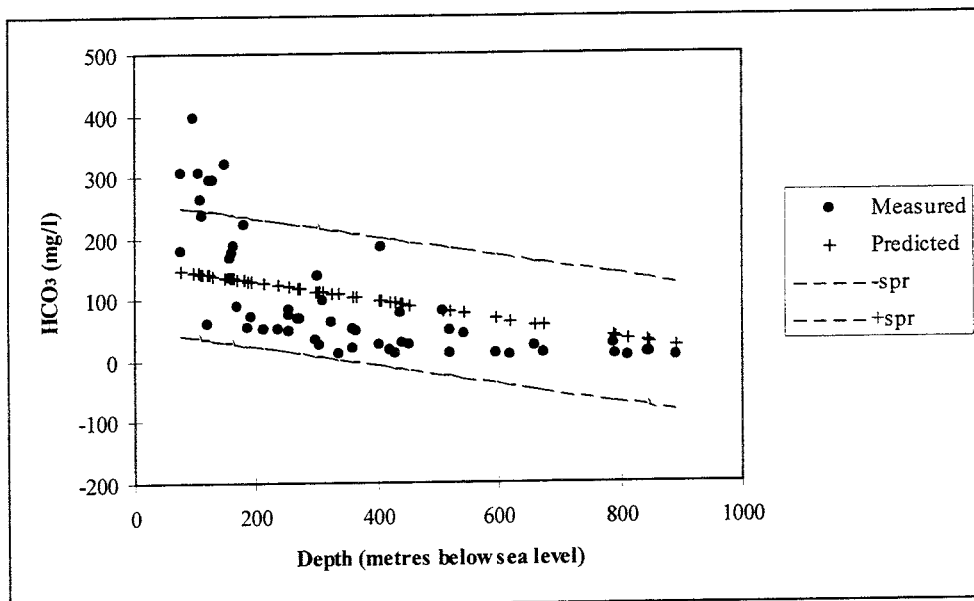


Figure 4-15. The measured (dots) and predicted (crosses) HCO_3 content at the Äspö site in relation to the depth below sea level. The dotted lines show \pm the standard deviation of the prediction (s_{pr}).

The trend of the Ca predictions at the Äspö site is not steep enough to correspond to the measurements. The predictions are generally low (Figure 4-16).

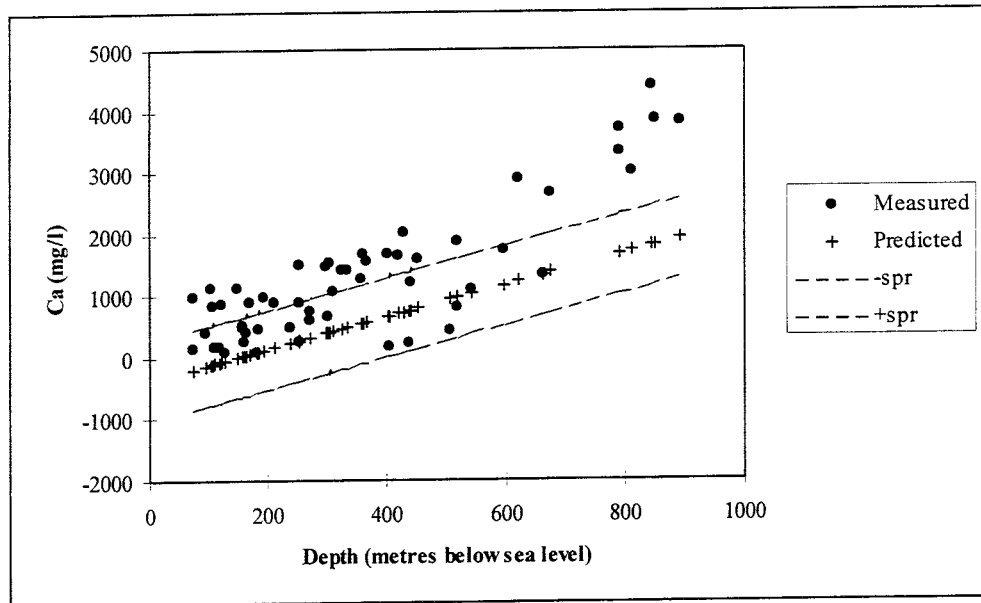


Figure 4-16. The measured (dots) and predicted (crosses) Ca content at the Äspö site in relation to the depth below sea level. The dotted lines show \pm the standard deviation of the prediction (s_{pr}).

The trend of the SO_4 predictions at the Äspö site is not steep enough to correspond to the measurements. The predictions are generally low (Figure 4-17).

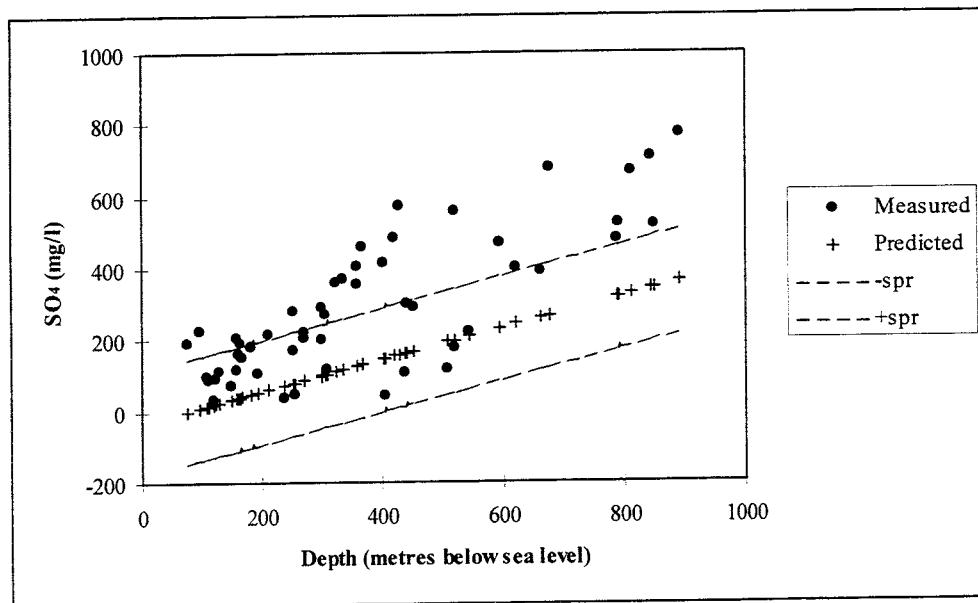


Figure 4-17. The measured (dots) and predicted (crosses) SO_4 content at the Äspö site in relation to the depth below sea level. The dotted lines show \pm the standard deviation of the prediction (s_{pr}).

The K at the Äspö site is well predicted. However, the high measured values in the shallow part are not recognised by the prediction model (Figure 4-18).

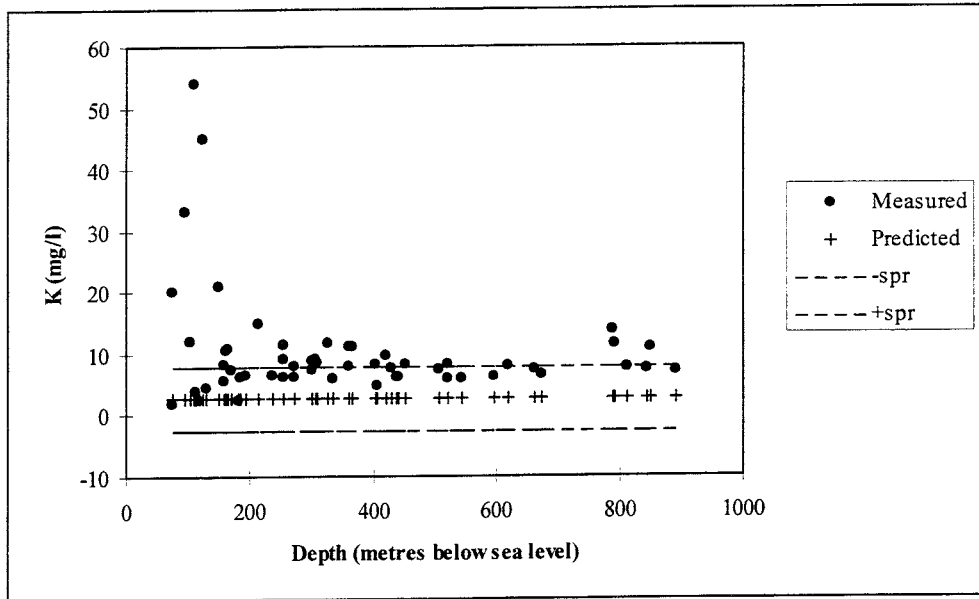


Figure 4-18. The measured (dots) and predicted (crosses) K content at the Äspö site in relation to the depth below sea level. The dotted lines show \pm the standard deviation of the prediction (s_{pr}).

The measured S at the Äspö site varies without any obvious trend. The predictions are good in most cases (Figure 4-19).

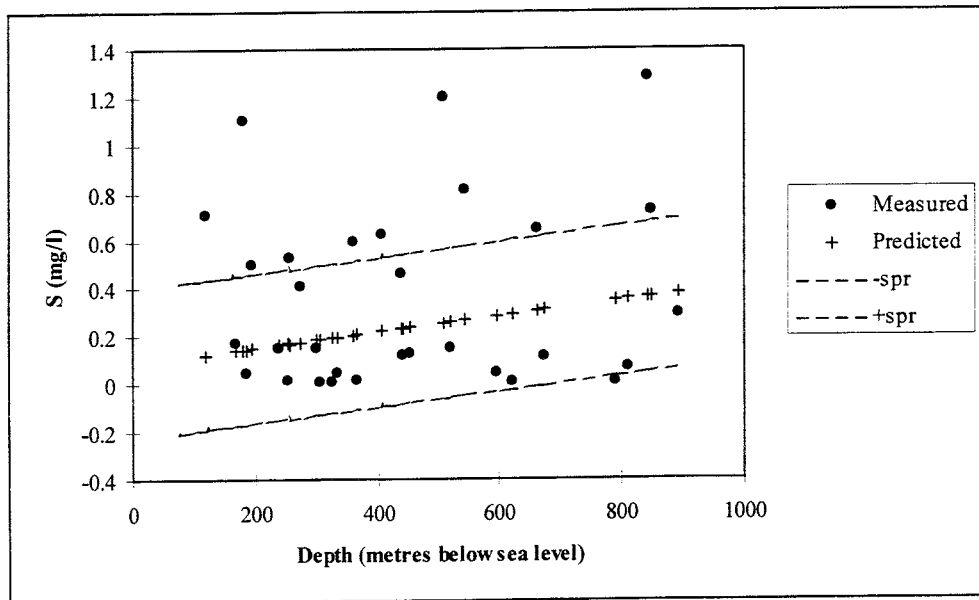


Figure 4-19. The measured (dots) and predicted (crosses) S content at the Äspö site in relation to the depth below sea level. The dotted lines show \pm the standard deviation of the prediction (s_{pr}).

Fe is well predicted at the Äspö site. No prediction is one standard deviation or more from the corresponding measurement (Figure 4-20).

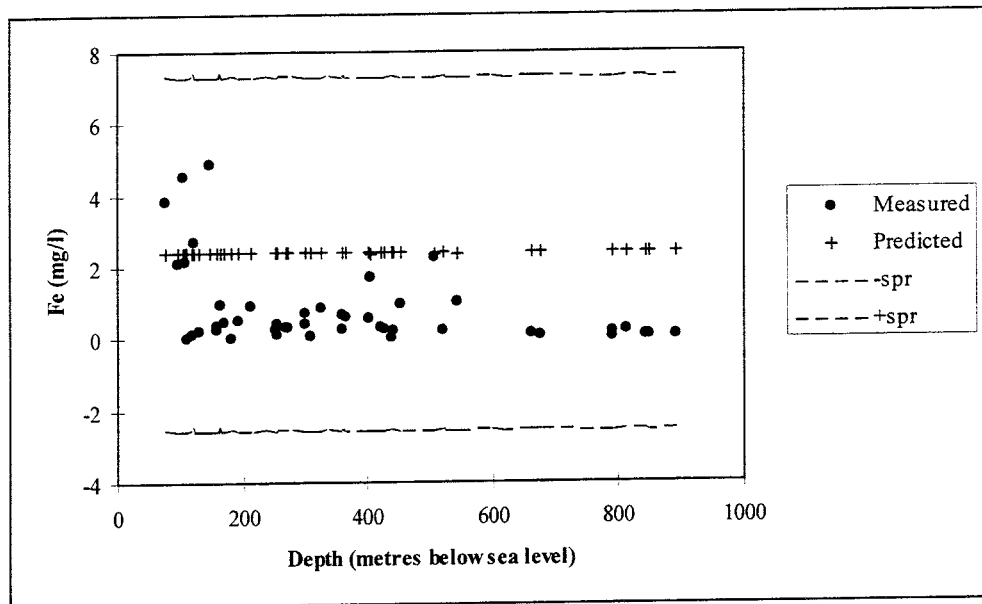


Figure 4-20. The measured (dots) and predicted (crosses) Fe content at the Äspö site in relation to the depth below sea level. The dotted lines show \pm the standard deviation of the prediction (s_{pr}).

TOC prediction is slightly high at the Äspö site. No prediction is one standard deviation or more from the corresponding measurement (Figure 4-21).

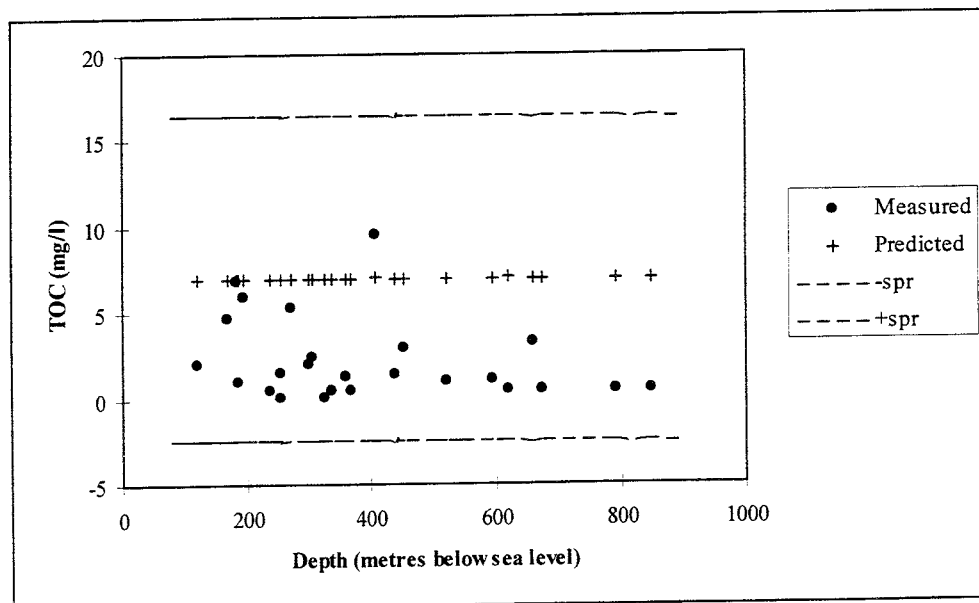


Figure 4-21. The measured (dots) and predicted (crosses) TOC content at the Äspö site in relation to the depth below sea level. The dotted lines show \pm the standard deviation of the prediction (s_{pr}).

pH prediction is slightly low at the Äspö site. No prediction is one standard deviation or more from the corresponding measurement (Figure 4-22).

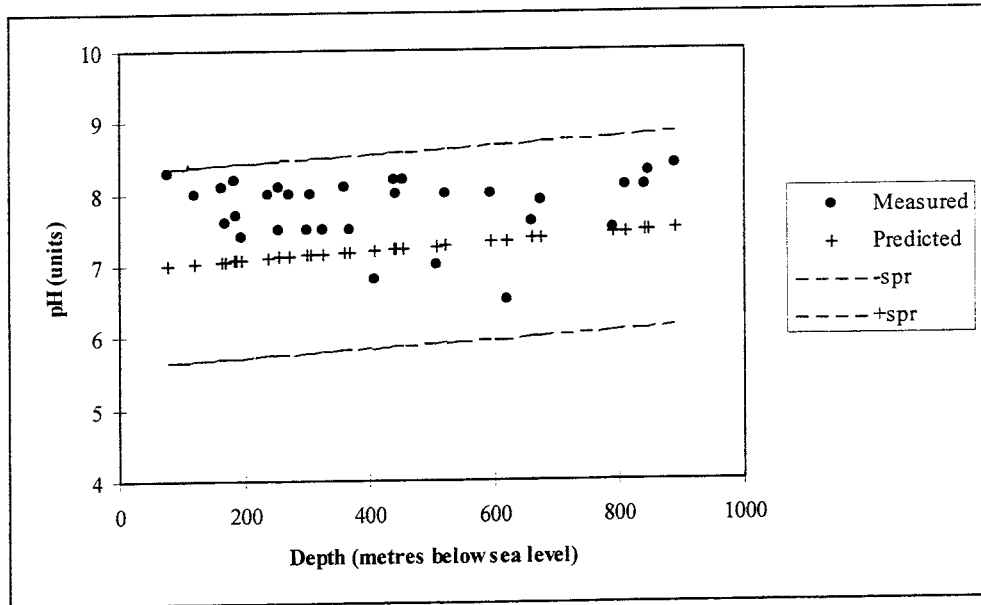


Figure 4-22. The measured (dots) and predicted (crosses) pH content at the Äspö site in relation to the depth below sea level. The dotted lines show \pm the standard deviation of the prediction (s_{pr}).

The results of the predictions for the elements and sites not shown in Figures 4-1 - 4-22 are found in Appendix 1. Only predictions with corresponding measurements are shown.

5. DISCUSSION

One of the questions initiating this work was: Is it possible to make groundwater predictions on a large scale throughout Sweden? The results show that it is possible but more work needs to be done to improve the prediction models. More measurements at depth are needed to enable the use of 3D models. It is also important to include hydrogeological parameters in the prediction models that are used.

ACKNOWLEDGEMENTS

The authors would like to thank Peter Wikberg (SKB) for helpful discussions. This work was financed by SKB.

REFERENCES

- Fortner B, 1992.** The Data Handbook. Spyglass Inc, Champaign, Illinois, USA.
- Henley S, 1981.** Nonparametric geostatistics. Elsevier Applied Science Publishers Ltd, Essex, England.
- Kleinbaum D G, Kupper L L, Muller K E, 1988.** Applied regression analysis and other multivariable methods. PWS-KENT Publishing Company, Boston, USA.
- STATGRAPHICS PLUS for Windows, 1994. Statistical graphics system by Manugistics Inc, Rockville, Maryland, USA.
- STATISTICA for Windows, 1995. Complete Statistical system by StatSoft Inc, Tulsa, Oklahoma, USA.
- SURFER for Windows, 1994. Contouring and 3D Surface Mapping by Golden Software Inc, Golden, Colorado, USA.
- Wikberg P, Skårman C, Laaksoharju M, Ittner T, 1994a.** Groundwater chemistry and transport of solutes. Evaluation of the data from tunnel section 1475-2265m. SKB Progress Report PR 25-93-12, Stockholm, Sweden.
- Wikberg P, Skårman C, Laaksoharju M, 1994b.** Groundwater chemistry and transport of solutes. Evaluation of the data from tunnel section 2265-2874m. SKB Progress Report PR 25-94-21, Stockholm, Sweden.

APPENDIX A: FINNSJÖN

The results of the predictions are compared with measured data and shown in relation to depth. The prediction error for the multiple linear regression is also shown. The error shown is the smallest assumable error. The true overall prediction error is larger. A general prediction error includes measurement error, analysis error, misfit to the applied distribution, kriging error etc. The error interval is not a confidence interval. Negative predictions would by definition be set at zero. Only predictions with corresponding measurements are shown.

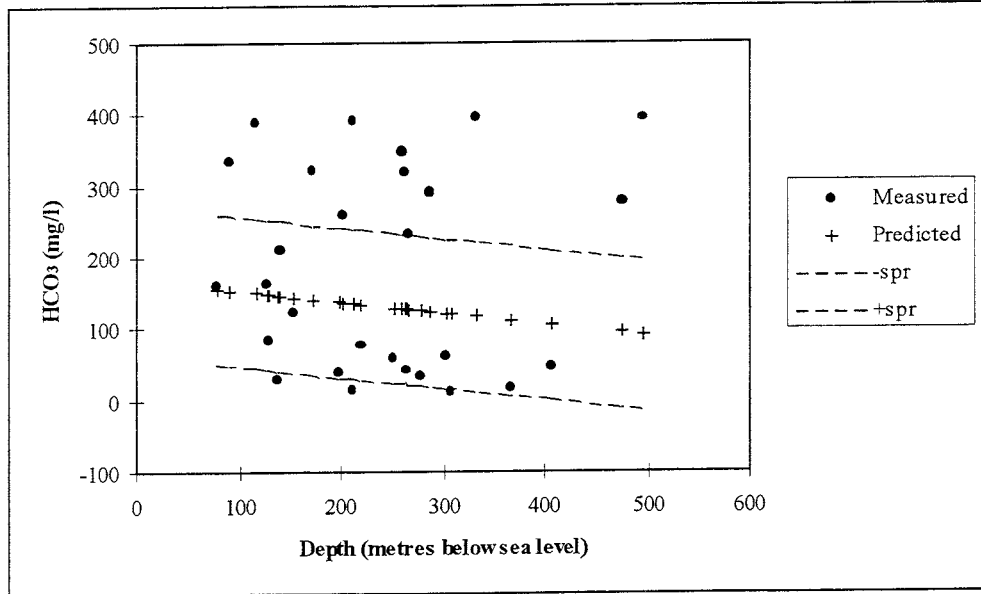


Figure A-1. The measured (dots) and predicted (crosses) HCO_3^- content at the Finnsjön site in relation to the depth below sea level. The dotted lines show \pm the standard deviation of the prediction (s_{pr}).

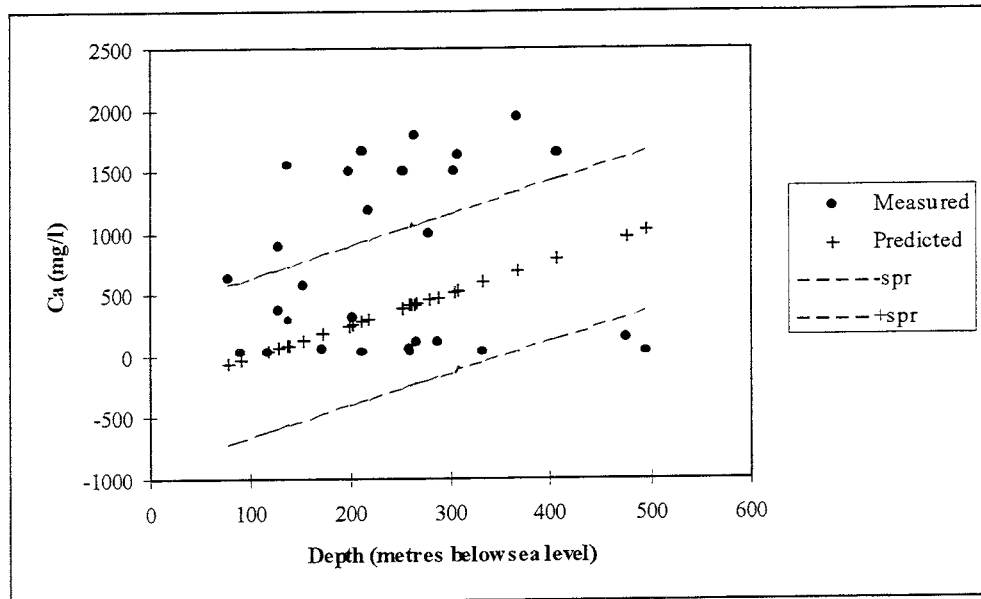


Figure A-2. The measured (dots) and predicted (crosses) Ca content at the Finnsjön site in relation to the depth below sea level. The dotted lines show \pm the standard deviation of the prediction (s_{pr}).

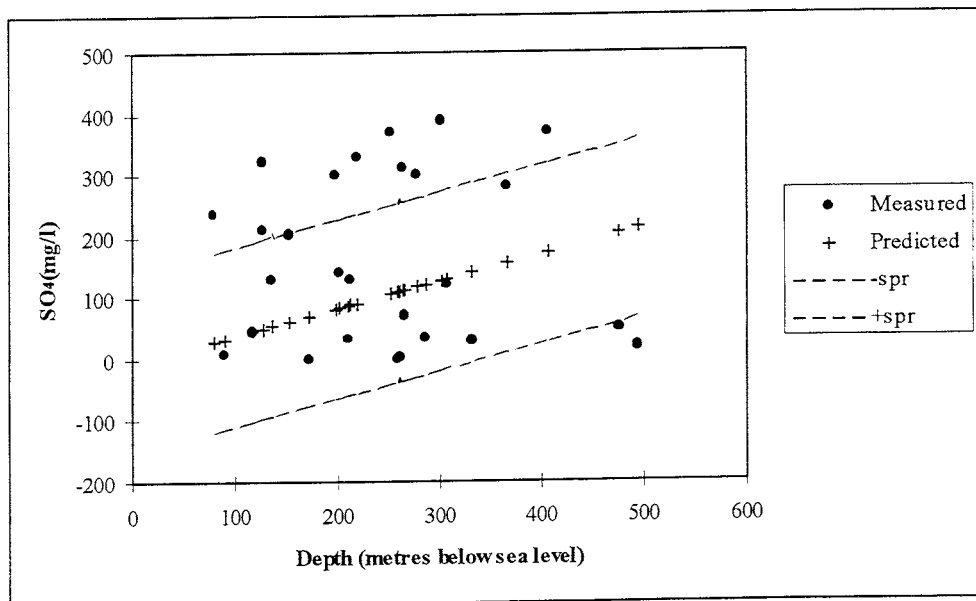


Figure A-3. The measured (dots) and predicted (crosses) SO_4 content at the Finnsjön site in relation to the depth below sea level. The dotted lines show \pm the standard deviation of the prediction (s_{pr}).

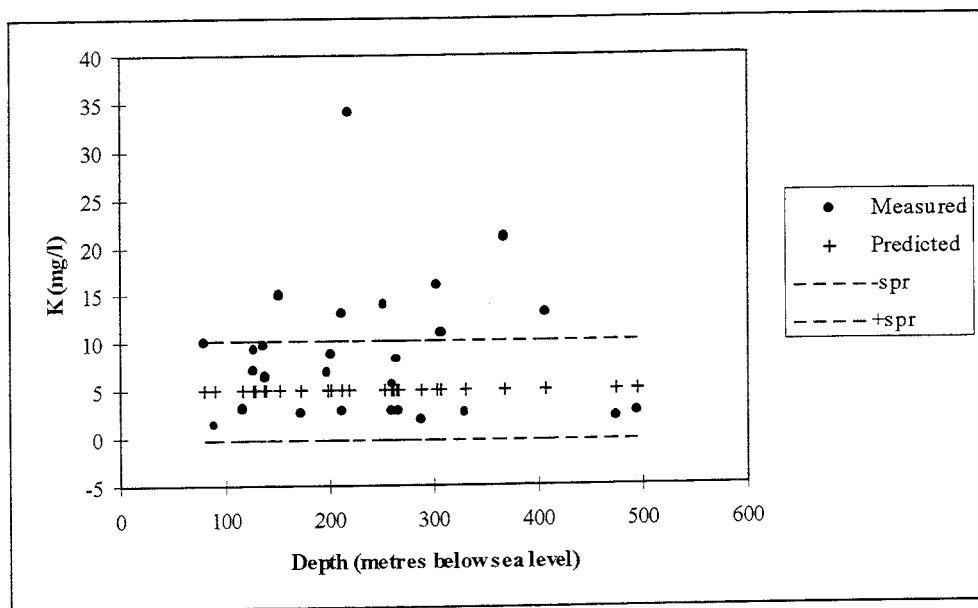


Figure A-4. The measured (dots) and predicted (crosses) K content at the Finnsjön site in relation to the depth below sea level. The dotted lines show \pm the standard deviation of the prediction (s_{pr}).

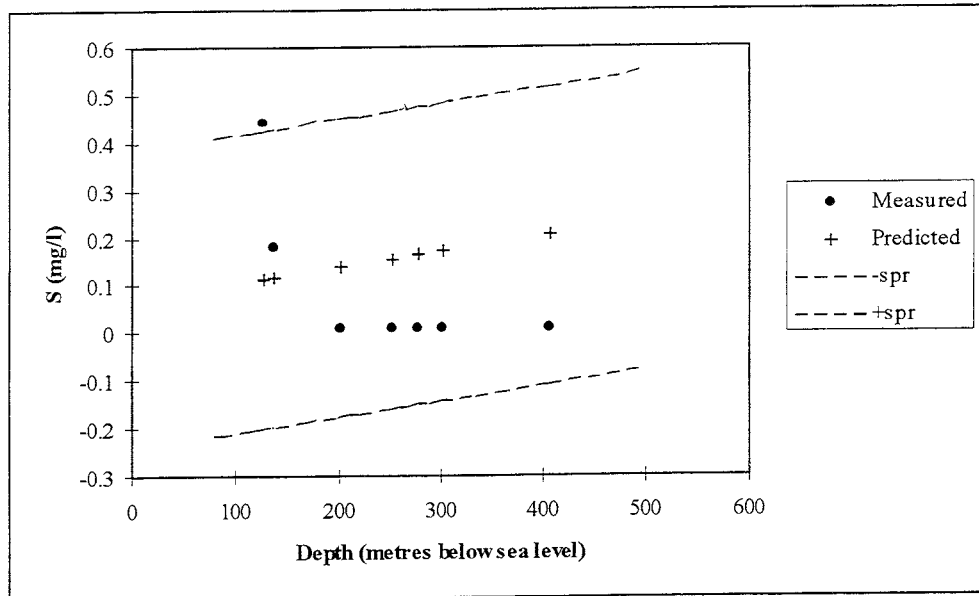


Figure A-5. The measured (dots) and predicted (crosses) S content at the Finnsjön site in relation to the depth below sea level. The dotted lines show \pm the standard deviation of the prediction (s_{pr}).

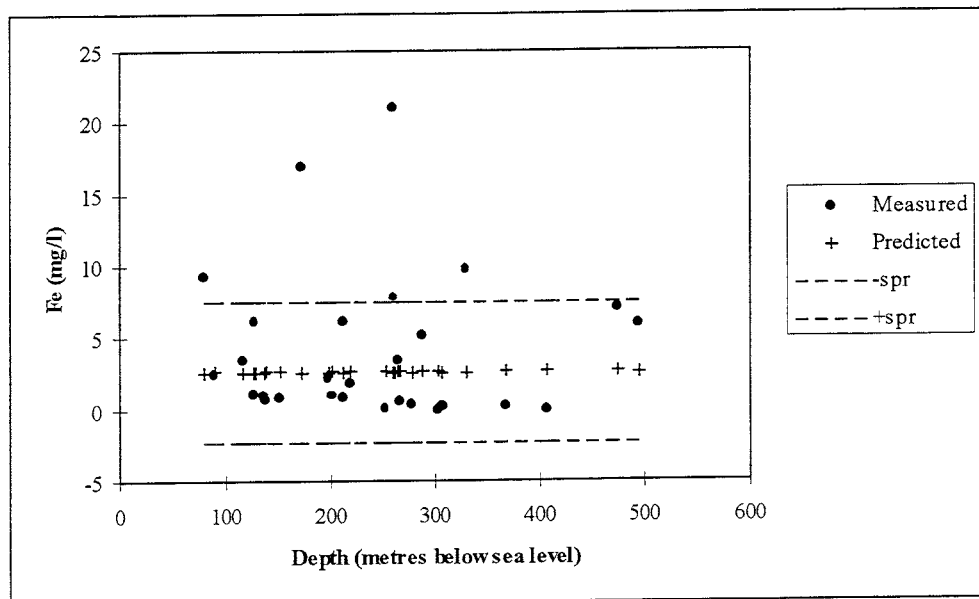


Figure A-6. The measured (dots) and predicted (crosses) Fe content at the Finnsjön site in relation to the depth below sea level. The dotted lines show \pm the standard deviation of the prediction (s_{pr}).

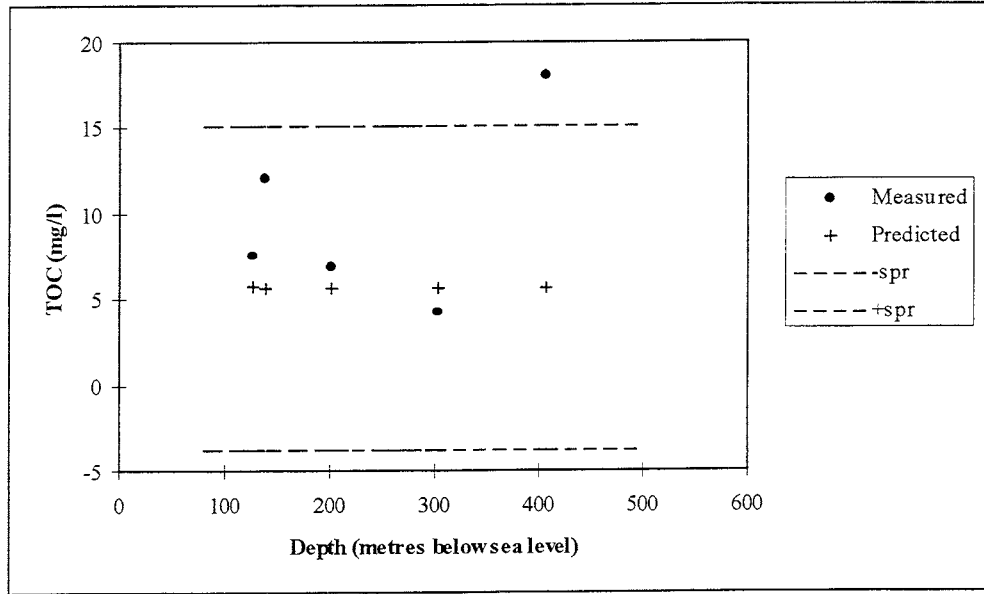


Figure A-7. The measured (dots) and predicted (crosses) TOC content at the Finnsjön site in relation to the depth below sea level. The dotted lines show \pm the standard deviation of the prediction (s_{pr}).

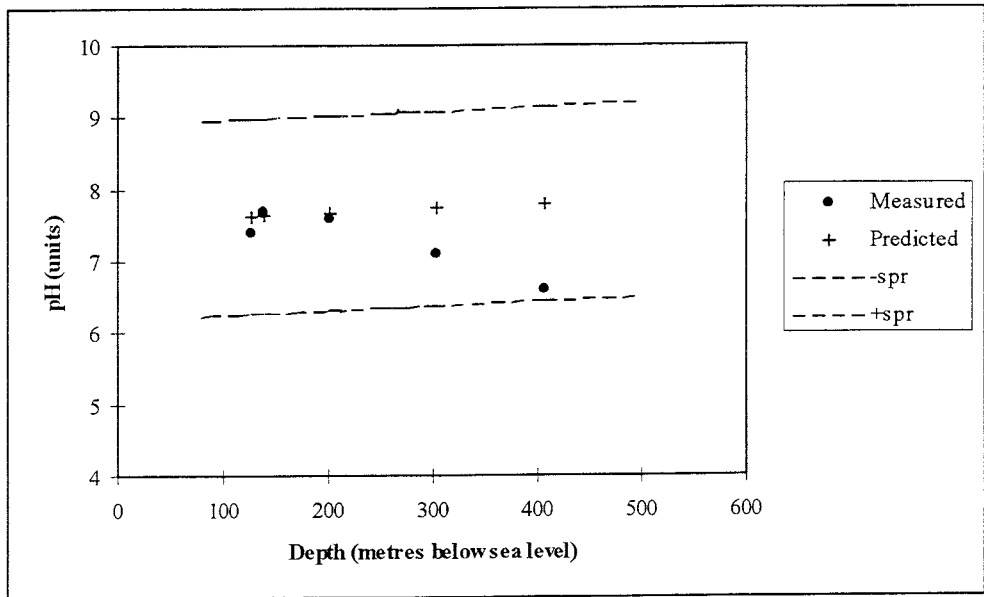


Figure A-8. The measured (dots) and predicted (crosses) pH content at the Finnsjön site in relation to the depth below sea level. The dotted lines show \pm the standard deviation of the prediction (s_{pr}).

APPENDIX B: FJÄLLVEDEN

The results of the predictions are compared with measured data and shown in relation to depth. The prediction error for the multiple linear regression is also shown. The error shown is the smallest assumable error. The true overall prediction error is larger. A general prediction error includes measurement error, analysis error, misfit to the applied distribution, kriging error etc. The error interval is not a confidence interval. Negative predictions would by definition be set at zero. Only predictions with corresponding measurements are shown.

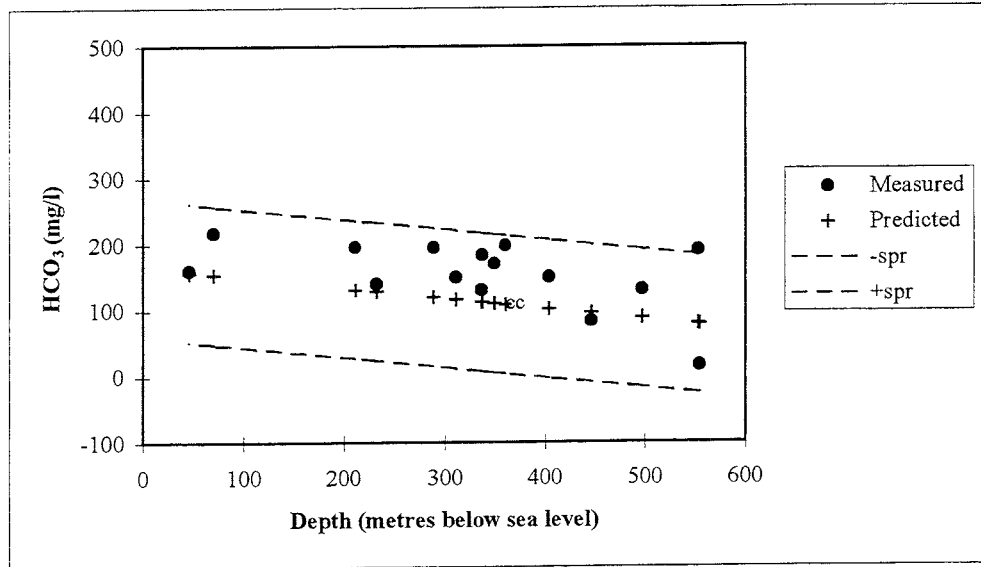


Figure B-1. The measured (dots) and predicted (crosses) HCO_3^- content at the Fjällveden site in relation to the depth below sea level. The dotted lines show \pm the standard deviation of the prediction (s_{pr}).

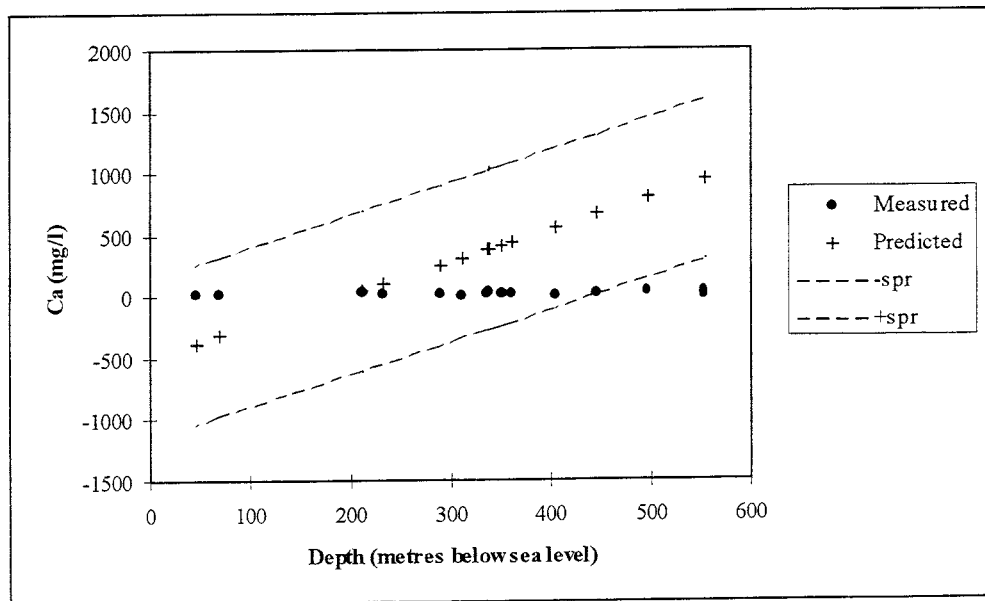


Figure B-2. The measured (dots) and predicted (crosses) Ca content at the Fjällveden site in relation to the depth below sea level. The dotted lines show \pm the standard deviation of the prediction (s_{pr}).

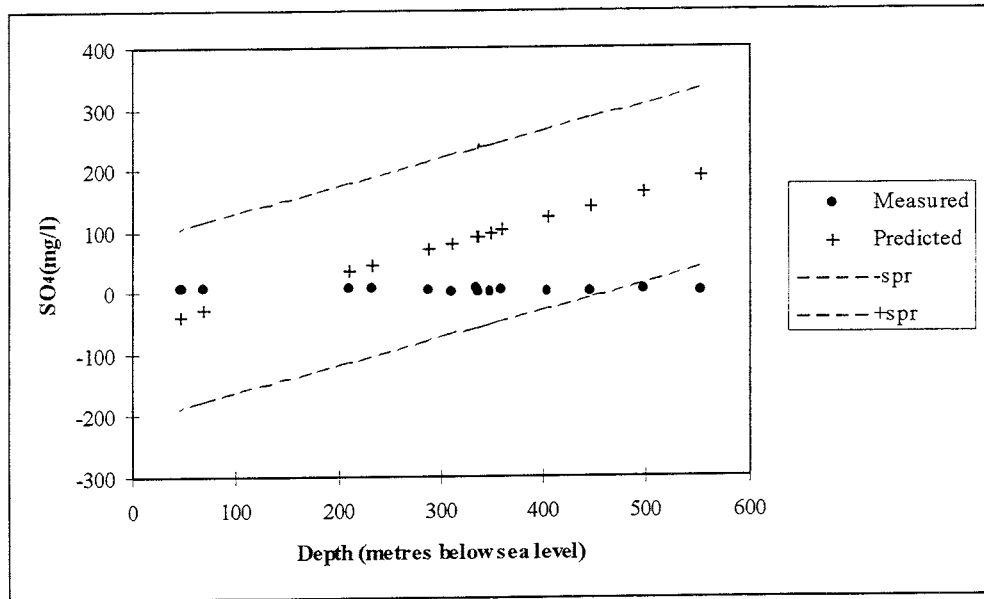


Figure B-3. The measured (dots) and predicted (crosses) SO_4 content at the Fjällveden site in relation to the depth below sea level. The dotted lines show \pm the standard deviation of the prediction (s_{pr}).

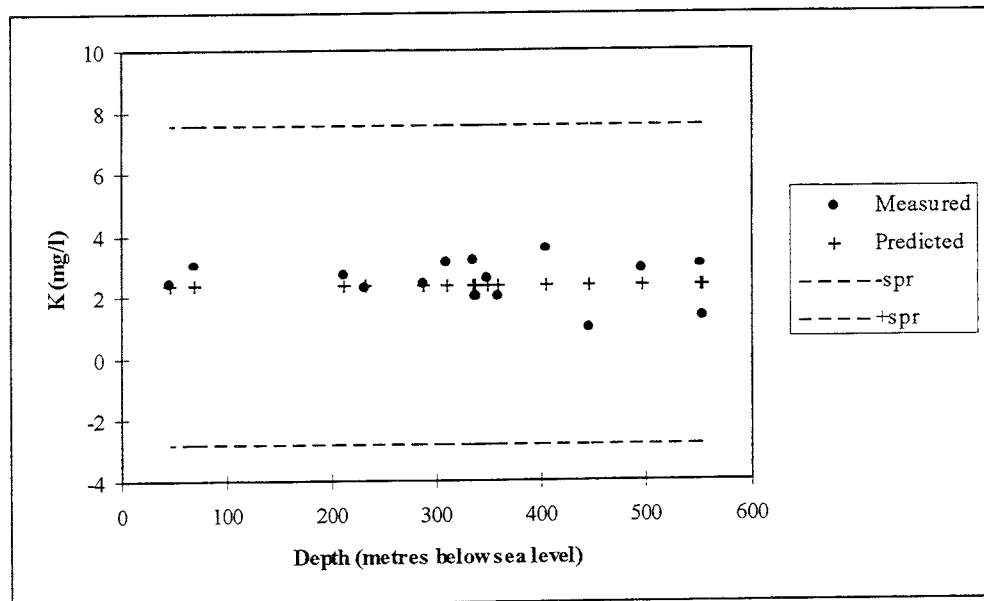


Figure B-4. The measured (dots) and predicted (crosses) K content at the Fjällveden site in relation to the depth below sea level. The dotted lines show \pm the standard deviation of the prediction (s_{pr}).

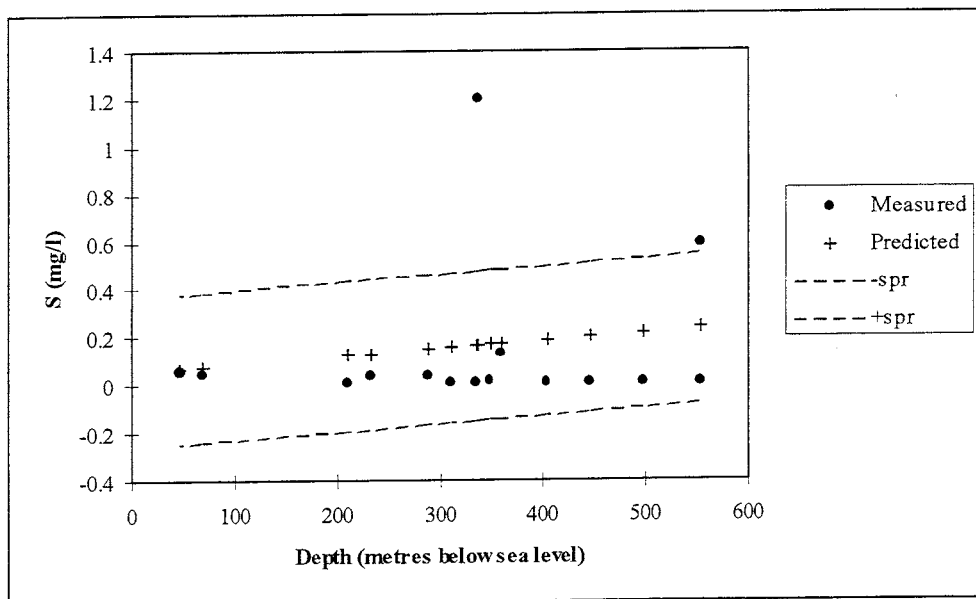


Figure B-5. The measured (dots) and predicted (crosses) S content at the Fjällveden site in relation to the depth below sea level. The dotted lines show \pm the standard deviation of the prediction (s_{pr}).

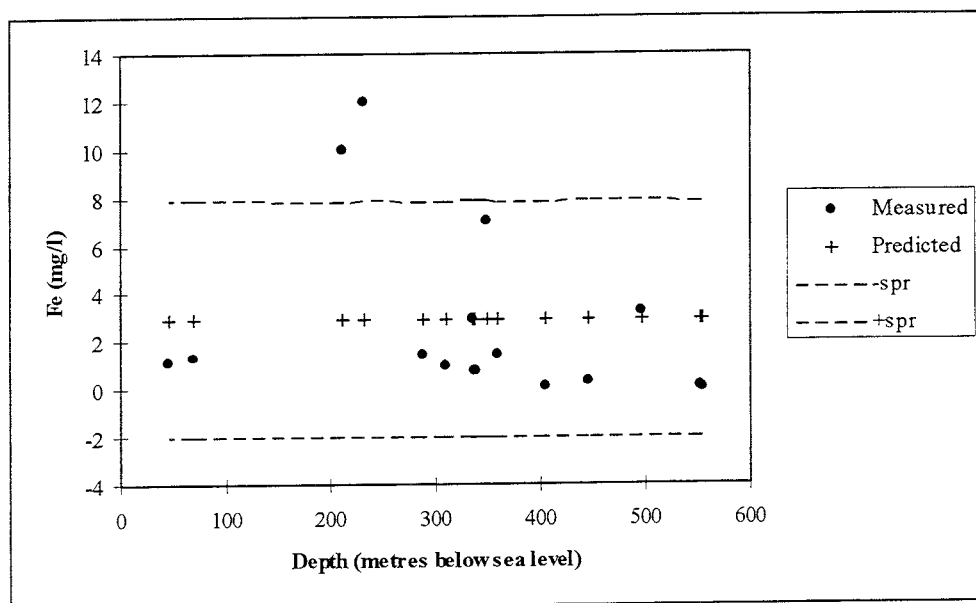


Figure B-6. The measured (dots) and predicted (crosses) Fe content at the Fjällveden site in relation to the depth below sea level. The dotted lines show \pm the standard deviation of the prediction (s_{pr}).

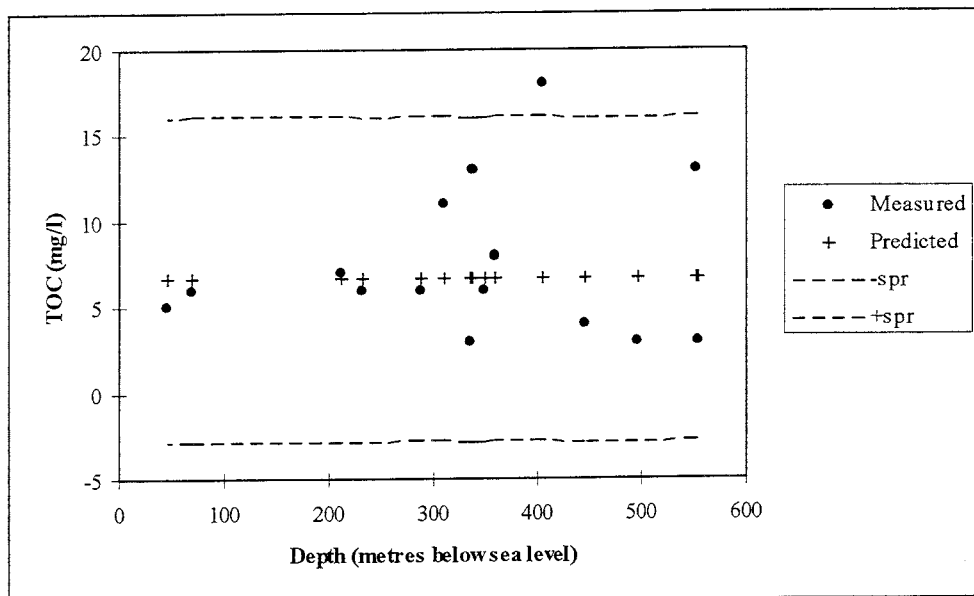


Figure B-7. The measured (dots) and predicted (crosses) TOC content at the Fjällveden site in relation to the depth below sea level. The dotted lines show \pm the standard deviation of the prediction (s_{pr}).

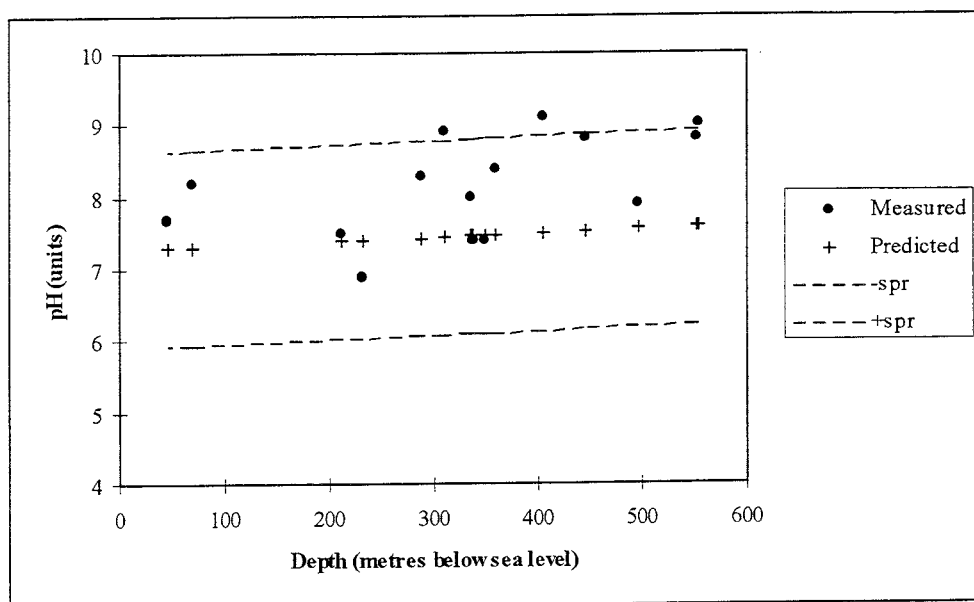


Figure B-8. The measured (dots) and predicted (crosses) pH content at the Fjällveden site in relation to the depth below sea level. The dotted lines show \pm the standard deviation of the prediction (s_{pr}).

APPENDIX C: FORSMARK

The results of the predictions are compared with measured data and shown in relation to depth. The prediction error for the multiple linear regression is also shown. The error shown is the smallest assumable error. The true overall prediction error is larger. A general prediction error includes measurement error, analysis error, misfit to the applied distribution, kriging error etc. The error interval is not a confidence interval. Negative predictions would by definition be set at zero. Only predictions with corresponding measurements are shown.

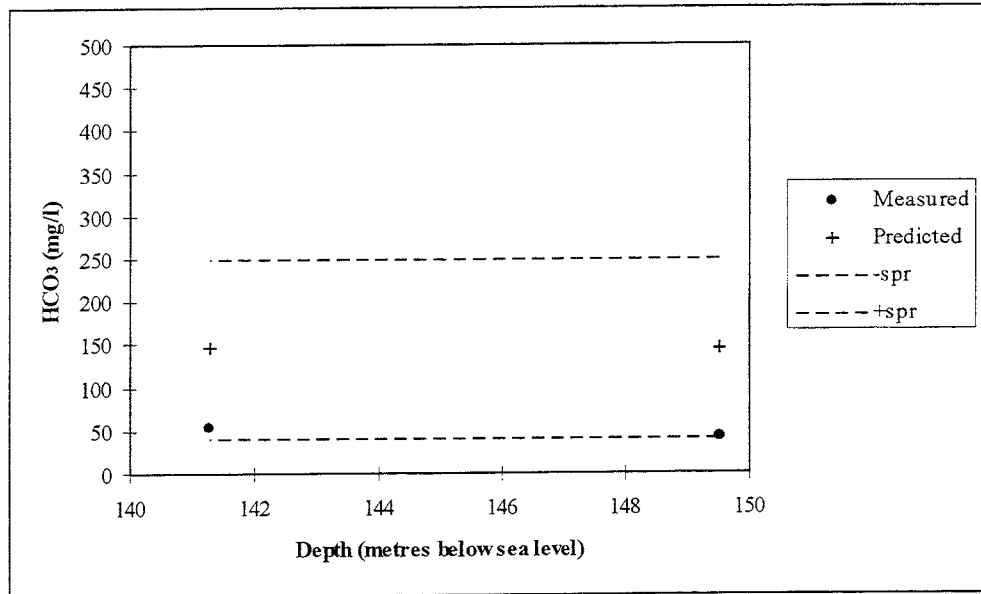


Figure C-1. The measured (dots) and predicted (crosses) HCO_3^- content at the Forsmark site in relation to the depth below sea level. The dotted lines show \pm the standard deviation of the prediction (s_{pr}).

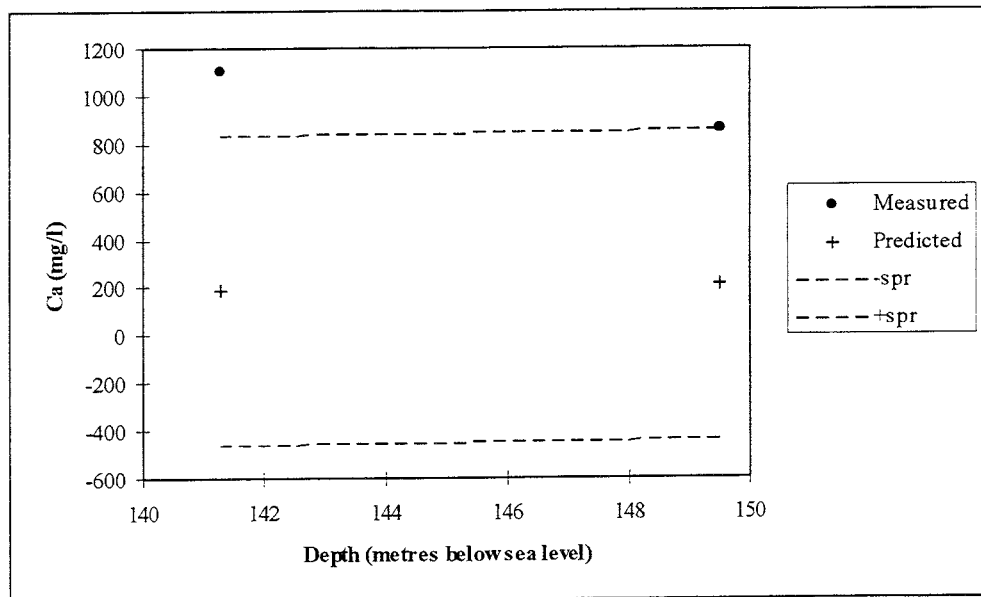


Figure C-2. The measured (dots) and predicted (crosses) Ca content at the Forsmark site in relation to the depth below sea level. The dotted lines show \pm the standard deviation of the prediction (s_{pr}).

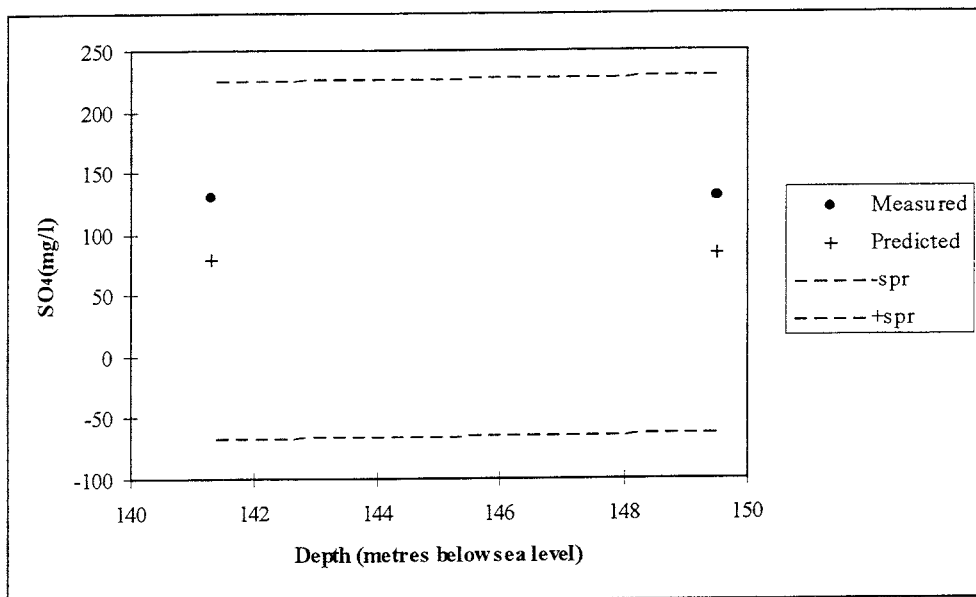


Figure C-3. The measured (dots) and predicted (crosses) SO_4 content at the Forsmark site in relation to the depth below sea level. The dotted lines show \pm the standard deviation of the prediction (s_{pr}).

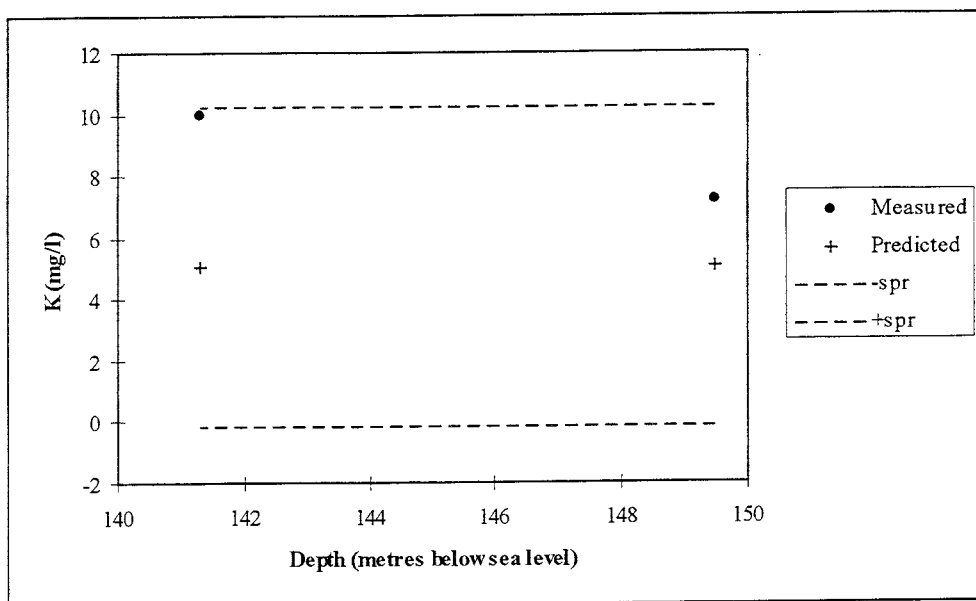


Figure C-4. The measured (dots) and predicted (crosses) K content at the Forsmark site in relation to the depth below sea level. The dotted lines show \pm the standard deviation of the prediction (s_{pr}).

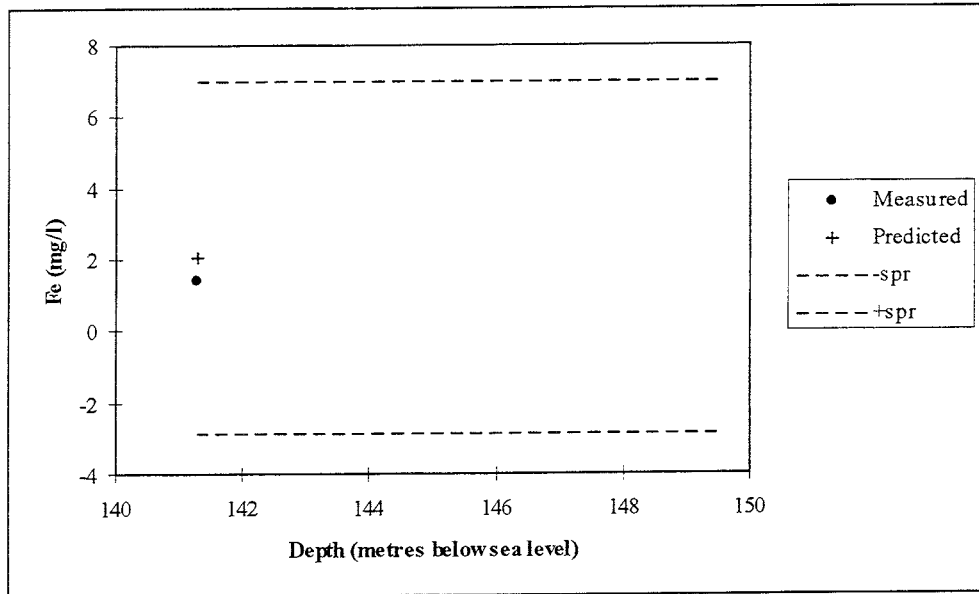


Figure C-5. The measured (dots) and predicted (crosses) Fe content at the Forsmark site in relation to the depth below sea level. The dotted lines show \pm the standard deviation of the prediction (s_{pr}).

APPENDIX D: GIDEÅ

The results of the predictions are compared with measured data and shown in relation to depth. The prediction error for the multiple linear regression is also shown. The error shown is the smallest assumable error. The true overall prediction error is larger. A general prediction error includes measurement error, analysis error, misfit to the applied distribution, kriging error etc. The error interval is not a confidence interval. Negative predictions would by definition be set at zero. Only predictions with corresponding measurements are shown.

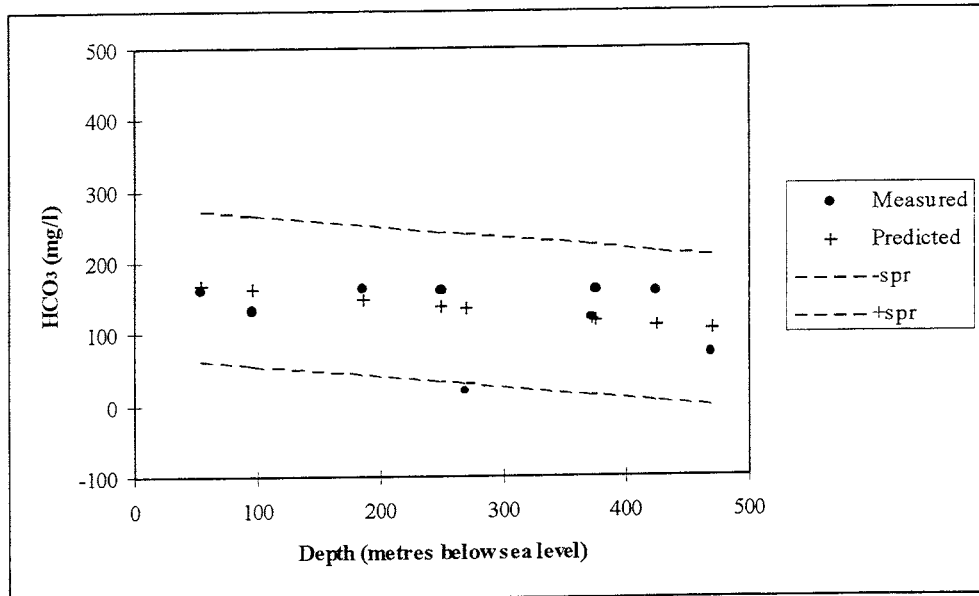


Figure D-1. The measured (dots) and predicted (crosses) HCO_3^- content at the Gideå site in relation to the depth below sea level. The dotted lines show \pm the standard deviation of the prediction (s_{pr}).

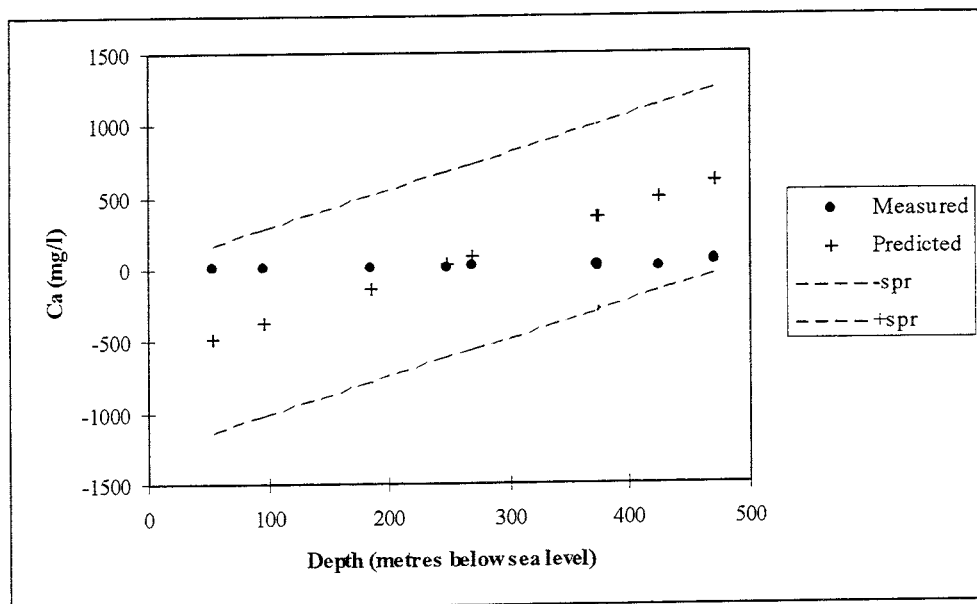


Figure D-2. The measured (dots) and predicted (crosses) Ca content at the Gideå site in relation to the depth below sea level. The dotted lines show \pm the standard deviation of the prediction (s_{pr}).

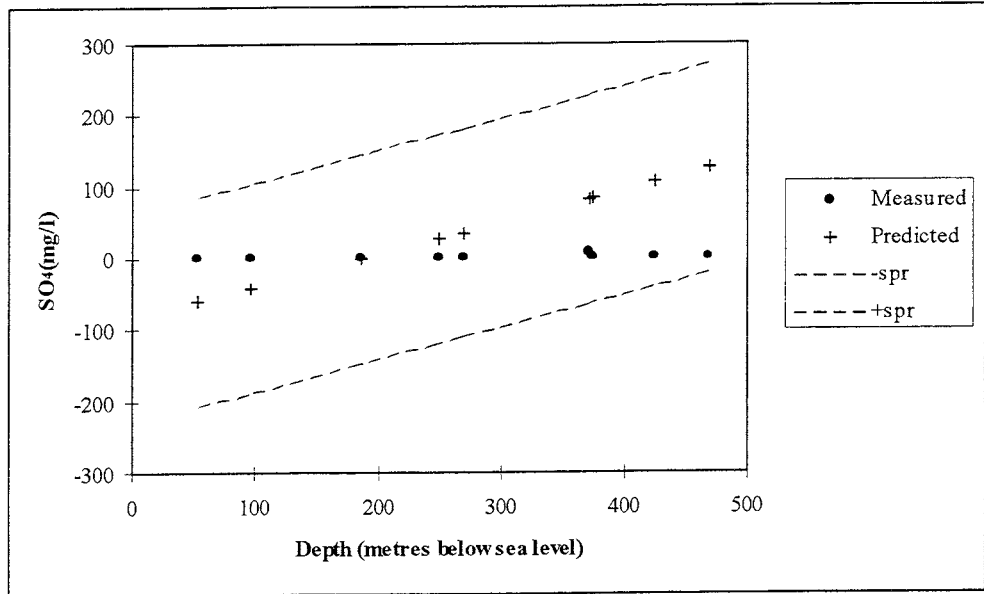


Figure D-3. The measured (dots) and predicted (crosses) SO_4 content at the Gideå site in relation to the depth below sea level. The dotted lines show \pm the standard deviation of the prediction (s_{pr}).

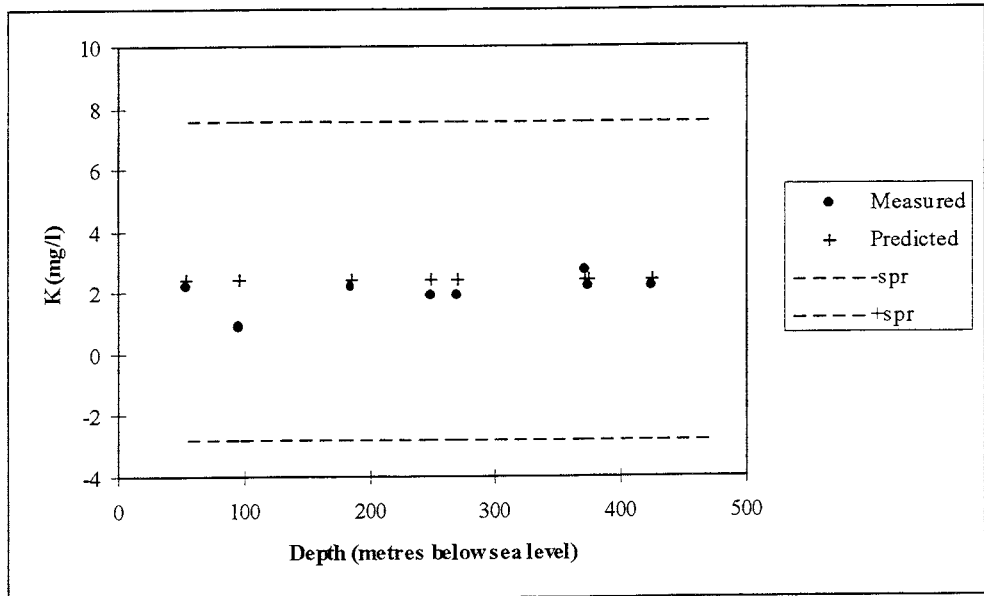


Figure D-4. The measured (dots) and predicted (crosses) K content at the Gideå site in relation to the depth below sea level. The dotted lines show \pm the standard deviation of the prediction (s_{pr}).

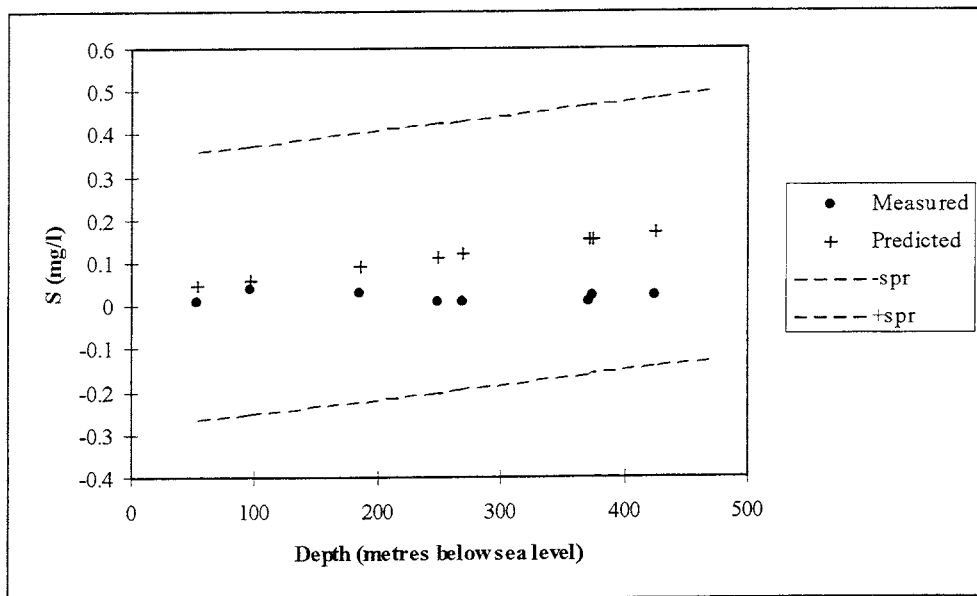


Figure D-5. The measured (dots) and predicted (crosses) S content at the Gideå site in relation to the depth below sea level. The dotted lines show \pm the standard deviation of the prediction (s_{pr}).

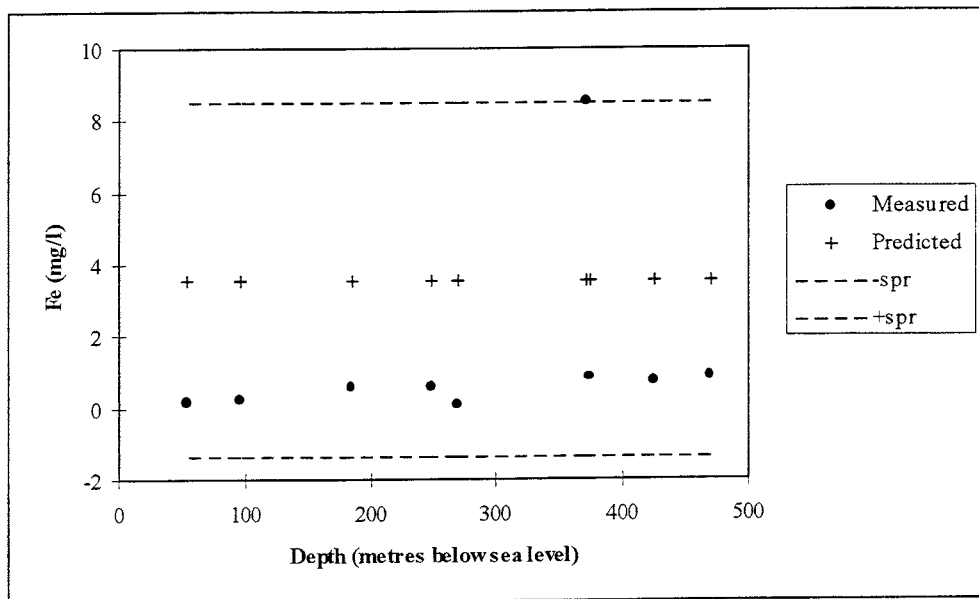


Figure D-6. The measured (dots) and predicted (crosses) Fe content at the Gideå site in relation to the depth below sea level. The dotted lines show \pm the standard deviation of the prediction (s_{pr}).

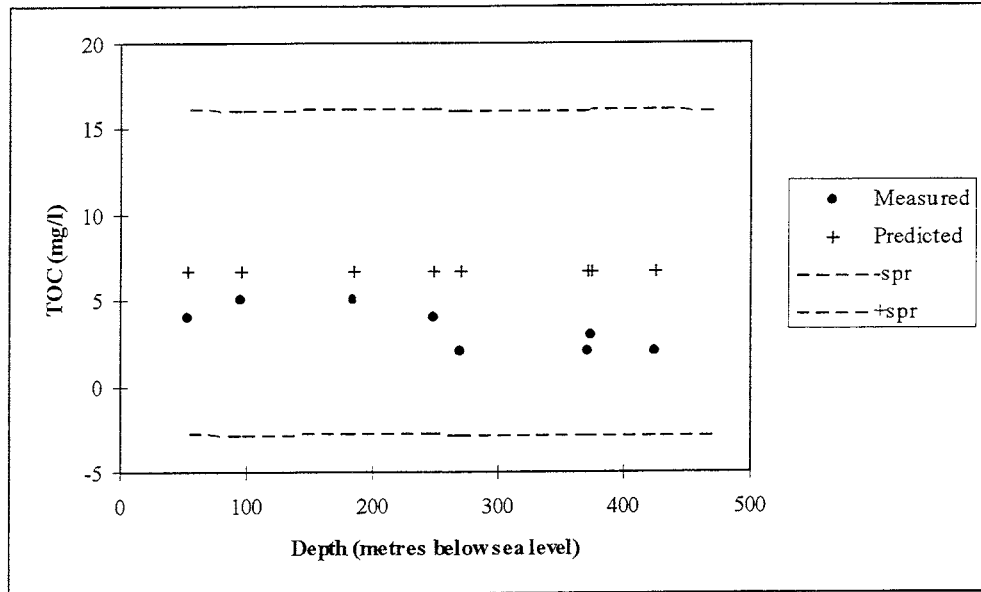


Figure D-7. The measured (dots) and predicted (crosses) TOC content at the Gideå site in relation to the depth below sea level. The dotted lines show \pm the standard deviation of the prediction (s_{pr}).

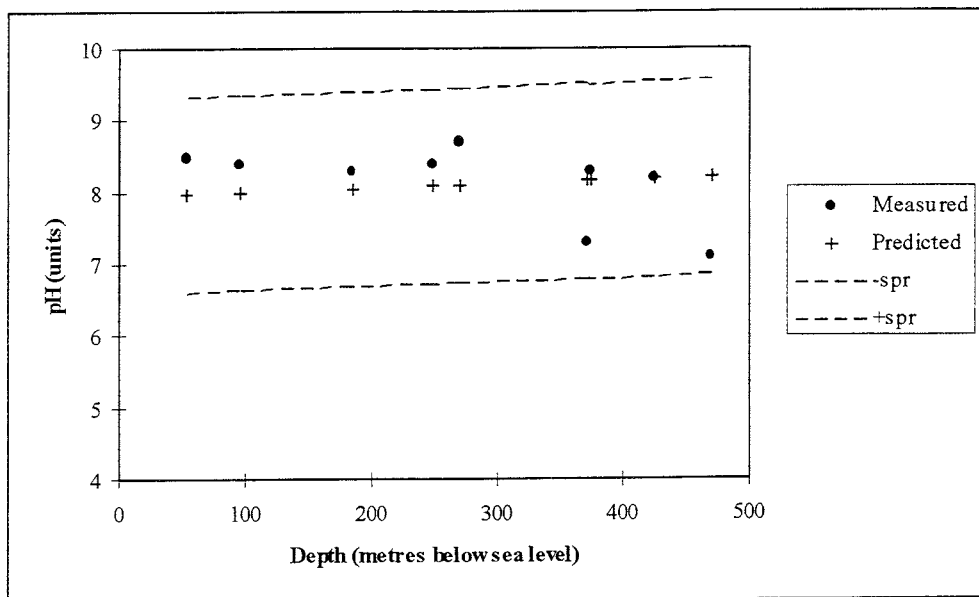


Figure D-8. The measured (dots) and predicted (crosses) pH content at the Gideå site in relation to the depth below sea level. The dotted lines show \pm the standard deviation of the prediction (s_{pr}).

APPENDIX E: KAMLUNGE

The results of the predictions are compared with measured data and shown in relation to depth. The prediction error for the multiple linear regression is also shown. The error shown is the smallest assumable error. The true overall prediction error is larger. A general prediction error includes measurement error, analysis error, misfit to the applied distribution, kriging error etc. The error interval is not a confidence interval. Negative predictions would by definition be set at zero. Only predictions with corresponding measurements are shown.

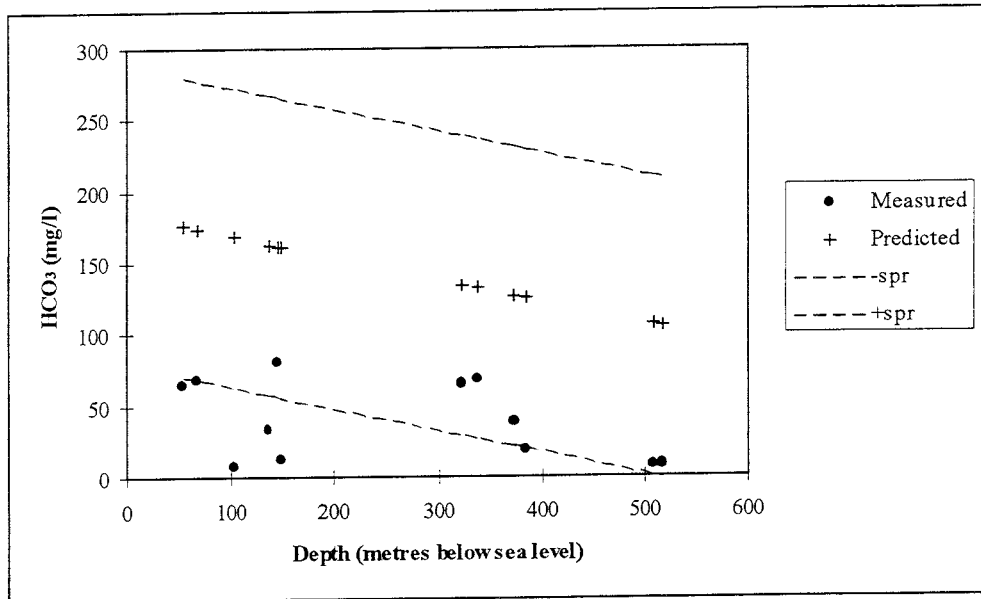


Figure E-1. The measured (dots) and predicted (crosses) HCO_3 content at the Kamlunge site in relation to the depth below sea level. The dotted lines show \pm the standard deviation of the prediction (s_{pr}).

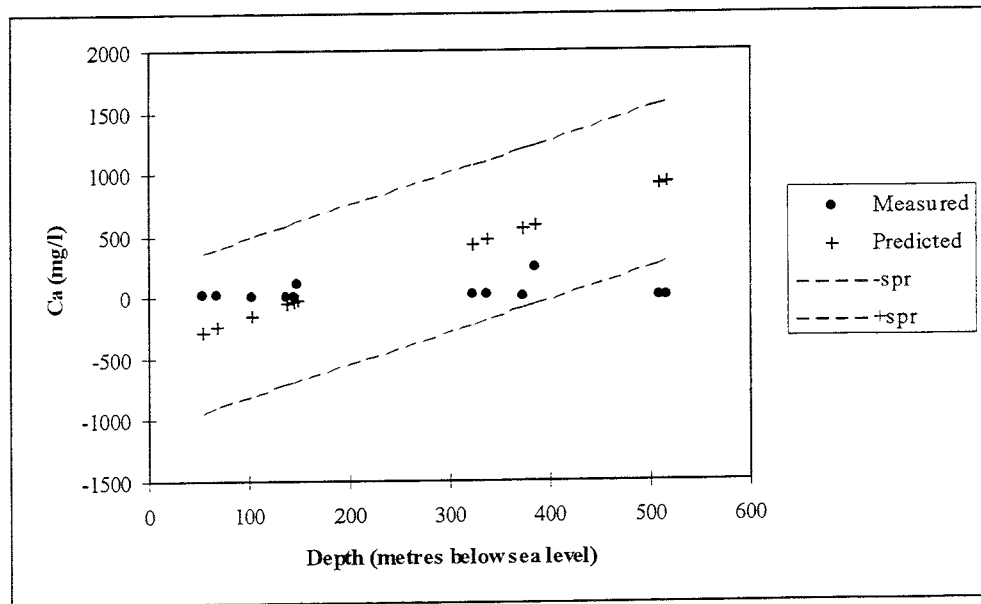


Figure E-2. The measured (dots) and predicted (crosses) Ca content at the Kamlunge site in relation to the depth below sea level. The dotted lines show \pm the standard deviation of the prediction (s_{pr}).

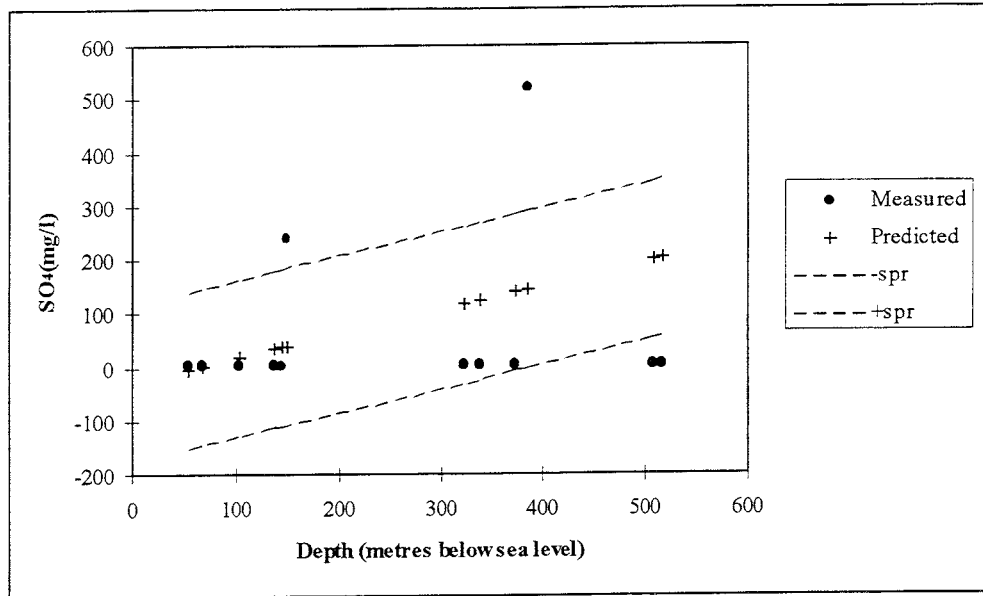


Figure E-3. The measured (dots) and predicted (crosses) SO_4 content at the Kamlunge site in relation to the depth below sea level. The dotted lines show \pm the standard deviation of the prediction (s_{pr}).

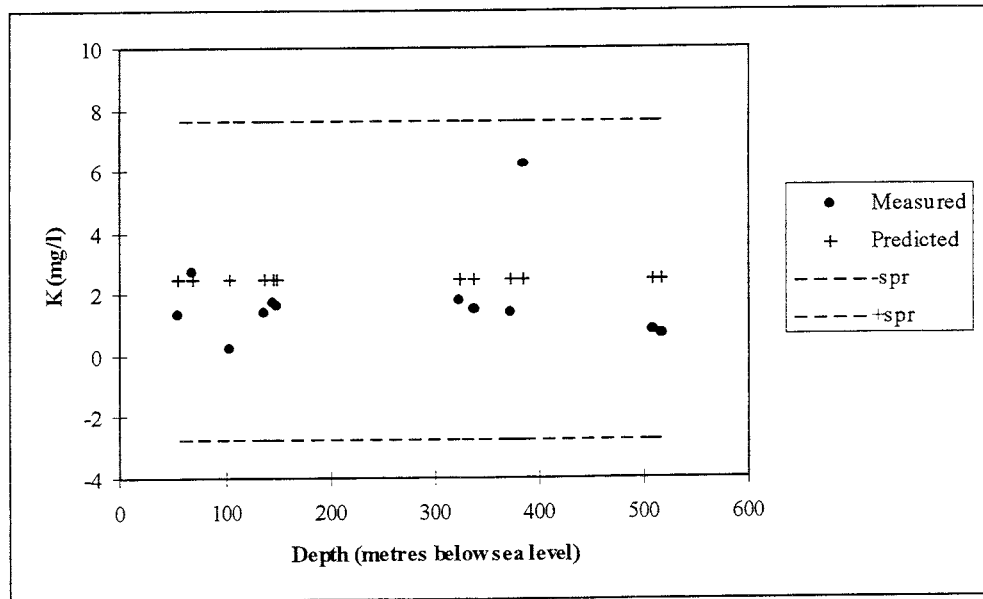


Figure E-4. The measured (dots) and predicted (crosses) K content at the Kamlunge site in relation to the depth below sea level. The dotted lines show \pm the standard deviation of the prediction (s_{pr}).

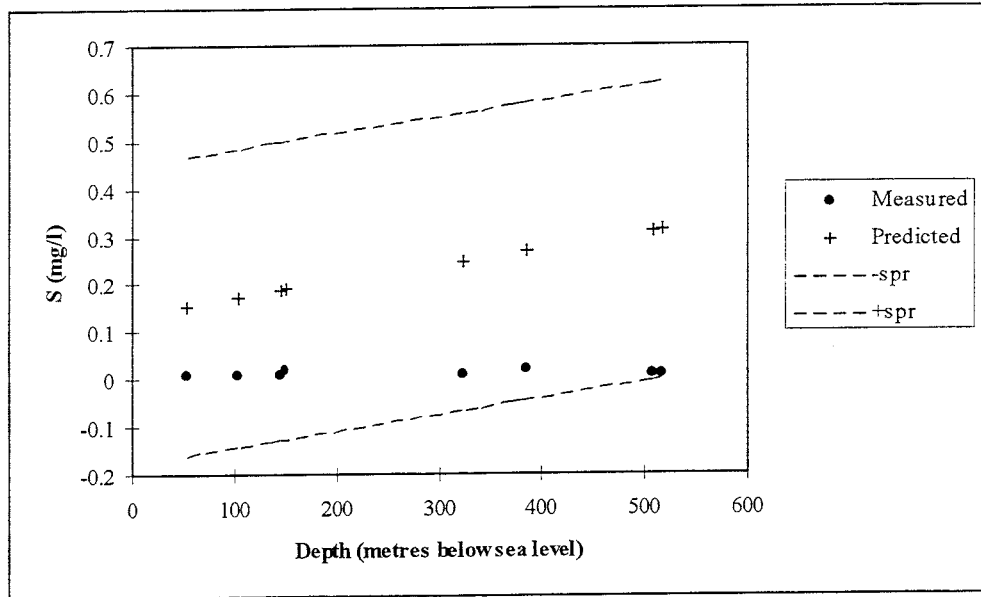


Figure E-5. The measured (dots) and predicted (crosses) S content at the Kamlunge site in relation to the depth below sea level. The dotted lines show \pm the standard deviation of the prediction (s_{pr}).

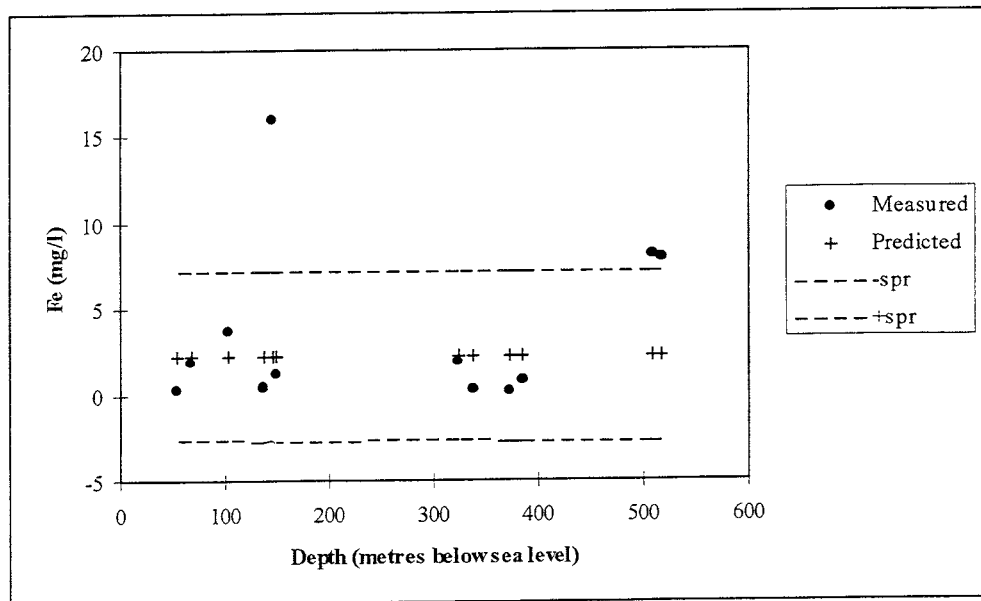


Figure E-6. The measured (dots) and predicted (crosses) Fe content at the Kamlunge site in relation to the depth below sea level. The dotted lines show \pm the standard deviation of the prediction (s_{pr}).

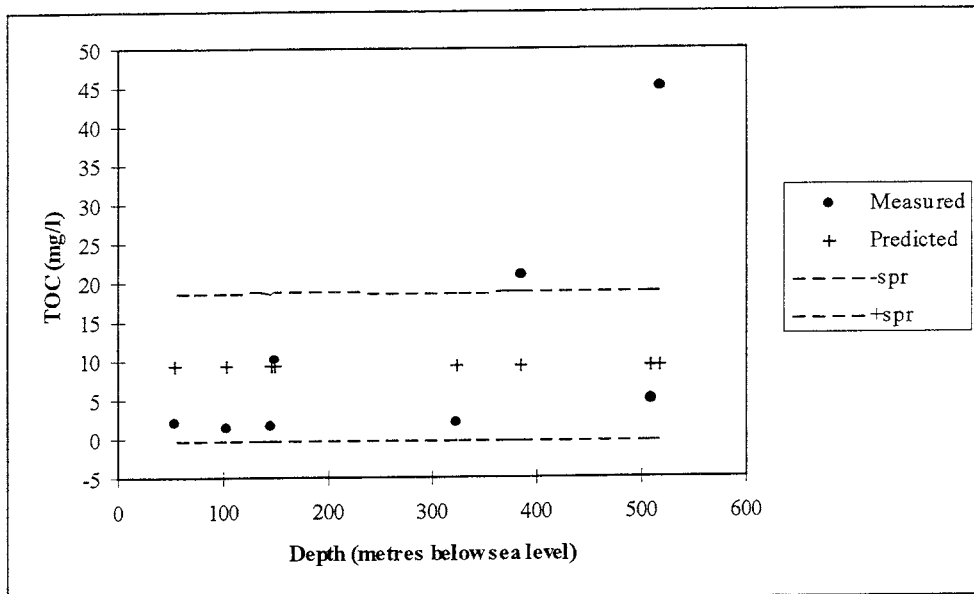


Figure E-7. The measured (dots) and predicted (crosses) TOC content at the Kamlunge site in relation to the depth below sea level. The dotted lines show \pm the standard deviation of the prediction (s_{pr}).

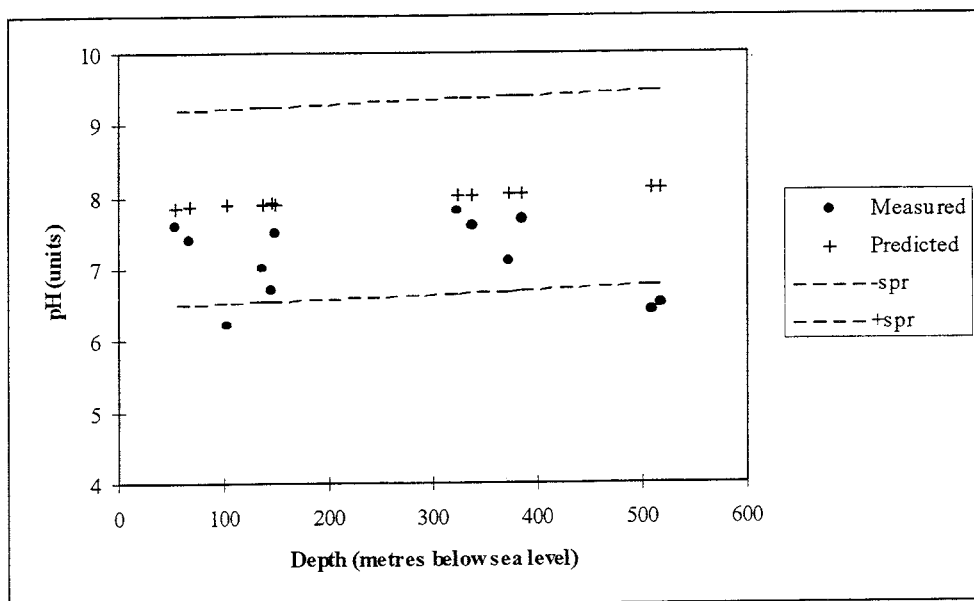


Figure E-8. The measured (dots) and predicted (crosses) pH content at the Kamlunge site in relation to the depth below sea level. The dotted lines show \pm the standard deviation of the prediction (s_{pr}).

APPENDIX F: KARLSHAMN

The results of the predictions are compared with measured data and shown in relation to depth. The prediction error for the multiple linear regression is also shown. The error shown is the smallest assumable error. The true overall prediction error is larger. A general prediction error includes measurement error, analysis error, misfit to the applied distribution, kriging error etc. The error interval is not a confidence interval. Negative predictions would by definition be set at zero. Only predictions with corresponding measurements are shown.

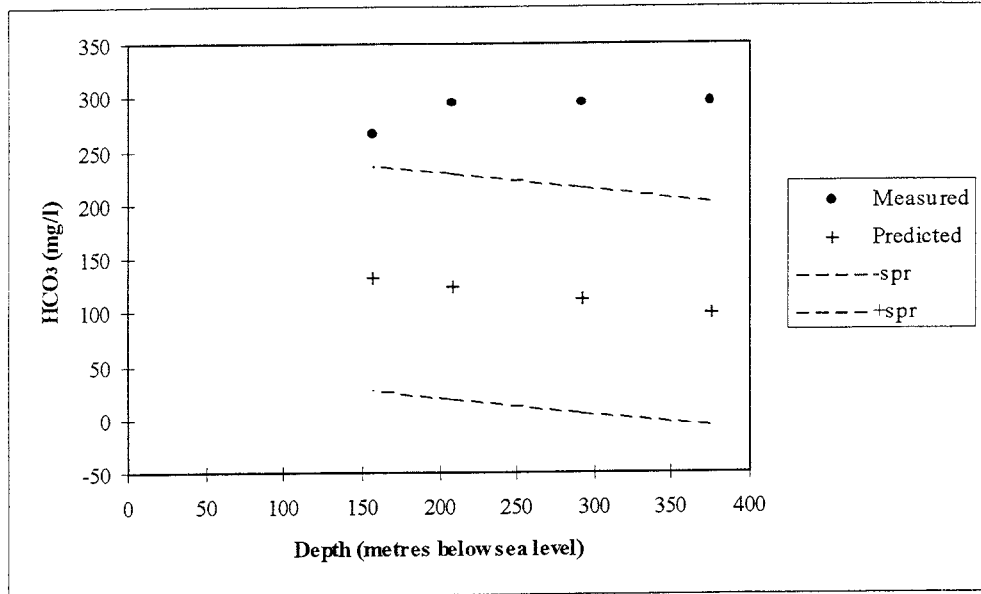


Figure F-1. The measured (dots) and predicted (crosses) HCO_3 content at the Karlshamn site in relation to the depth below sea level. The dotted lines show \pm the standard deviation of the prediction (s_{pr}).

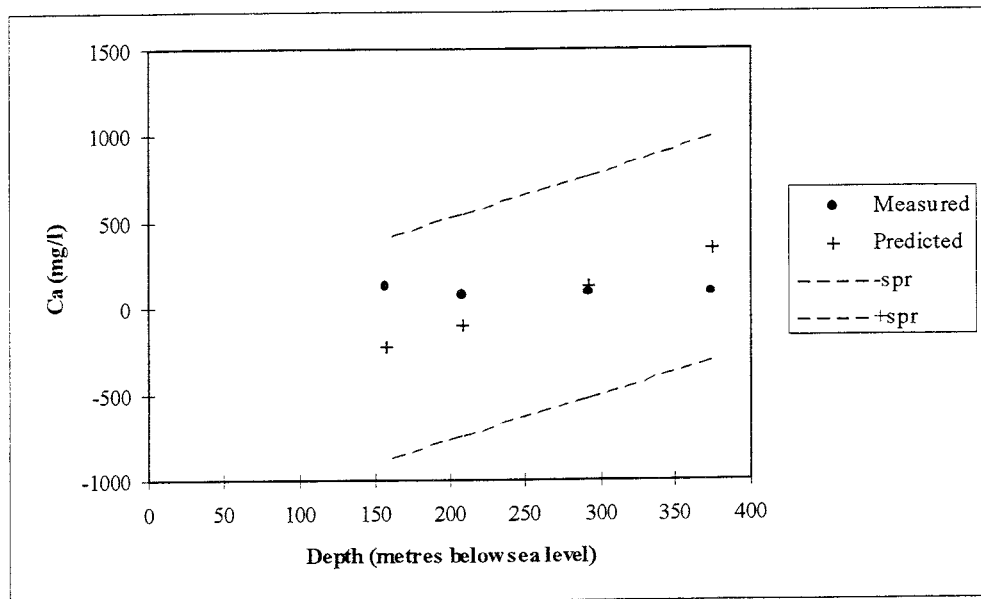


Figure F-2. The measured (dots) and predicted (crosses) Ca content at the Karlshamn site in relation to the depth below sea level. The dotted lines show \pm the standard deviation of the prediction (s_{pr}).

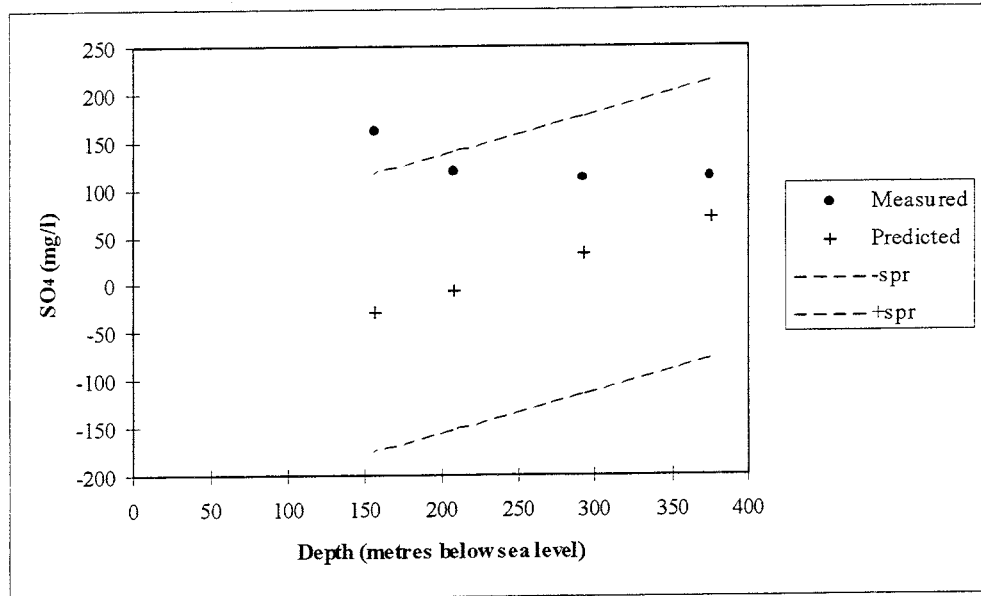


Figure F-3. The measured (dots) and predicted (crosses) SO₄ content at the Karlshamn site in relation to the depth below sea level. The dotted lines show \pm the standard deviation of the prediction (s_{pr}).

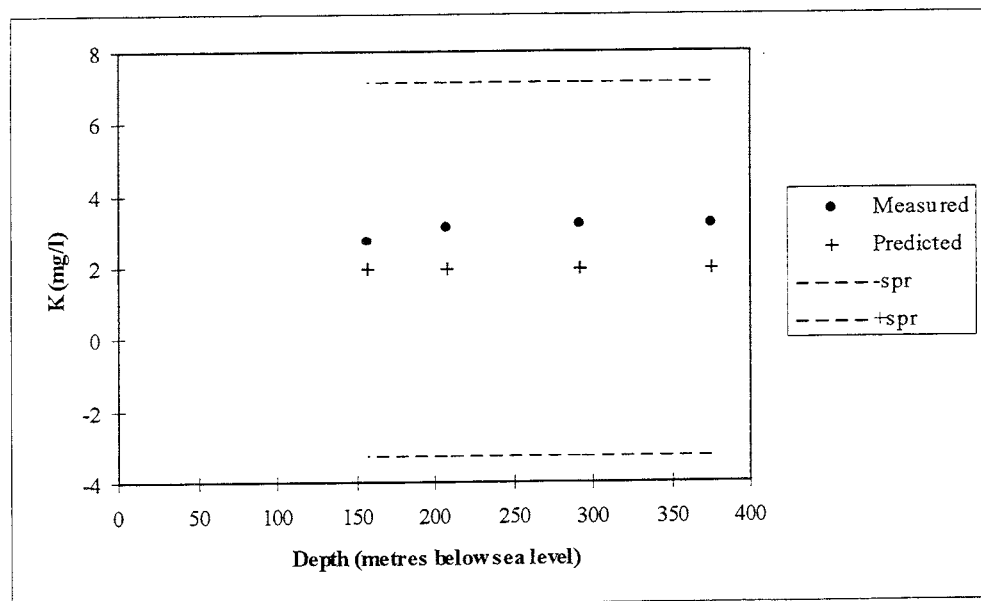


Figure F-4. The measured (dots) and predicted (crosses) K content at the Karlshamn site in relation to the depth below sea level. The dotted lines show \pm the standard deviation of the prediction (s_{pr}).

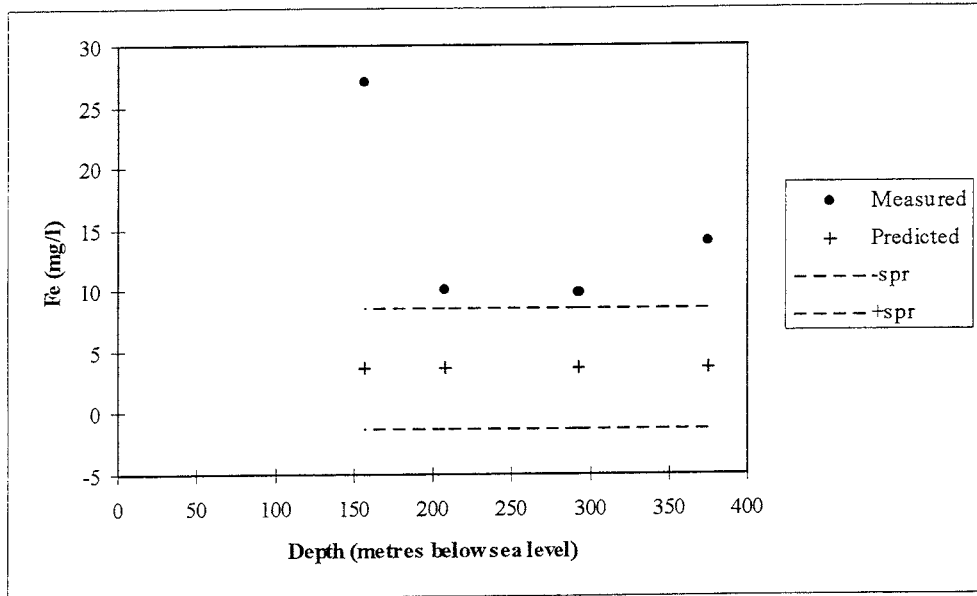


Figure F-5. The measured (dots) and predicted (crosses) Fe content at the Karlshamn site in relation to the depth below sea level. The dotted lines show \pm the standard deviation of the prediction (s_{pr}).

APPENDIX G: KLIPPERÅS

The results of the predictions are compared with measured data and shown in relation to depth. The prediction error for the multiple linear regression is also shown. The error shown is the smallest assumable error. The true overall prediction error is larger. A general prediction error includes measurement error, analysis error, misfit to the applied distribution, kriging error etc. The error interval is not a confidence interval. Negative predictions would by definition be set at zero. Only predictions with corresponding measurements are shown.

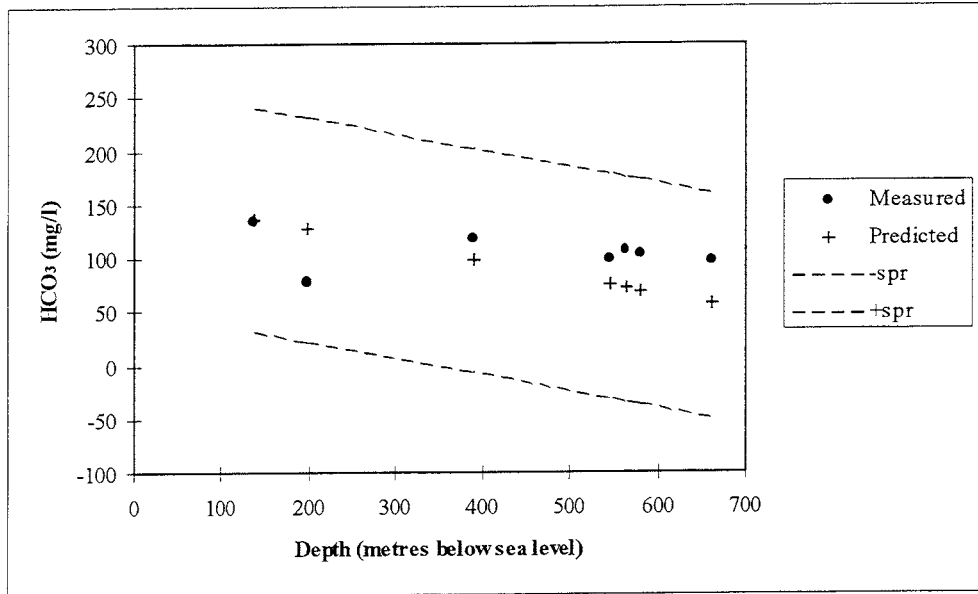


Figure G-1. The measured (dots) and predicted (crosses) HCO_3 content at the Klipperås site in relation to the depth below sea level. The dotted lines show \pm the standard deviation of the prediction (s_{pr}).

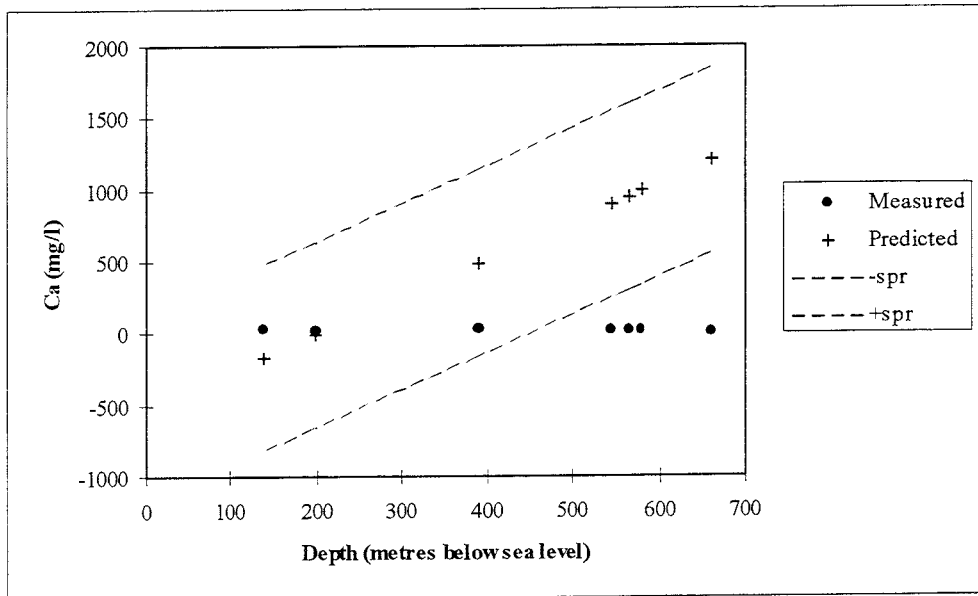


Figure G-2. The measured (dots) and predicted (crosses) Ca content at the Klipperås site in relation to the depth below sea level. The dotted lines show \pm the standard deviation of the prediction (s_{pr}).

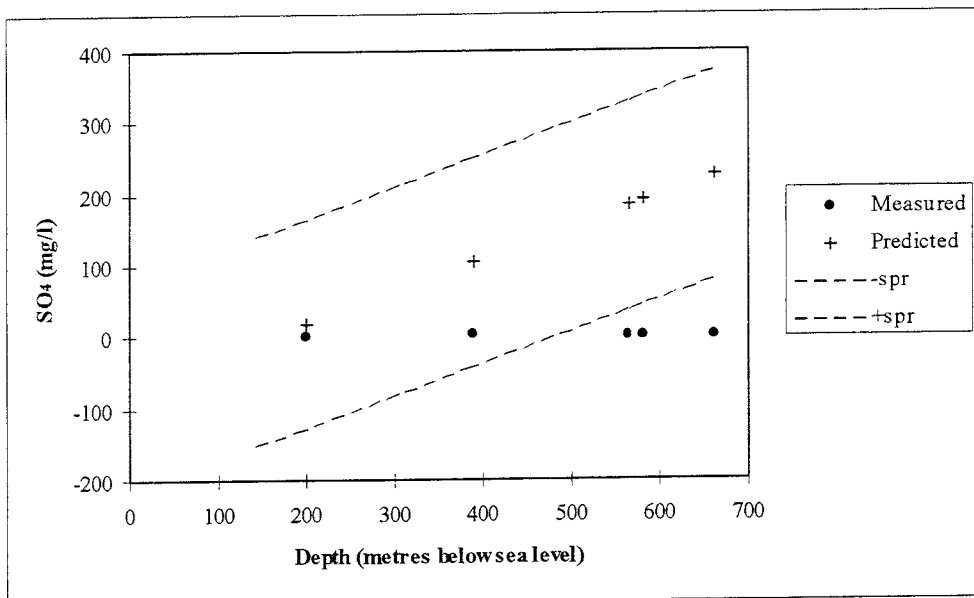


Figure G-3. The measured (dots) and predicted (crosses) SO_4 content at the Klipperås site in relation to the depth below sea level. The dotted lines show \pm the standard deviation of the prediction (s_{pr}).

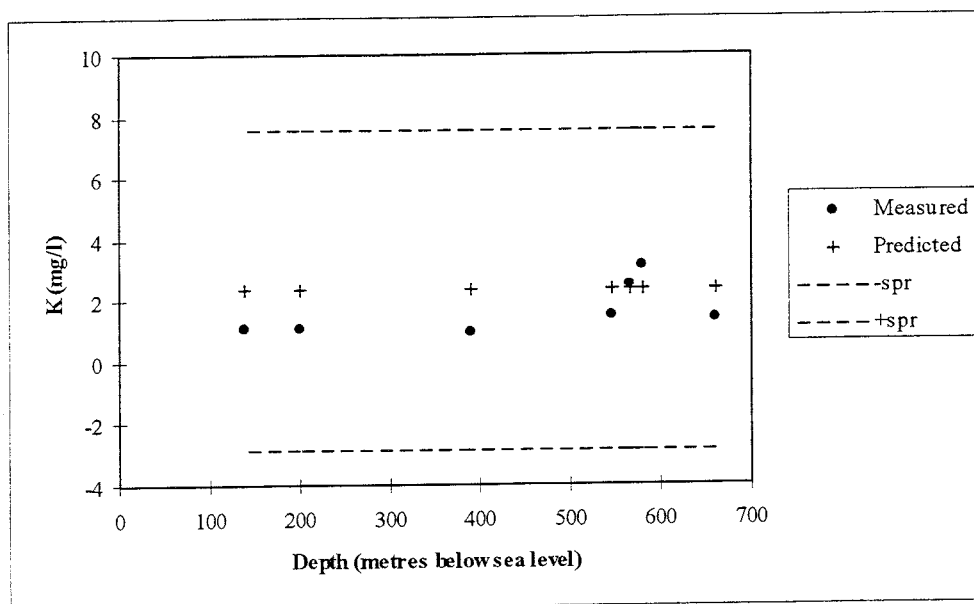


Figure G-4. The measured (dots) and predicted (crosses) K content at the Klipperås site in relation to the depth below sea level. The dotted lines show \pm the standard deviation of the prediction (s_{pr}).

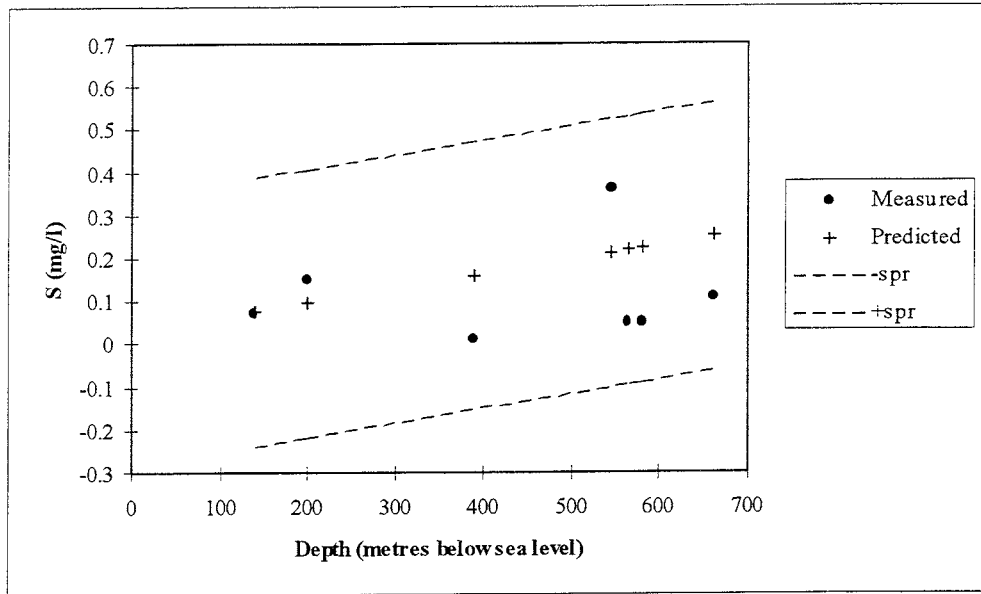


Figure G-5. The measured (dots) and predicted (crosses) S content at the Klipperås site in relation to the depth below sea level. The dotted lines show \pm the standard deviation of the prediction (s_{pr}).

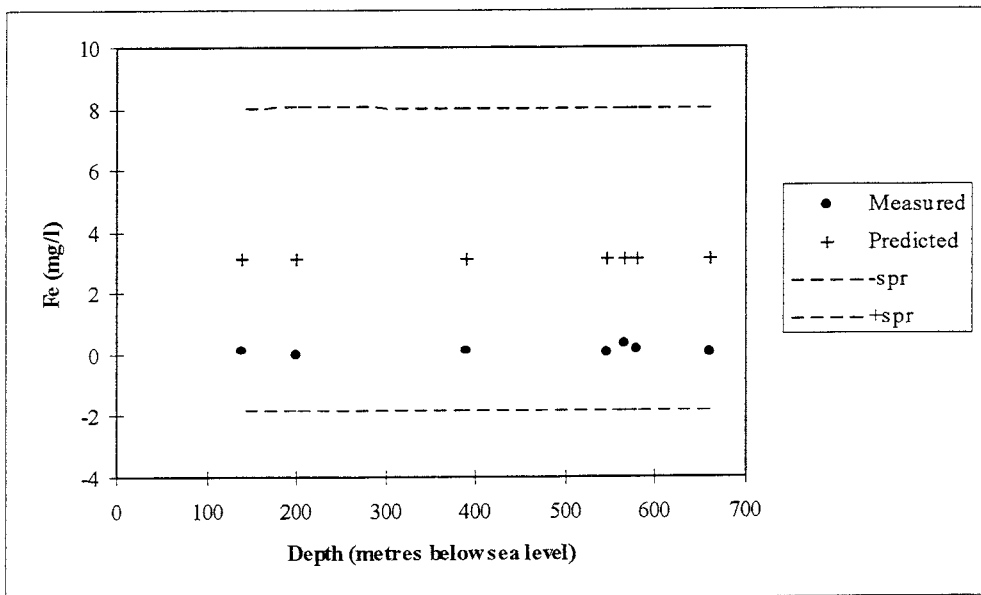


Figure G-6. The measured (dots) and predicted (crosses) Fe content at the Klipperås site in relation to the depth below sea level. The dotted lines show \pm the standard deviation of the prediction (s_{pr}).

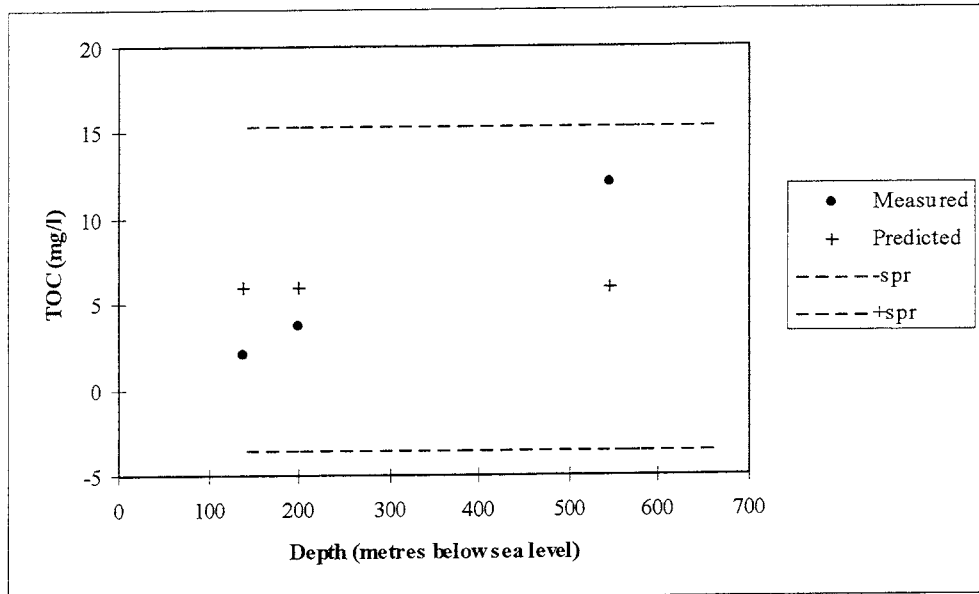


Figure G-7. The measured (dots) and predicted (crosses) TOC content at the Klipperås site in relation to the depth below sea level. The dotted lines show \pm the standard deviation of the prediction (s_{pr}).

APPENDIX H: KRÅKEMÅLA

The results of the predictions are compared with measured data and shown in relation to depth. The prediction error for the multiple linear regression is also shown. The error shown is the smallest assumable error. The true overall prediction error is larger. A general prediction error includes measurement error, analysis error, misfit to the applied distribution, kriging error etc. The error interval is not a confidence interval. Negative predictions would by definition be set at zero. Only predictions with corresponding measurements are shown.

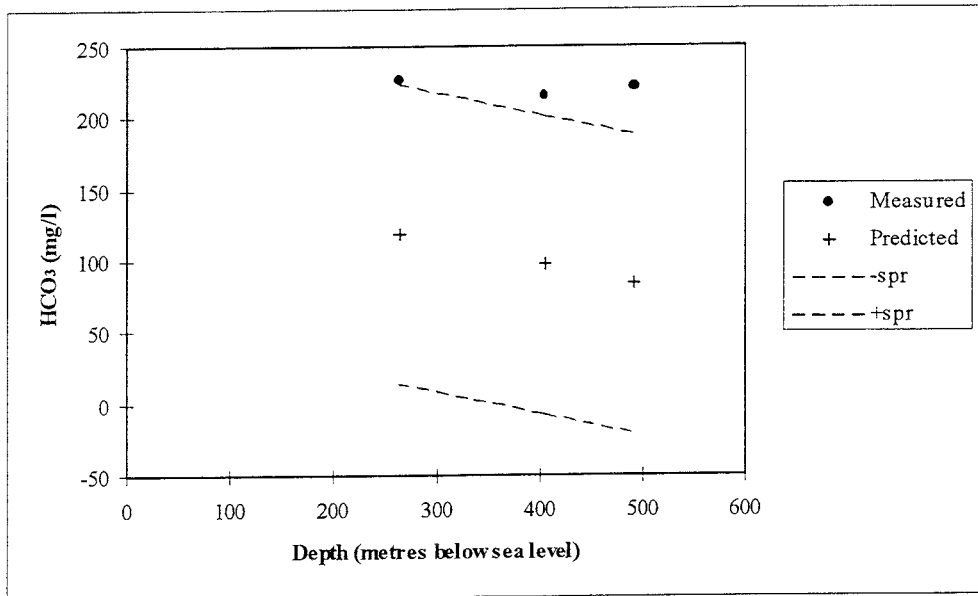


Figure H-1. The measured (dots) and predicted (crosses) HCO_3^- content at the Kråkemåla site in relation to the depth below sea level. The dotted lines show \pm the standard deviation of the prediction (s_{pr}).

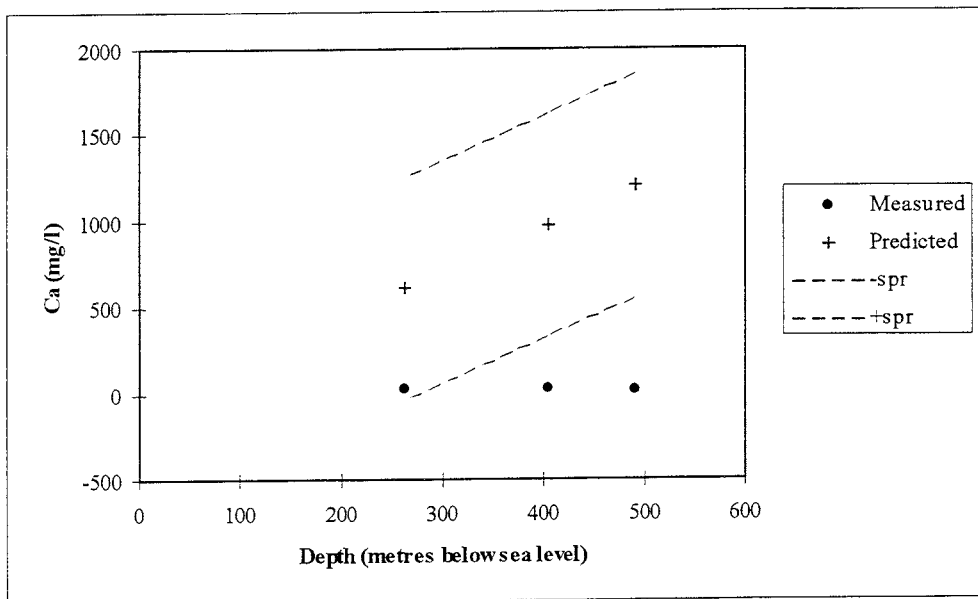


Figure H-2. The measured (dots) and predicted (crosses) Ca content at the Kråkemåla site in relation to the depth below sea level. The dotted lines show \pm the standard deviation of the prediction (s_{pr}).

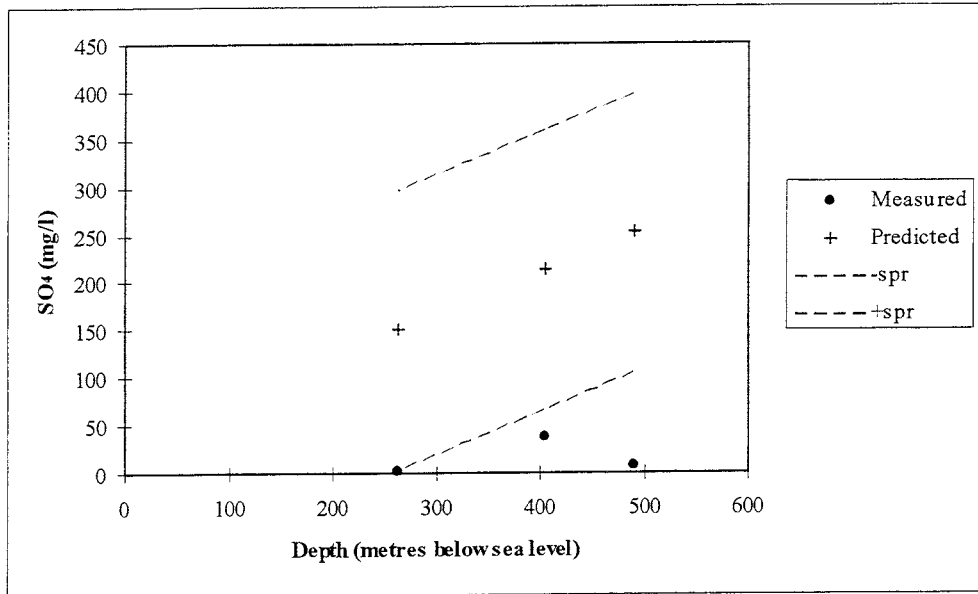


Figure H-3. The measured (dots) and predicted (crosses) SO_4 content at the Kråkemåla site in relation to the depth below sea level. The dotted lines show \pm the standard deviation of the prediction (s_{pr}).

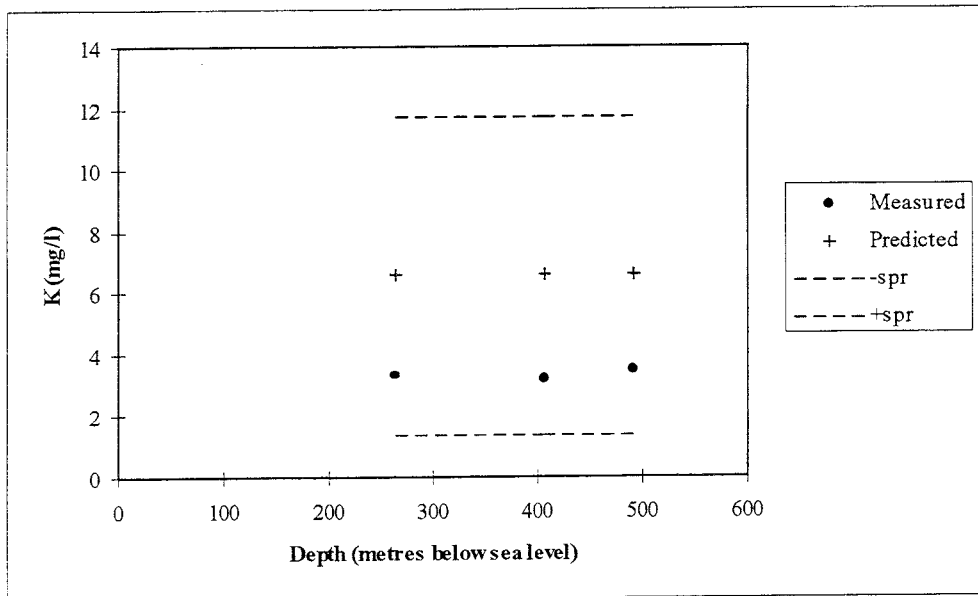


Figure H-4. The measured (dots) and predicted (crosses) K content at the Kråkemåla site in relation to the depth below sea level. The dotted lines show \pm the standard deviation of the prediction (s_{pr}).

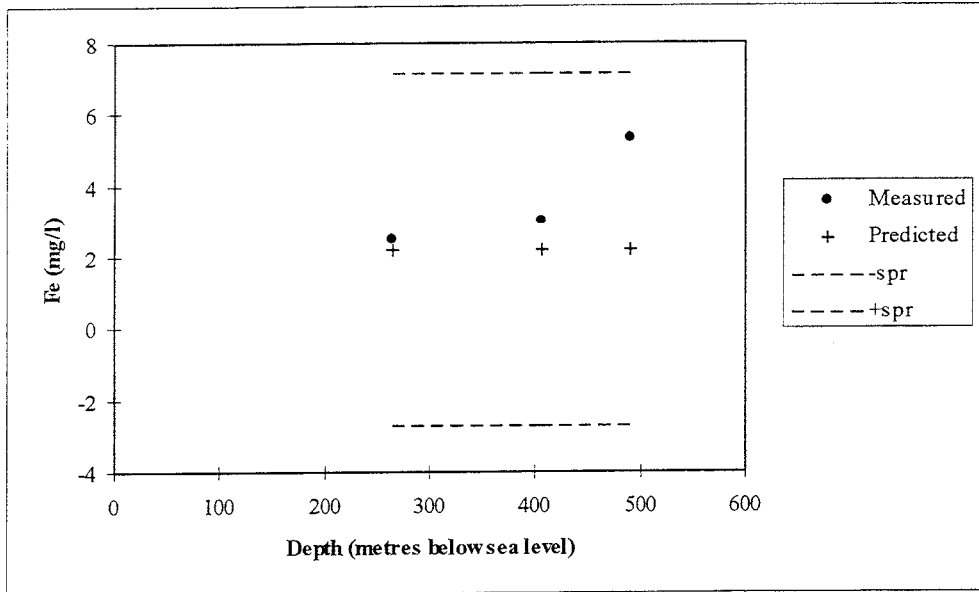


Figure H-5. The measured (dots) and predicted (crosses) Fe content at the Kråkemåla site in relation to the depth below sea level. The dotted lines show \pm the standard deviation of the prediction (s_{pr}).

APPENDIX I: LANSJÄRV

The results of the predictions are compared with measured data and shown in relation to depth. The prediction error for the multiple linear regression is also shown. The error shown is the smallest assumable error. The true overall prediction error is larger. A general prediction error includes measurement error, analysis error, misfit to the applied distribution, kriging error etc. The error interval is not a confidence interval. Negative predictions would by definition be set at zero. Only predictions with corresponding measurements are shown.

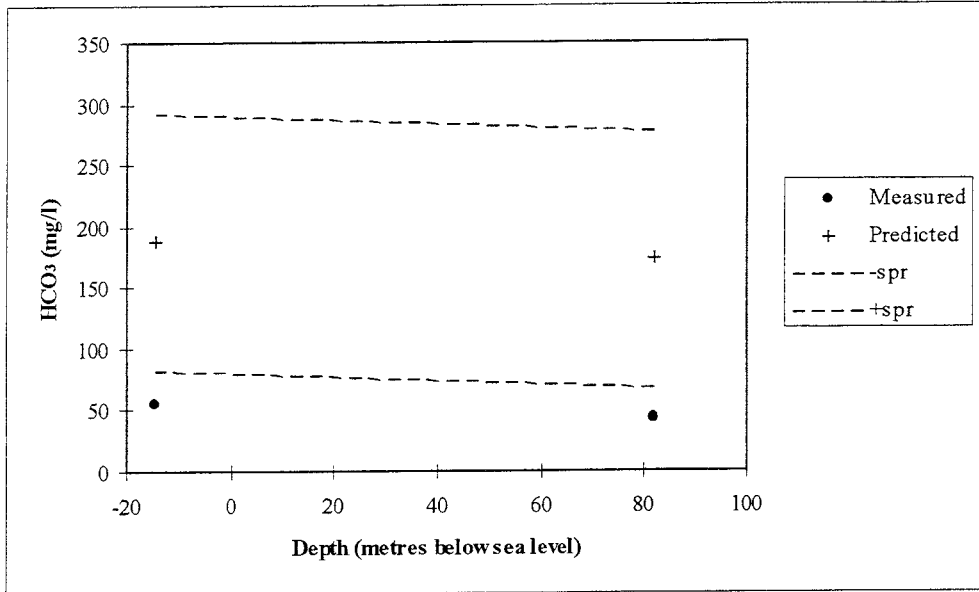


Figure I-1. The measured (dots) and predicted (crosses) HCO_3 content at the Lansjärv site in relation to the depth below sea level. The dotted lines show \pm the standard deviation of the prediction (s_{pr}).

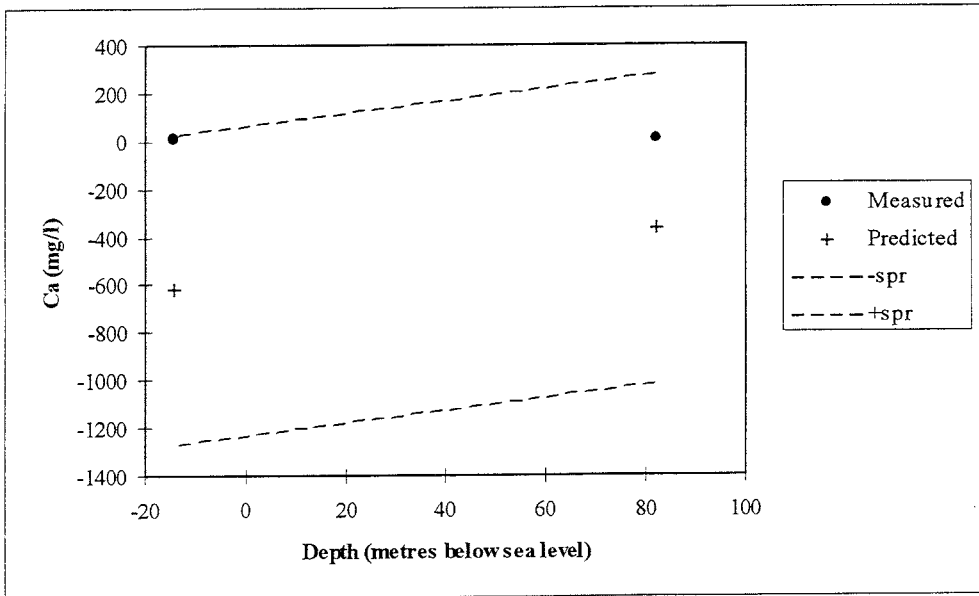


Figure I-2. The measured (dots) and predicted (crosses) Ca content at the Lansjärv site in relation to the depth below sea level. The dotted lines show \pm the standard deviation of the prediction (s_{pr}).

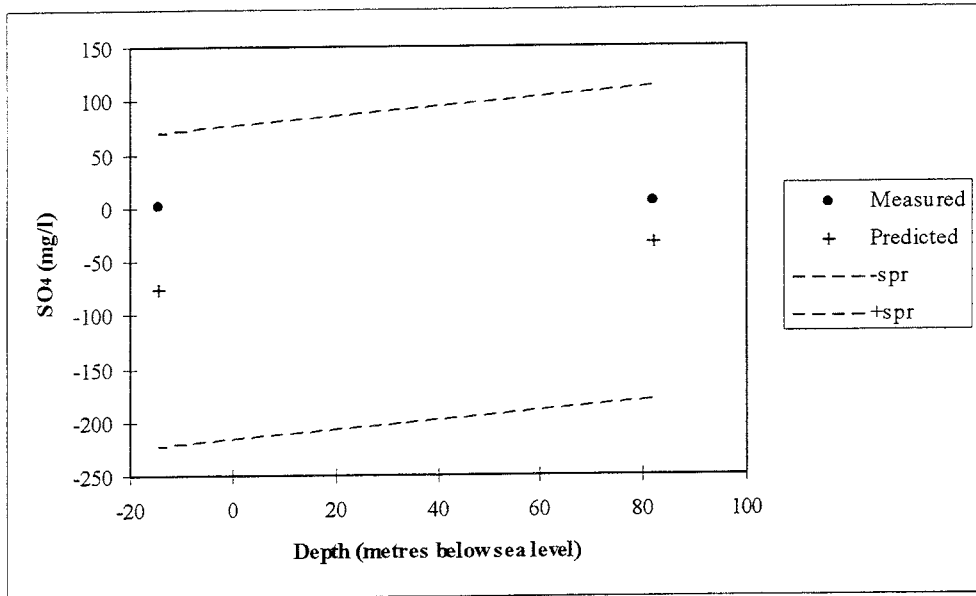


Figure I-3. The measured (dots) and predicted (crosses) SO₄ content at the Lansjärv site in relation to the depth below sea level. The dotted lines show \pm the standard deviation of the prediction (s_{pr}).

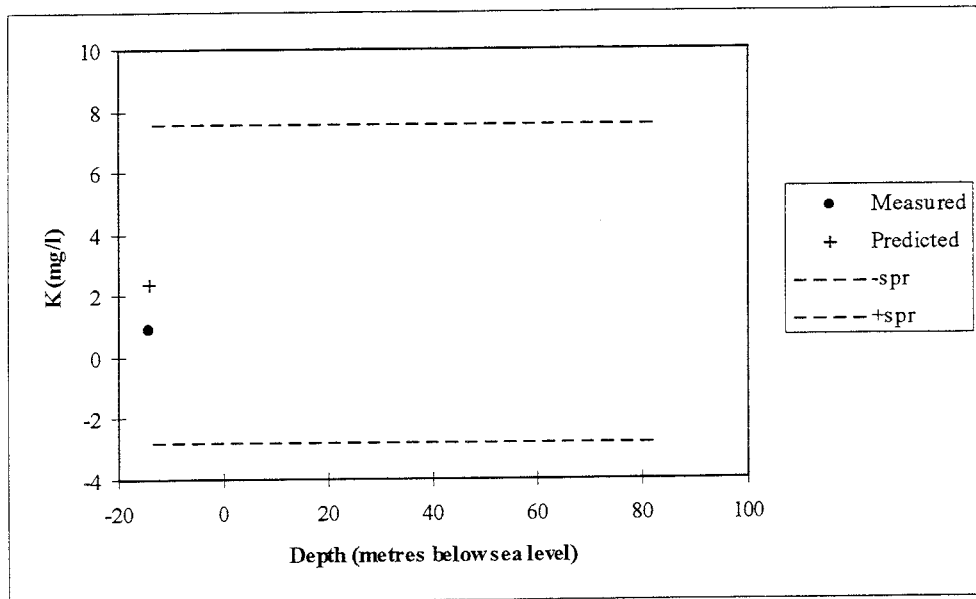


Figure I-4. The measured (dots) and predicted (crosses) K content at the Lansjärv site in relation to the depth below sea level. The dotted lines show \pm the standard deviation of the prediction (s_{pr}).

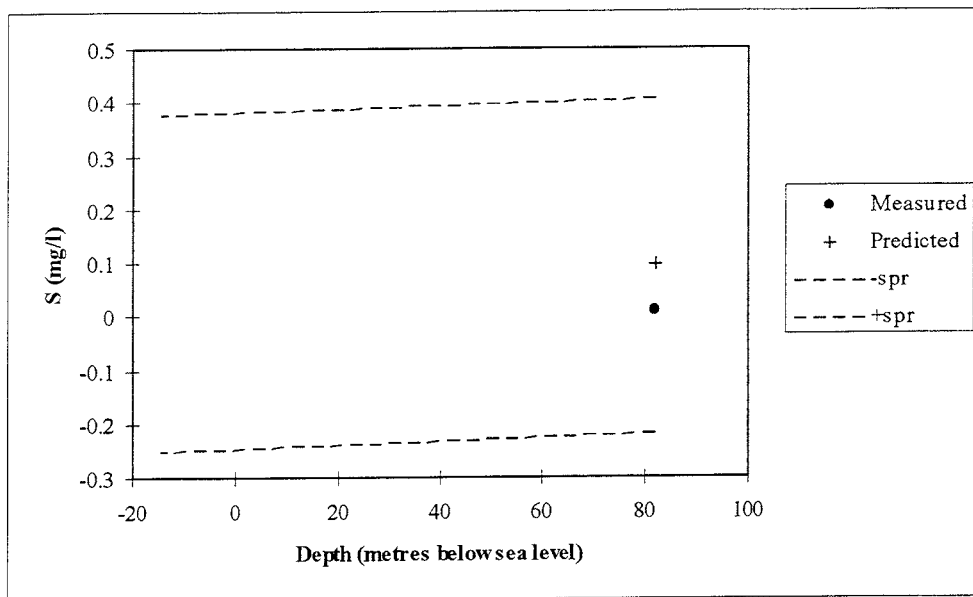


Figure I-5. The measured (dots) and predicted (crosses) S content at the Lansjärv site in relation to the depth below sea level. The dotted lines show \pm the standard deviation of the prediction (s_{pr}).

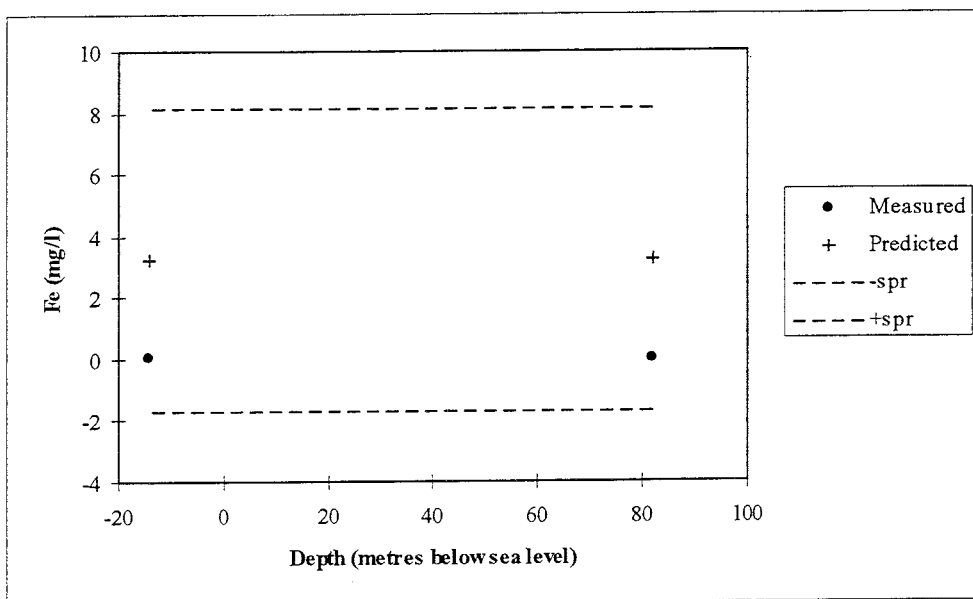


Figure I-6. The measured (dots) and predicted (crosses) Fe content at the Lansjärv site in relation to the depth below sea level. The dotted lines show \pm the standard deviation of the prediction (s_{pr}).

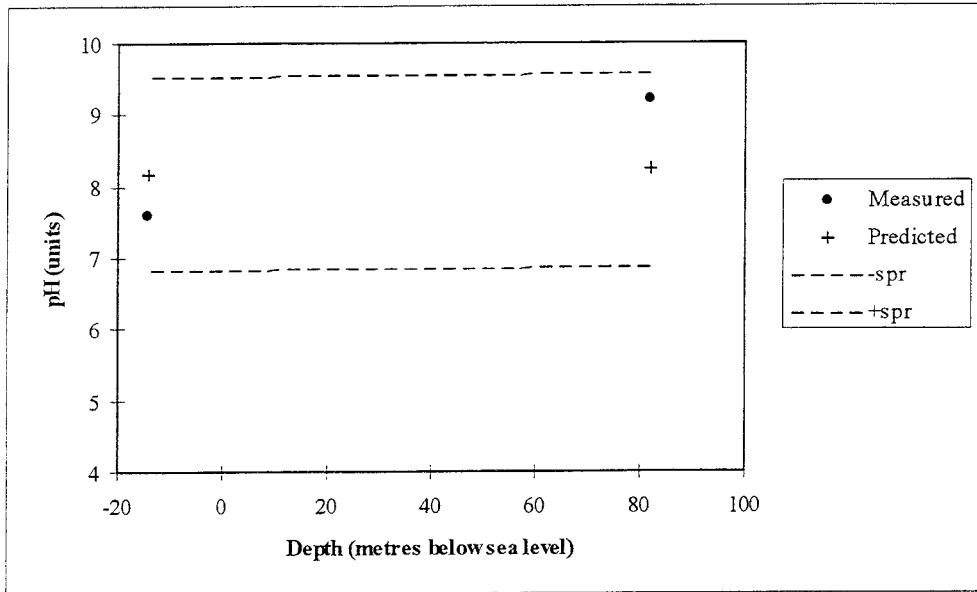


Figure I-7. The measured (dots) and predicted (crosses) pH content at the Lansjärv site in relation to the depth below sea level. The dotted lines show \pm the standard deviation of the prediction (s_{pr}).

APPENDIX J: STRIPA

The results of the predictions are compared with measured data and shown in relation to depth. The prediction error for the multiple linear regression is also shown. The error shown is the smallest assumable error. The true overall prediction error is larger. A general prediction error includes measurement error, analysis error, misfit to the applied distribution, kriging error etc. The error interval is not a confidence interval. Negative predictions would by definition be set at zero. Only predictions with corresponding measurements are shown.

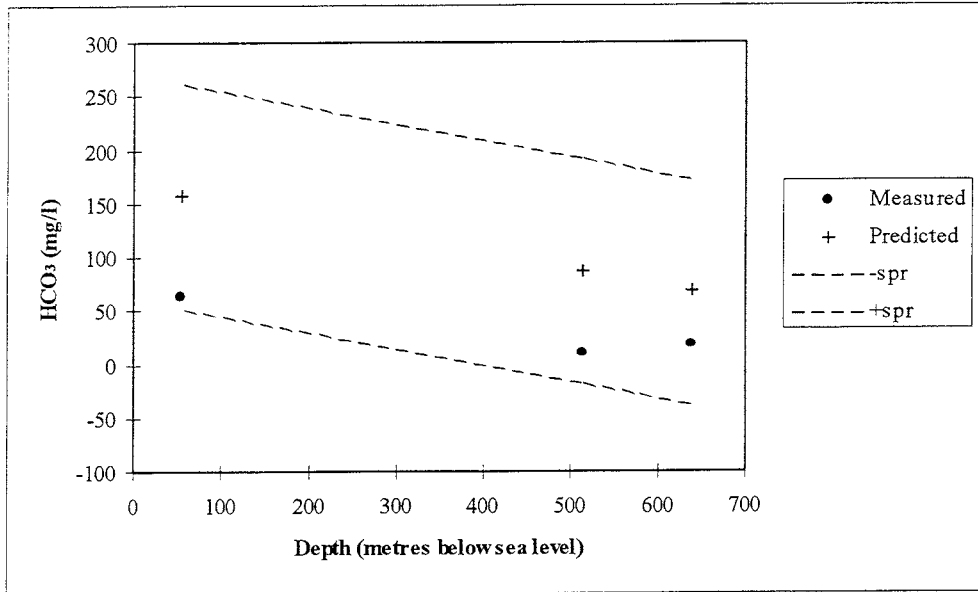


Figure J-1. The measured (dots) and predicted (crosses) HCO_3 content at the Stripa site in relation to the depth below sea level. The dotted lines show \pm the standard deviation of the prediction (s_{pr}).

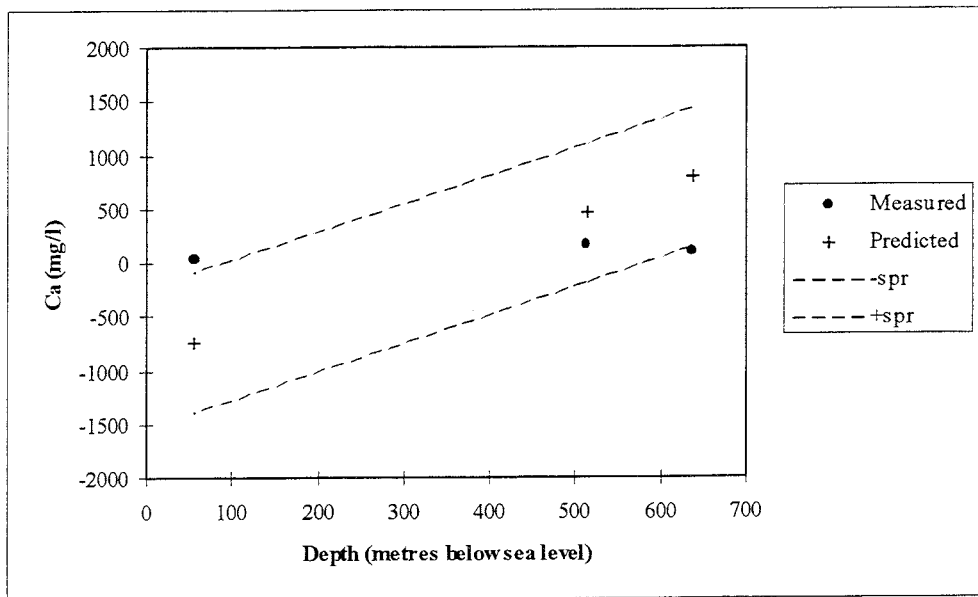


Figure J-2. The measured (dots) and predicted (crosses) Ca content at the Stripa site in relation to the depth below sea level. The dotted lines show \pm the standard deviation of the prediction (s_{pr}).

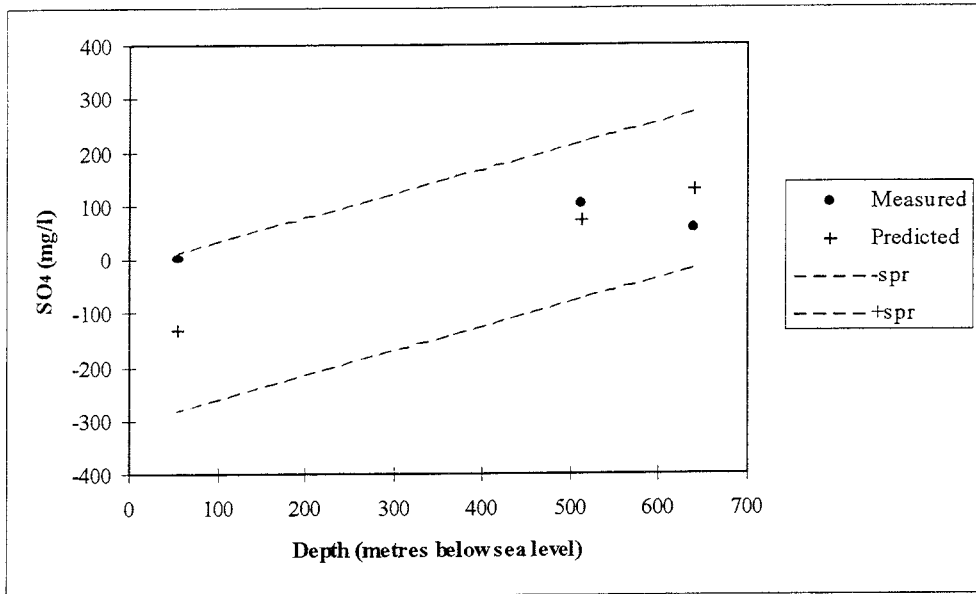


Figure J-3. The measured (dots) and predicted (crosses) SO_4 content at the Stripa site in relation to the depth below sea level. The dotted lines show \pm the standard deviation of the prediction (s_{pr}).

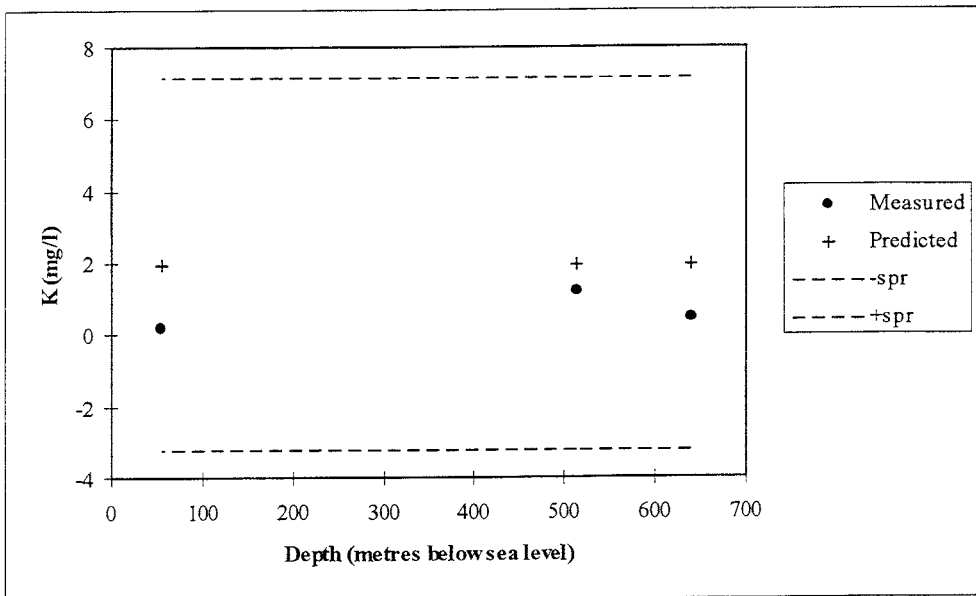


Figure J-4. The measured (dots) and predicted (crosses) K content at the Stripa site in relation to the depth below sea level. The dotted lines show \pm the standard deviation of the prediction (s_{pr}).

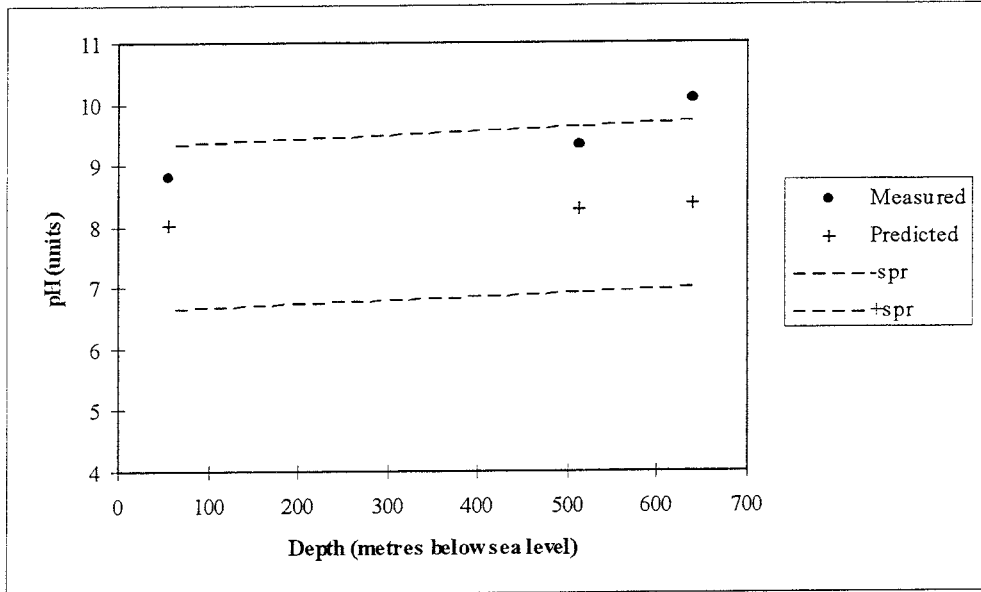


Figure J-5. The measured (dots) and predicted (crosses) pH content at the Stripa site in relation to the depth below sea level. The dotted lines show \pm the standard deviation of the prediction (s_{pr}).

APPENDIX K: SVARTBOBERGET

The results of the predictions are compared with measured data and shown in relation to depth. The prediction error for the multiple linear regression is also shown. The error shown is the smallest assumable error. The true overall prediction error is larger. A general prediction error includes measurement error, analysis error, misfit to the applied distribution, kriging error etc. The error interval is not a confidence interval. Negative predictions would by definition be set at zero. Only predictions with corresponding measurements are shown.

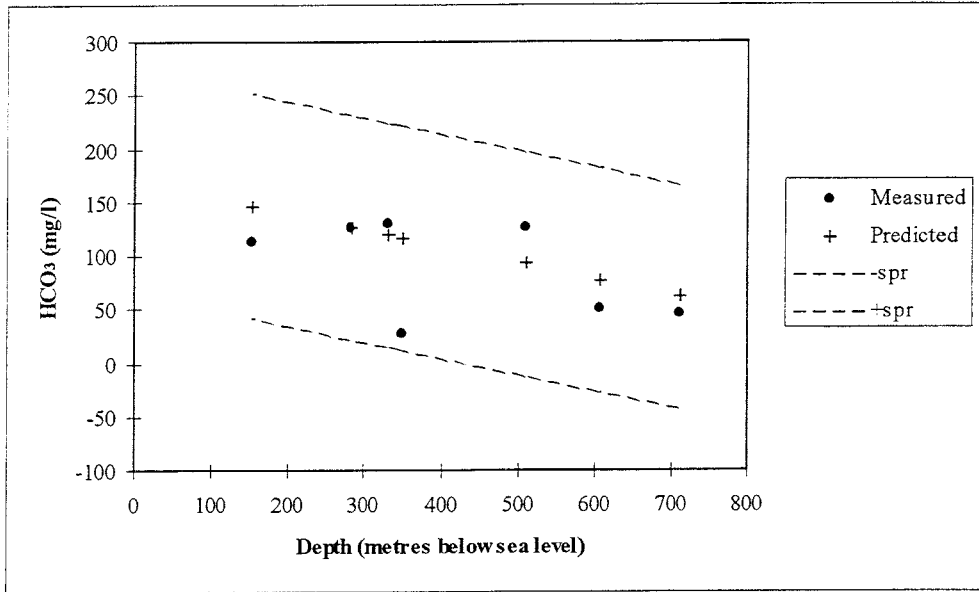


Figure K-1. The measured (dots) and predicted (crosses) HCO_3^- content at the Svartboberget site in relation to the depth below sea level. The dotted lines show \pm the standard deviation of the prediction (s_{pr}).

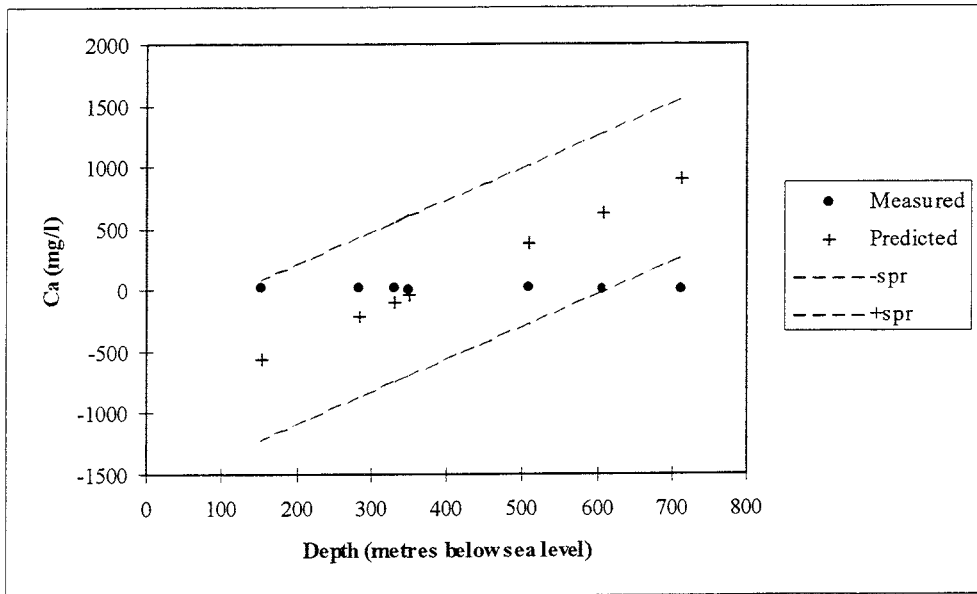


Figure K-2. The measured (dots) and predicted (crosses) Ca content at the Svartboberget site in relation to the depth below sea level. The dotted lines show \pm the standard deviation of the prediction (s_{pr}).

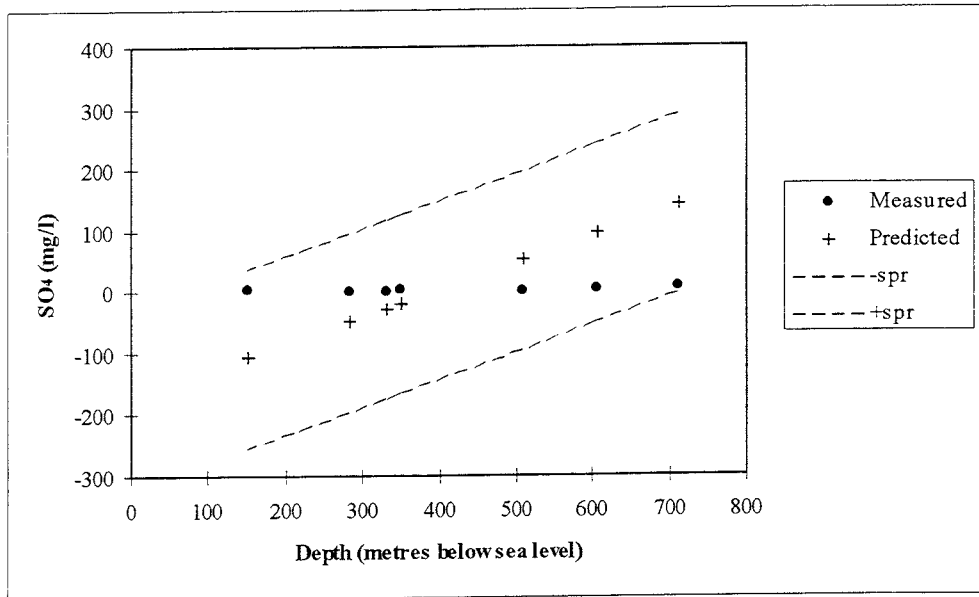


Figure K-3. The measured (dots) and predicted (crosses) SO₄ content at the Svartboberget site in relation to the depth below sea level. The dotted lines show \pm the standard deviation of the prediction (s_{pr}).

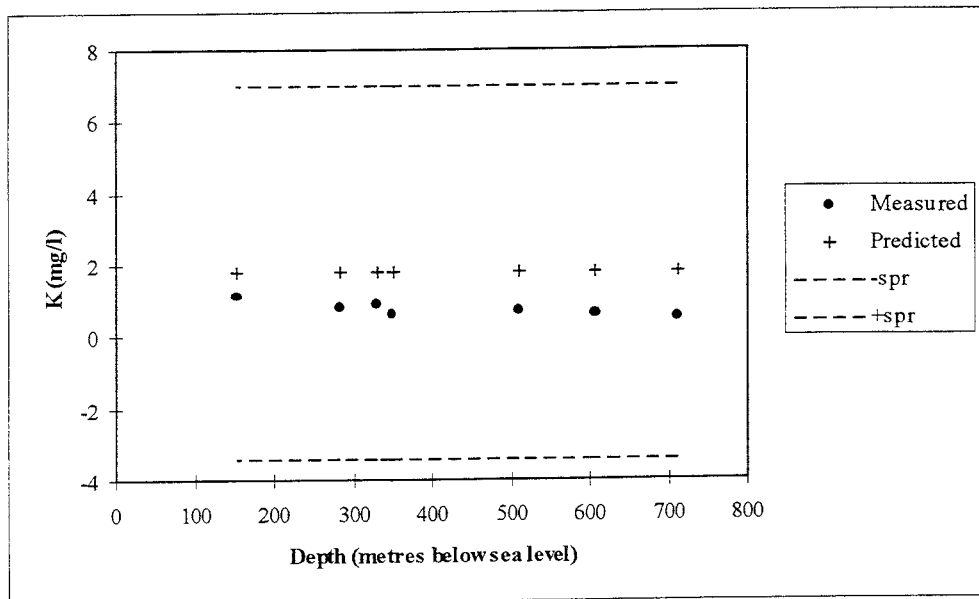


Figure K-4. The measured (dots) and predicted (crosses) K content at the Svartboberget site in relation to the depth below sea level. The dotted lines show \pm the standard deviation of the prediction (s_{pr}).

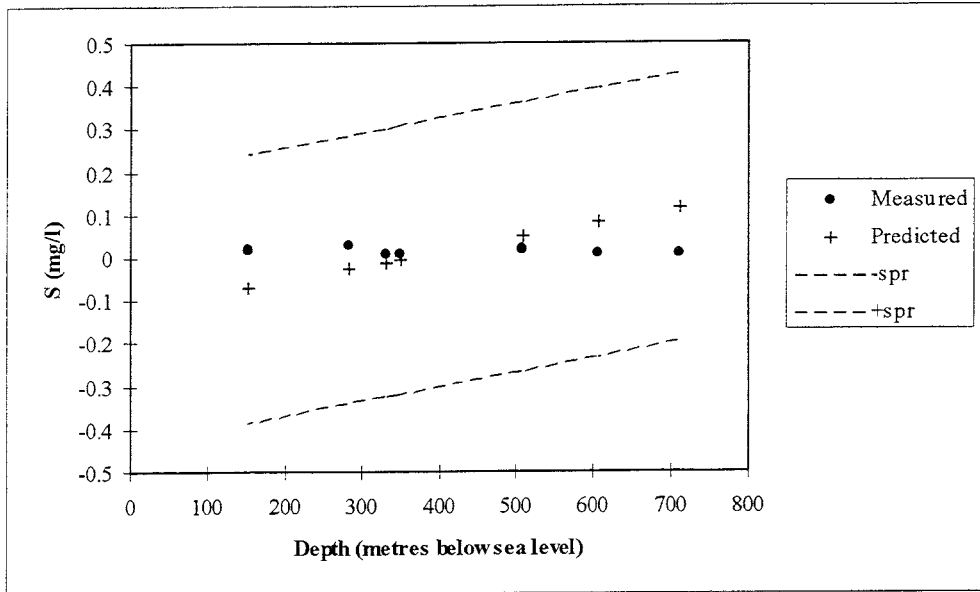


Figure K-5. The measured (dots) and predicted (crosses) S content at the Svartboberget site in relation to the depth below sea level. The dotted lines show \pm the standard deviation of the prediction (s_{pr}).

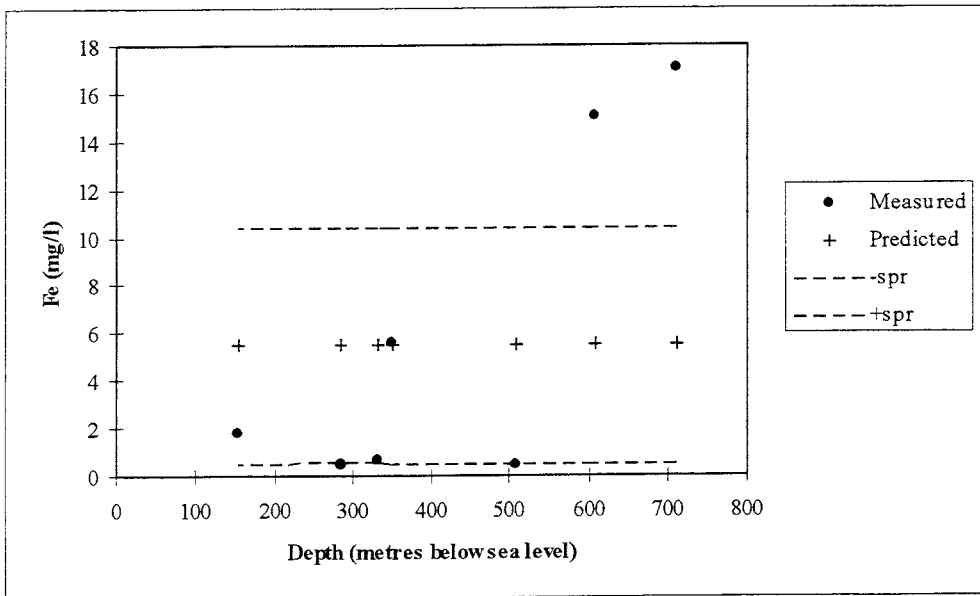


Figure K-6. The measured (dots) and predicted (crosses) Fe content at the Svartboberget site in relation to the depth below sea level. The dotted lines show \pm the standard deviation of the prediction (s_{pr}).

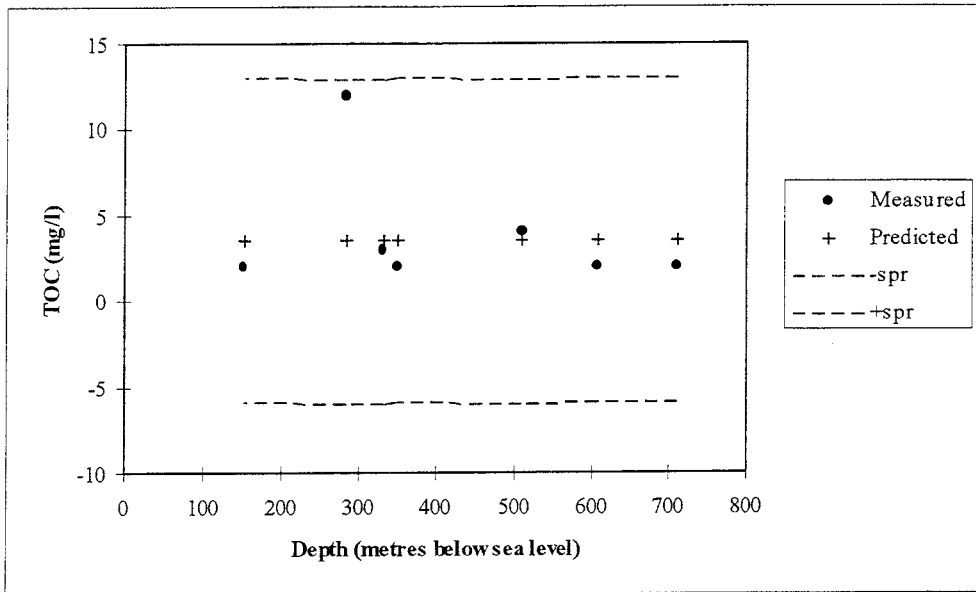


Figure K-7. The measured (dots) and predicted (crosses) TOC content at the Svartboberget site in relation to the depth below sea level. The dotted lines show \pm the standard deviation of the prediction (s_{pr}).

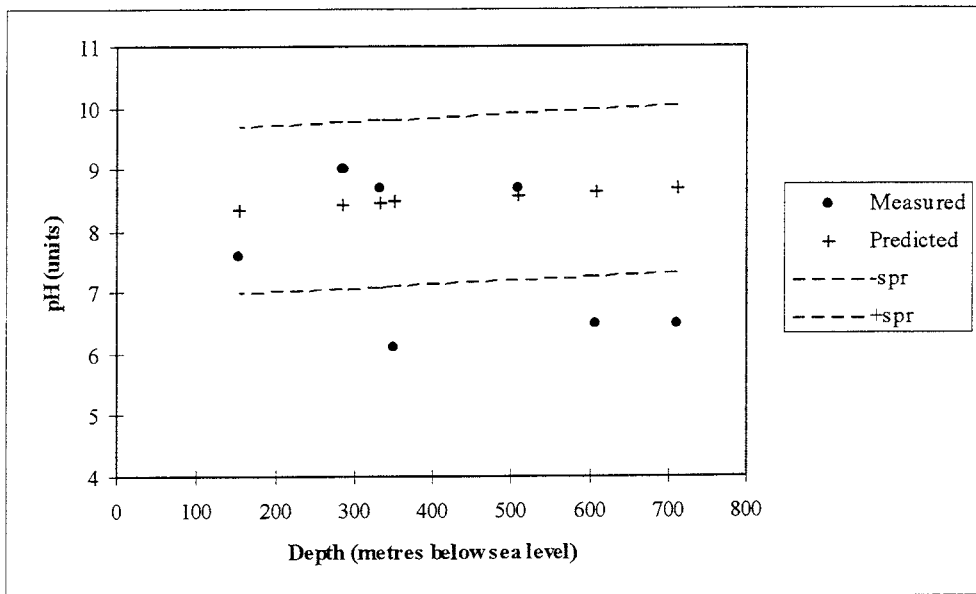


Figure K-8. The measured (dots) and predicted (crosses) pH content at the Svartboberget site in relation to the depth below sea level. The dotted lines show \pm the standard deviation of the prediction (s_{pr}).

APPENDIX L: TAAVINUNNANEN

The results of the predictions are compared with measured data and shown in relation to depth. The prediction error for the multiple linear regression is also shown. The error shown is the smallest assumable error. The true overall prediction error is larger. A general prediction error includes measurement error, analysis error, misfit to the applied distribution, kriging error etc. The error interval is not a confidence interval. Negative predictions would by definition be set at zero. Only predictions with corresponding measurements are shown.

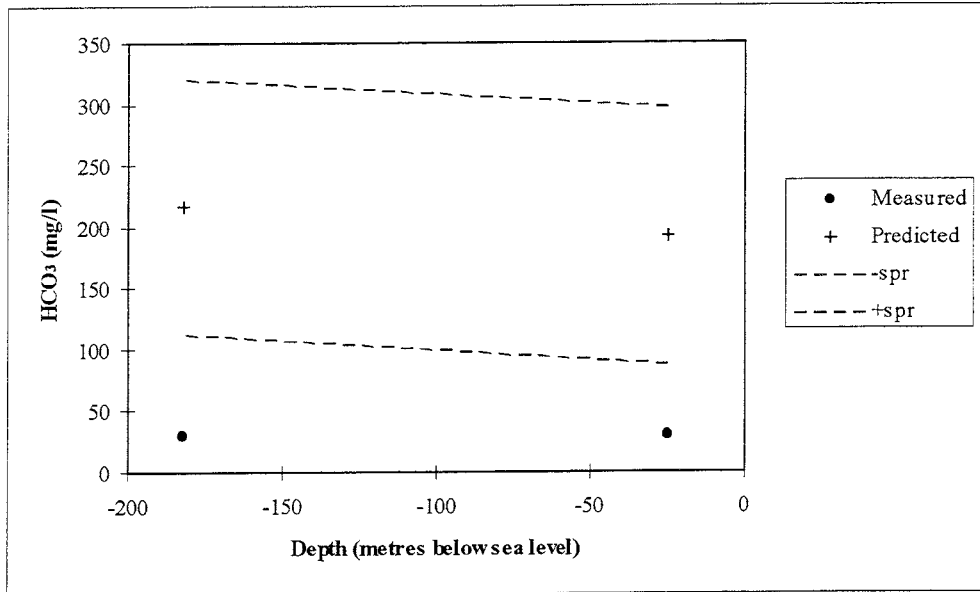


Figure L-1. The measured (dots) and predicted (crosses) HCO_3 content at the Taavimunnanen site in relation to the depth below sea level. The dotted lines show \pm the standard deviation of the prediction (s_{pr}).

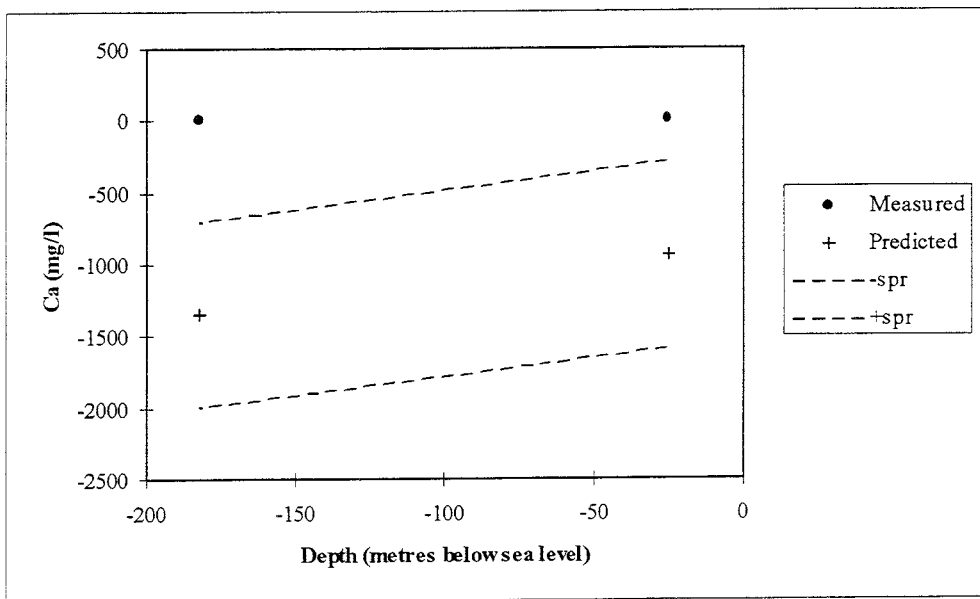


Figure L-2. The measured (dots) and predicted (crosses) Ca content at the Taavimunnanen site in relation to the depth below sea level. The dotted lines show \pm the standard deviation of the prediction (s_{pr}).

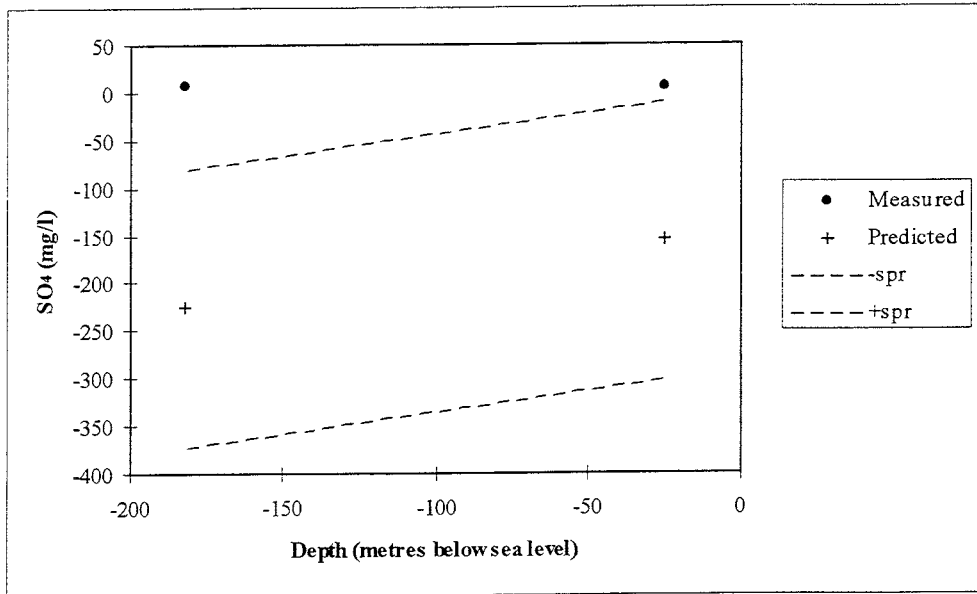


Figure L-3. The measured (dots) and predicted (crosses) SO_4 content at the Taavinummanen site in relation to the depth below sea level. The dotted lines show \pm the standard deviation of the prediction (S_{pr}).

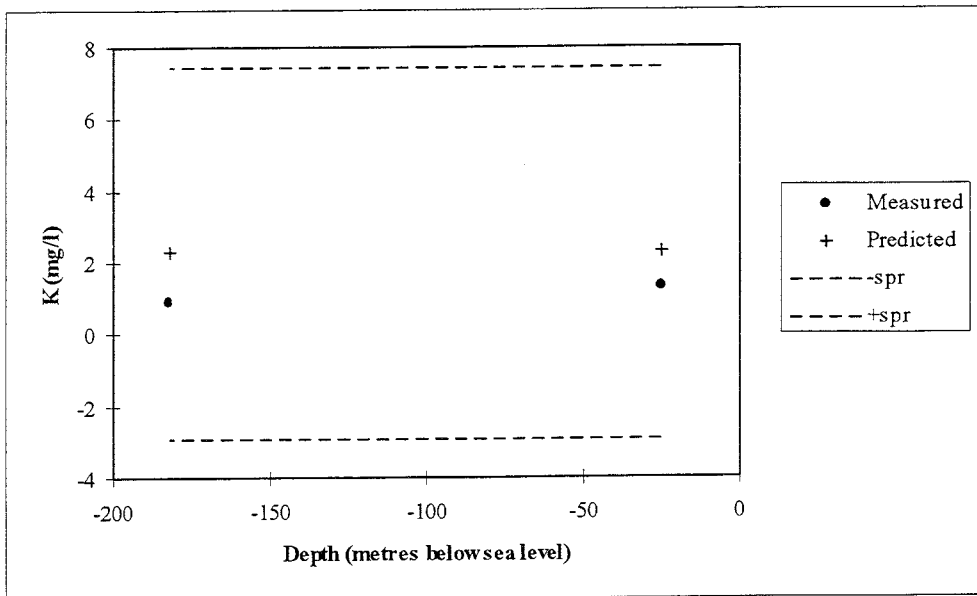


Figure L-4. The measured (dots) and predicted (crosses) K content at the Taavinummanen site in relation to the depth below sea level. The dotted lines show \pm the standard deviation of the prediction (S_{pr}).

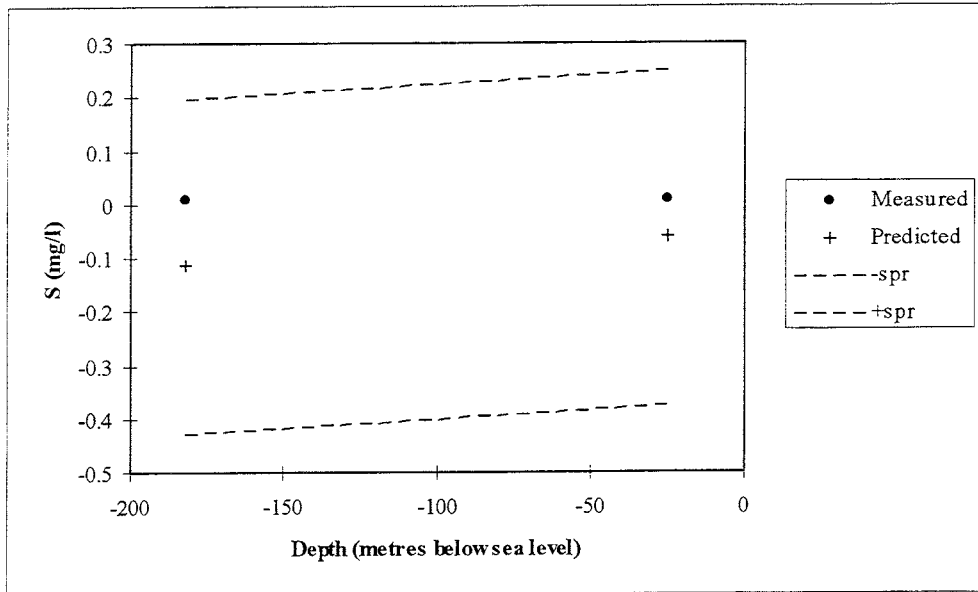


Figure L-5. The measured (dots) and predicted (crosses) S content at the Taavinunnen site in relation to the depth below sea level. The dotted lines show \pm the standard deviation of the prediction (s_{pr}).

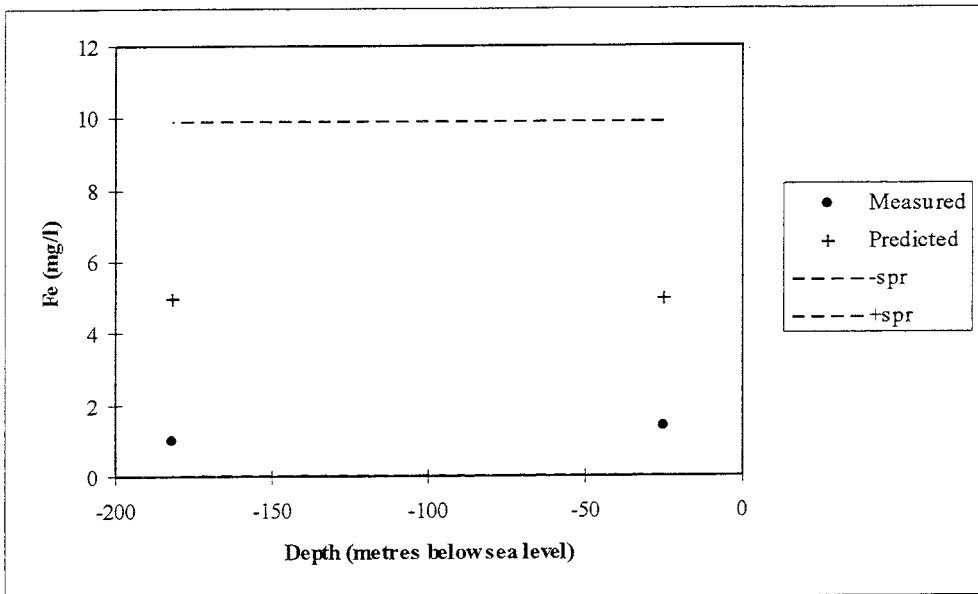


Figure L-6. The measured (dots) and predicted (crosses) Fe content at the Taavinunnen site in relation to the depth below sea level. The dotted lines show \pm the standard deviation of the prediction (s_{pr}).

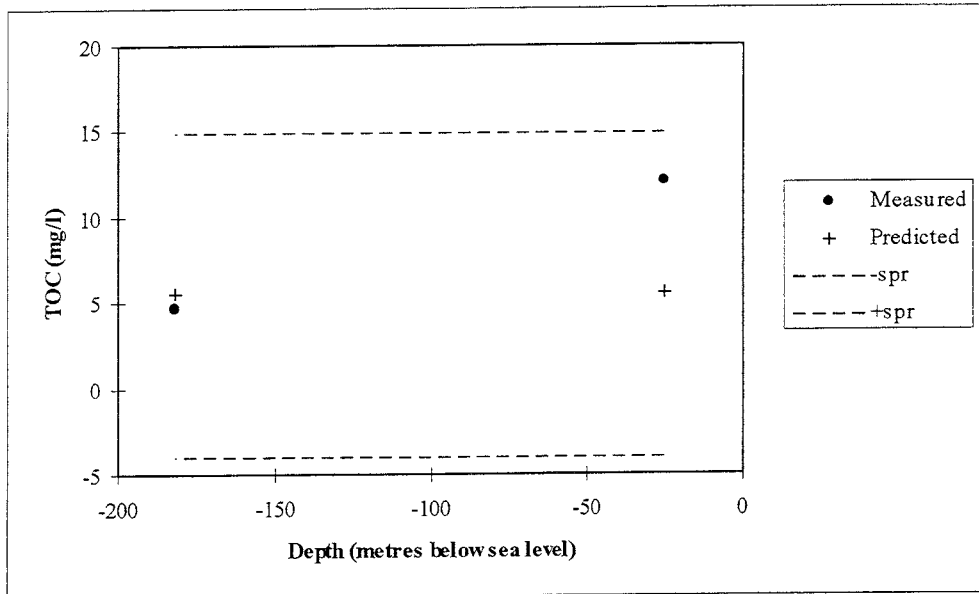


Figure L-7. The measured (dots) and predicted (crosses) TOC content at the Taavinunnen site in relation to the depth below sea level. The dotted lines show \pm the standard deviation of the prediction (s_{pr}).

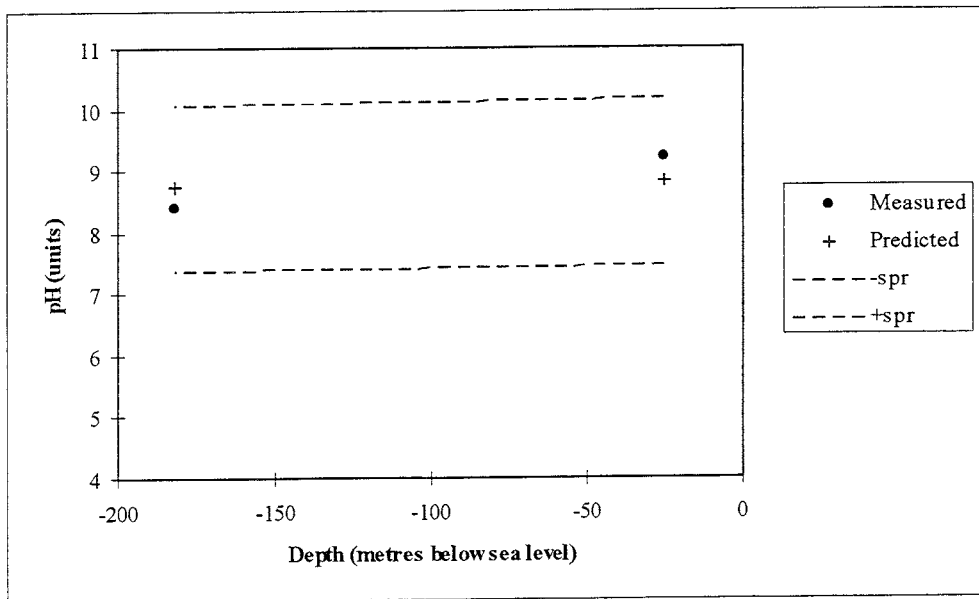


Figure L-8. The measured (dots) and predicted (crosses) pH content at the Taavinunnen site in relation to the depth below sea level. The dotted lines show \pm the standard deviation of the prediction (s_{pr}).

APPENDIX M: ZINKGRUVAN

The results of the predictions are compared with measured data and shown in relation to depth. The prediction error for the multiple linear regression is also shown. The error shown is the smallest assumable error. The true overall prediction error is larger. A general prediction error includes measurement error, analysis error, misfit to the applied distribution, kriging error etc. The error interval is not a confidence interval. Negative predictions would by definition be set at zero. Only predictions with corresponding measurements are shown.

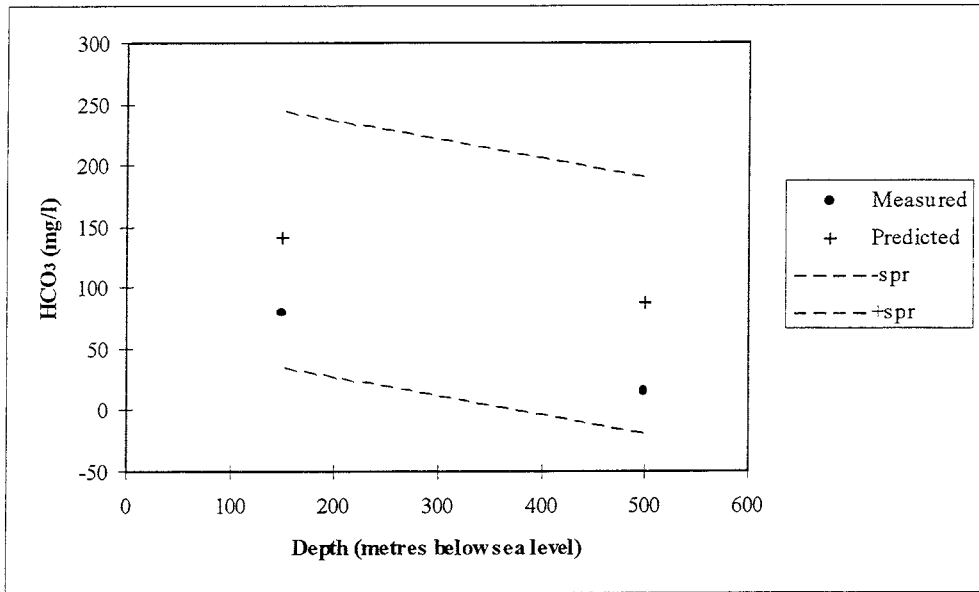


Figure M-1. The measured (dots) and predicted (crosses) HCO_3 content at the Zinkgruvan site in relation to the depth below sea level. The dotted lines show \pm the standard deviation of the prediction (s_{pr}).

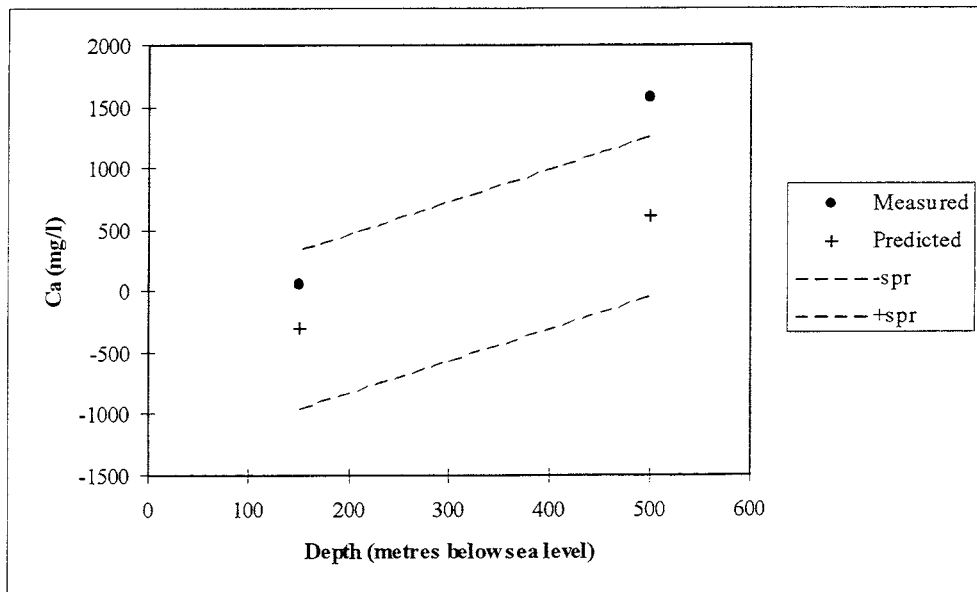


Figure M-2. The measured (dots) and predicted (crosses) Ca content at the Zinkgruvan site in relation to the depth below sea level. The dotted lines show \pm the standard deviation of the prediction (s_{pr}).

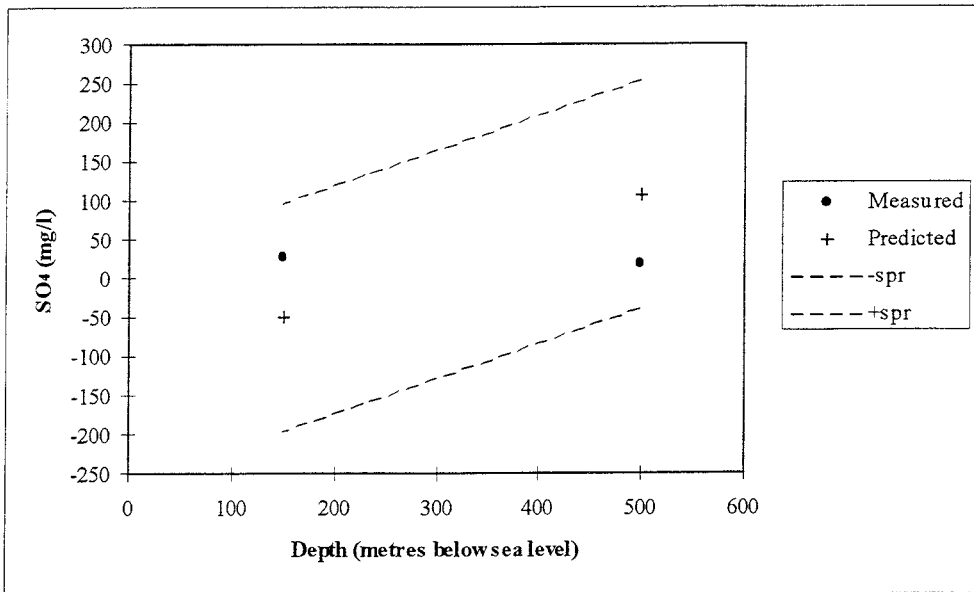


Figure M-3. The measured (dots) and predicted (crosses) SO_4 content at the Zinkgruvan site in relation to the depth below sea level. The dotted lines show \pm the standard deviation of the prediction (s_{pr}).

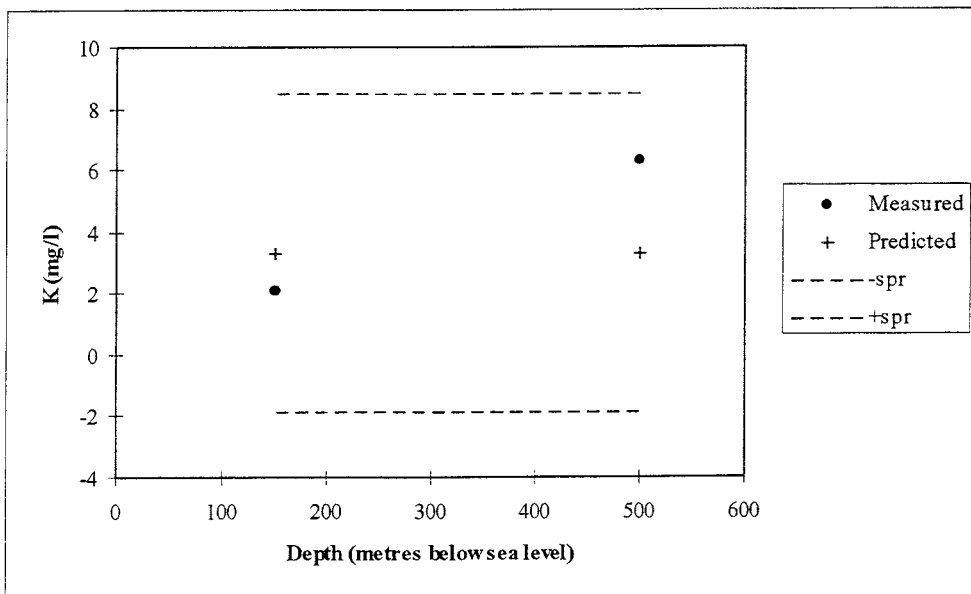


Figure M-4. The measured (dots) and predicted (crosses) K content at the Zinkgruvan site in relation to the depth below sea level. The dotted lines show \pm the standard deviation of the prediction (s_{pr}).

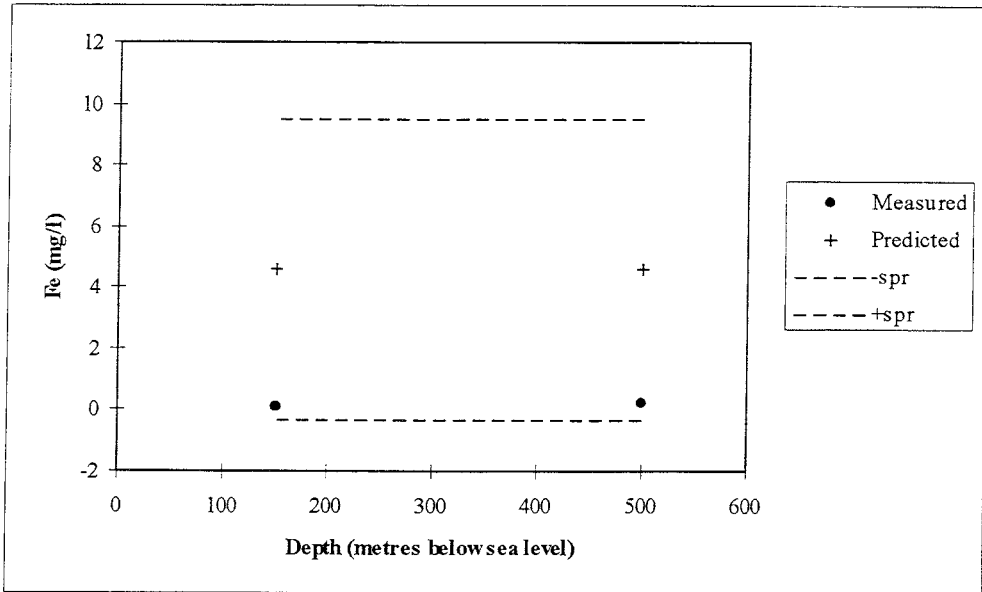


Figure M-5. The measured (dots) and predicted (crosses) Fe content at the Zinkgruvan site in relation to the depth below sea level. The dotted lines show \pm the standard deviation of the prediction (s_{pr}).